Investigating the role of apoptosis regulator EndoG on exogenous DNA uptake, stability, replication and recombination

by

Vanja Misic, B.Sc.

Biological Sciences (Cell and Molecular Biology)

Submitted in partial fulfillment

of the requirements for the degree of

Doctor of Philosophy

Faculty of Mathematics and Science,

Department of Biological Sciences, Brock University

St. Catharines, Ontario

Abstract

Endonuclease G (EndoG) is a well conserved mitochondrial nuclease with dual lethal and vital roles in the cell. It non-specifically cleaves endogenous DNA following apoptosis induction, but is also active in non-apoptotic cells for mitochondrial DNA (mtDNA) replication and may also be important for replication, repair and recombination of genomic DNA. The aim of our study was to examine whether EndoG exerts similar activities on exogenous DNA substrates such as plasmid DNA (pDNA) and viral DNA vectors, considering their importance in gene therapy applications. The effects of EndoG knockdown on pDNA stability and levels of encoded reporter gene expression were evaluated in the cervical carcinoma HeLa cells. Transfection of pDNA vectors encoding short-hairpin RNAs (shRNAs) reduced levels of EndoG mRNA and nuclease activity in HeLa cells. In physiological circumstances, EndoG knockdown did not have an effect on the stability of pDNA or the levels of encoded transgene expression as measured over a four day time-course. However, when endogenous expression of EndoG was induced by an extrinsic stimulus (a cationic liposome transfection reagent), targeting of EndoG by shRNA improved the perceived stability and transgene expression of pDNA vectors. Therefore, EndoG is not a mediator of exogenous DNA clearance, but in non-physiological circumstances it may non-specifically cleave intracellular DNA regardless of its origin. To investigate possible effects of EndoG on viral DNA vectors, we constructed and evaluated AdsiEndoG, a first generation adenovirus (Ad5 ΔE1) vector encoding a shRNA directed against EndoG mRNA, along with appropriate Ad5 ΔE1 controls. Infection of HeLa cells with AdsiEndoG at a multiplicity of infection (MOI) of 10 p.f.u./cell resulted in an early cell proliferation defect, absent from cells infected at

equivalent MOI with control Ad5 ΔE1 vectors. Replication of Ad5 ΔE1 DNA was detected for all vectors, but AdsiEndoG DNA accumulated to levels that were 50 fold higher than initially, four days after infection, compared to 14 fold for the next highest control Ad5 ΔE1 vector. Deregulation of the cell cycle by EndoG depletion, which is characterized by an accumulation of cells in the G2/M transition, is the most likely reason for the observed cell proliferation defect. The enhanced replication of AdsiEndoG is consistent with this conclusion, as Ad5 ΔE1 DNA replication is intimately related to cell cycling and prolongation or delay in G2/M greatly enhances this process. Furthermore, infection of HeLa with AdsiEndoG at MOI of 50 p.f.u./cell resulted in an almost complete disappearance of viable, adherent tumour cells from culture, whereas almost a third of the cells were still adherent after infection with control Ad5 ΔE1 vectors, relative to the non-infected control. Therefore, targeting of EndoG by RNAi is a viable strategy for improving the oncolytic properties of first generation adenovirus vectors. In addition, AdsiEndoG-mediated knockdown of EndoG reduced homologous recombination between pDNA substrates in HeLa cells. The effect was modest but, nevertheless demonstrated that the proposed role of EndoG in homologous recombination of cellular DNA also extends to exogenous DNA substrates.

Acknowledgements

First and foremost, I would like to thank my mentor and supervisor Dr. Yousef Haj-Ahmad for giving me the opportunity to pursue my doctorate studies under his guidance and supervision. He provided me with the freedom to explore my research interests and to do so with a high degree of independence. I will forever be indebted to Dr. Haj-Ahmad for investing in my professional and personal development and for his inexhaustible support, encouragement, enthusiasm and patience in leading me to achieving my goal. Throughout the years that it took to complete my thesis I could always lean on Dr. Haj-Ahmad for wisdom and expertise to keep me on the right path. It is difficult to express in words the gratitude that I feel towards Dr. Haj-Ahmad, other than to say that I feel truly privileged to have been his student.

I would also like to thank my committee members, Dr. Alan Castle and Dr. Adonis Skandalis, whose input and guidance were instrumental for steering my thesis to completion. I will always be grateful for their contribution. Furthermore, I would like thank them for the careful review of this manuscript and all of their suggestions and advice that have helped me in its preparation.

My endless thanks go to the staff of Norgen Biotek for their invaluable help in my research endeavors. They were a constant source of knowledge, expertise and encouragement and it is my great privilege to be able to call them friends. Thank you: Dr. Mohamed El-Mogy, Dr. Moemen Abdalla, Dr. Bernard Lam, Dr. Won-Sik Kim, Elisa Bibby, Ismail Aljourmi, Thomas Hunter, Nezar Rghei, Seema Shamim, David Findlay, Angela Duarte, Jaclyn Ugulini, Chris O'Brien, Sherry Amery, Katelynn Fenner, Saleem Khan, Pam Roberts and Amy Whittard.

For their support, help and encouragement, but especially for their friendship and companionship I would like to thank all of my lab mates: Taha Haj-Ahmad, Song Song Geng, Basma Abbas, Lei Zhang, Hayam Mansour, Hadeel Zamakhshari, Brittany Umer and Melissa Simkin. Thank you for creating a fun and stimulating environment for learning and achieving.

Thank you also to my friends outside of the laboratory who have always encouraged me and kept my spirits up throughout the years. Thank you: Gorana Zubic, Vladimir Popovic, Mladen Djukic and Zoran Kubat.

Finally, I would like to acknowledge my parents and my brother whose love and devotion allowed me to achieve my goal. I dedicate this work to them. Thank you for all of your sacrifices and all of your hard work. All of my accomplishments are equally yours, for without you none of this would be possible.

Table of Contents

Table of Abbreviations

CAD	caspase activated DNase
CSR	class switch DNA recombination
CMVie	cytomegalovirus immediate/early
CPE	cytopathic effect
DNase	deoxyribonuclease
dsDNA	double stranded DNA
EndoG	Endonuclease G
E. coli	*Escherichia coli*
Ad5 ΔE1	first generation adenovirus
FEN-1	flap endonuclease 1
fDNA	foreign DNA
GFP	green fluorescent protein
HSV I	herpes simplex type I
HEK293	human embryonic kidney 293
HPV-18	human papilloma virus 18
MEM	minimum essential medium
mtDNA	mitochondrial DNA
MOI	multiplicity of infection
PBS	phosphate buffered saline
pDNA	plasmid DNA
p.f.u.	plaque forming units
Pol	polymerase

PCR	polymerase chain reaction
PTE	primary tubular epithelial
qPCR	quantitative PCR
ROS	reactive oxygen species
Rb	retinoblastoma
RNAi	RNA interference
shRNA	short-hairpin RNA
ssDNA	single stranded DNA

List of Tables

List of Figures

General Introduction and Aim of the Study

The human genome encodes multiple deoxyribonucleases (DNases), yet they all function to hydrolyze the phosphodiester bond on a single substrate: DNA. From an evolutionary perspective, the question that presents itself is: Why does our genome encode so many different enzymes that have overlapping activities? Although genetic redundancy cannot be discounted, it appears that the answer may lie in the diverse biological roles these enzymes perform, or in which they are speculated to participate. Below is a brief review of the major human DNases that outline this diversity of functions, which is well highlighted in the case of the conserved and ubiquitously expressed mitochondrial endonuclease G (EndoG).

Caspase activated deoxyribonuclease

Caspase activated deoxyribonuclease (CAD) is the "professional" apoptotic endonuclease in human cells (reviewed in Baranovskii et al., 2004 and Samejima and Earnshaw, 2005). It non-specifically cleaves endogenous chromatin substrates during the last stages of apoptosis, after the cell has already committed to death (Enari et al., 1998). Unlike many other apoptotic proteins, activity of CAD is restricted exclusively to apoptosis and it has no known functions in physiological circumstances (reviewed in Samejima and Earnshaw, 2005). Tight regulation of CAD activity in the cells is facilitated by an inhibitor of CAD (ICAD) protein that is normally always bound to CAD to prevent formation of functional CAD homodimers (Korn et al., 2005). Apart from acting as an inhibitor of CAD, ICAD is also a protein chaperone that is required for proper CAD

folding (Enari et al., 1998). Therefore, ICAD regulates CAD at the level of protein expression, as well as enzymatic activity.

The CAD/ICAD protein complex is normally localized in the nucleus along with an excess of free ICAD proteins that serve as a failsafe against accidental CAD activation (Samejima and Earnshaw, 1998; Widlak et al., 2003). When apoptosis is induced through the death receptors, proteolytic activities of caspases 3 and 7 facilitate the release of CAD from ICAD, which subsequently leads to the assembly of enzymatically active CAD homodimers (Widlak et al., 2003; Woo et al., 2004). Active CAD cleaves the chromatin at internucleosomal regions to produce the characteristic laddering of DNA when visualized on an agarose gel, which is a hallmark event in programmed cell death (reviewed in Samejima and Earnshaw, 2005).

Deoxyribonuclease I

Deoxyribonuclease I (DNase I) is a neutral Mg^{2+}/Ca^{2+} dependent endonuclease mainly expressed in the pancreas (Shiokawa and Tanuma, 2001). It is the major secretory endonuclease, as evidenced by a hydrophobic signal peptide at its amino terminus and a high glycosylation level. In the cell, DNase I is found in the rough endoplasmic reticulum, Golgi apparatus and secretory granules, which corresponds to the traditional secretory route (reviewed in Baranovskii et al., 2004). Neutral DNase activity matching DNase I catalytic properties can be detected at low levels in the circulation and at higher levels in urine (Nadano et al., 1993).

Due to its presence in blood, DNase I is perceived as a "waste management" nuclease that prevents accumulation of DNA in the circulation (reviewed in Baranovskii et al.,

2004 and Samejima and Earnshaw, 2005). As such, downregulation of DNase I activity has been correlated with development of the autoimmune disorder, systemic lupus erythematosus, which is characterized by an inappropriate immune response to DNA auto-antigens (reviewed in Martinez Valle et al., 2008).

Deoxyribonuclease II

Deoxyribonuclease II (DNase II) is an acid hydrolase with a pH optimum of 4.8-5.2 that has a lysosomal cellular localization (Baker et al., 1998). It activity is reduced by a 100 fold at neutral pH compared to optimum. The compartmentalization of DNase II in the lysosome, coupled with its requirement for an acidic environment and the fact that its catalytic activity leaves a 3`-terminal phosphate make it unlikely that it participates in DNA replication, repair and recombination (reviewed in Baranovskii et al., 2004).

DNase II has been suggested to participate in cell-autonomous DNA degradation during apoptosis, but this role has not been definitively established (Nakagami et al., 2003; reviewed in Baranovskii et al., 2004). The primary role of DNase II is in engulfment-mediated degradation of DNA (McIlroy et al., 2000; reviewed in Samejima and Earnshaw, 2005). Therefore, macrophages depend on the action of DNase II for catabolism of DNA found in engulfed apoptotic bodies and also DNA of engulfed pathogens (reviewed in Evans et al., 2003; Krieser et al., 2002).

Deoxyribonuclease gamma

Deoxyribonuclease gamma (DNase γ) belongs to DNase I-like nucleases as it is closely related to DNase I based on sequence homology and catalytic activity (reviwed in Baranovskii et al., 2004). It is mainly expressed in macrophages, liver and spleen, but can

be found in other organs (Baron et al., 1998). Although some authors have argued that DNase γ is secreted into the extracellular space, others have localized this enzyme in the perinuclear space (Baron et al., 1998; Shiokawa and Tanuma, 2001). In addition, the polypeptide chain of DNase γ contains two nuclear localization signals, suggesting that it may participate in the degradation of chromatin following the induction of apoptosis (Shiokawa et al., 2002). Furthermore, studies of neuronal apoptosis showed that DNase γ replaces CAD as the primary low molecular weight DNA degradation nuclease based on the differentiation of the cells (Shiokawa and Tanuma, 2004).

Endonuclease G

Endonuclease G (EndoG) is encoded on nuclear DNA, but its primary cellular localization is in the intermembrane space of mitochondria (Diener et al., 2010). Its cellular location suggested a role in mitochondrial DNA (mtDNA) replication, however, some controversy arose after initial studies on EndoG knockout mice failed to demonstrate any mtDNA-associated phenotypes (Ohsato et al., 2002; David et al., 2006). Subsequently, EndoG has been shown to be an apoptosis regulator that responds to intrinsic and extrinsic stimuli that compromise the mitochondrial membrane potential and facilitate its release from the intermembrane space (Li et al., 2001). Translocation of EndoG from its cellular compartment to the nucleus coincides with high scale genomic DNA degradation and commits the cell to death. Although other nucleases with more defined roles in apoptosis have been discovered, of which the caspase activated DNase (CAD) is the most specialized for this function, EndoG is thought to be important for responding to cell-death stimuli which bypass caspase activation (Arnoult et al., 2003; Bahi et al., 2006; Strauss et al., 2008).

Apart from its pro-death role, EndoG has been shown to have a dual vital role in the cell which is centered on the maintenance of both mitochondrial and nuclear DNA (McDermott et al., 2011; Huang et al., 2006). As mentioned previously initial studies on EndoG knockout mice did not demonstrate any readily observable phenotypes on mtDNA synthesis, however, a recent study by McDermott et al. (2011), showed a physical interaction of EndoG with mtDNA and furthermore, discovered that EndoG knockout mice do, in fact, display a mtDNA synthesis defect that leads to an increase in the left-ventricular mass of the heart.

The presence of EndoG in nuclei of viable, non-apoptotic cells, suggested that its function is not restricted exclusively to mtDNA and apoptotic DNA degradation (Côté and Ruiz-Carrillo, 1993; Ikeda et al., 1997; Huang et al., 2002; Huang et al., 2006; Buttner et al., 2007b; Zan et al., 2011). Circumstantial evidence for the role of EndoG in the maintenance of nuclear DNA has come from observations that EndoG has an affinity for sites of DNA damage and that it co-immunoprecipitates with enzymes with established roles in genome stability and mutation sensitivity (Ikeda and Ozaki, 1997; Guo et al., 2008). In addition, EndoG is a cell cycle regulator in physiological circumstances and its depletion from cultured cells results in a proliferation defect, characterized by an accumulation of cells in the G2/M transition, which is consistent with an increase in unrepaired DNA damage (Huang et al, 2006; Buttner et al., 2007a,b; reviewed in Galluzzi et al., 2012). Therefore, EndoG may participate in the processes of cellular DNA repair and/or replication.

EndoG has also been shown to participate in homologous recombination. Specifically, it cleaves the alpha (α) sequence in the genome of herpes simplex type I (HSV I) virus,

which is an initial event in viral genome isomerization (Huang et al., 2002; Huang et al., 2006). Similarly, EndoG induces double stranded breaks in switch regions of immunoglobulin genes, resulting in class switch DNA recombination in mouse B cells (Zan et al., 2011). Furthermore, EndoG depletion results in nearly complete eradication of polyploidy in mammalian and yeast cell cultures (Diener et al., 2010; Buttner et al., 2007a). Maintenance of polyploidy is much more dependent on efficient homologous recombination, relative to haploid or diploid phenotypes, suggesting that EndoG is involved in this process.

Taking all of the above into consideration, it is clear that the proposed biological roles of EndoG are extremely varied, as exemplified by the fact they extend into both pro-death and vital cellular functions. However, the one thing they have in common is the requirement for the enzyme to exert its nuclease activity on endogenous DNA substrates. The question that presents itself is whether EndoG also interacts with exogenous DNA and if it does, what are the consequences of that interaction?

EndoG has already been implicated as a cellular defence enzyme by Buzder et al., (2009) who demonstrated improved transfection efficiency of cultured mouse cells upon EndoG depletion. It is unknown whether this extends to other mammalian cells and tissues, but would be important to investigate considering the importance of efficient transgene delivery in gene therapy applications. In addition to foreign DNA (fDNA) uptake, proposed biological roles of EndoG also lend themselves for speculation about other possible effects on exogenous DNA substrates, including its effects on exogenous DNA intranuclear stability, expression of encoded genes, replication and recombination.

Therefore the aim of this study was to investigate the biological role of EndoG on:

1. Plasmid DNA (pDNA) stability and gene expression,
2. Adenovirus vector replication, and
3. pDNA uptake and recombination efficiency.

Chapter I

EndoG silencing does not increase stability of exogenous DNA in HeLa cells

1.1 Introduction

Endonuclease G (EndoG) is a member of the conserved DNA/RNA nonspecific ββα-metal-ion-finger nuclease family (Diener et al., 2010). It was first isolated from calf thymus, but homologues have been described in many model organisms such as *Caenorhabditis elegans* (Parrish et al., 2001), *Mus musculus* (Li et al., 2001), *Saccharomyces cerevisiae* (Buttner et al., 2007b) and importantly in humans (Kieper et al., 2010). It is a nuclear encoded mitochondrial enzyme, which is translated as a 33 kDa preprotein with a mitochondria localization signal (MLS) and further processed by cleavage to a 28 kDa mature protein upon translocation into the mitochondrial intermembrane space (Diener et al., 2010). EndoG exerts its nuclease activity on double and single stranded DNA, RNA and DNA/RNA heteroduplexes. EndoG derives its name from the observed preference of the enzyme to first attack (dG)n.(dC)n tracts of double stranded DNA (dsDNA) by introducing single stranded breaks in its substrate, however, it is able to catalyze phosphodiesters in a non-specific fashion (Widlak et al., 2001). It is dependent on Mn2+ or Mg2+ (but not Ca2+) as its divalent cation and shows much greater activity on single stranded nucleic acid substrates (like ssDNA and RNA) than dsDNA (Widlak et al., 2001). EndoG is characterized as a nickase, an enzyme that introduces "nicks" (or single stranded breaks) in dsDNA, as illustrated by first-hit kinetics analysis, which shows that supercoiled plasmids are first relaxed by this action of the enzyme (Widlak et al., 2001). The substrate becomes completely degraded when nicks accumulate on opposite strands of the dsDNA, resulting in double stranded breaks. For catalysis, the conserved residues His143, Asn174, and Glu182 are important for metal binding and Arg141 for substrate binding (Schafer et al., 2004).

1.1.1 Biological functions of EndoG

Although biochemical studies have answered how EndoG acts on its substrates, the question that still remains unanswered is: What is the biological function of EndoG? Initially it was thought that EndoG participates in mitochondrial DNA (mtDNA) replication for primer generation, but that view generated some controversy, partly because EndoG was not readily detected in the matrix where replication occurs and because EndoG homozygous knockout mice did not show obvious defects in this process (Ohsato et al., 2002; David et al., 2006). However, a recent study by McDermott et al. (2011) showed a physical interaction of EndoG with mtDNA and furthermore, discovered that EndoG knockout mice do, in fact, display a mtDNA synthesis defect that leads to an increase in the left-ventricular mass of the heart.

EndoG has mostly been investigated in the context of programmed cell death as one of the executioners of apoptotic degradation of genomic DNA (Strauss et al., 2008). In this function, EndoG has been shown to translocate from the mitochondrial intermembrane space to the nucleus in response to various apoptotic stimuli that compromise the function of mitochondria (Li et al., 2001). There is still some uncertainty whether the apoptotic function of EndoG is dependent on caspase activation or if it is caspase independent, however, recent studies have skewed the opinion towards the latter (Arnoult et al., 2003; Bahi et al., 2006; Strauss et al., 2008). Once in the nucleus, it exerts its nuclease activity on the chromatin and results in genomic DNA laddering, which is a hallmark event in end-stage apoptosis.

The pro-death role of EndoG appears to depend greatly on its expression level in the cell (Wang et al., 2008; Basnakian et al., 2006). Cell lines of aggressive prostate and breast cancer, which display reduced EndoG expression, due to CpG methylation of EndoG promoter/exon1, are more resistant to chemotherapeutic agents such as cisplatin and etoposide (Wang et al., 2008; Basnakian et al., 2006). Furthermore, depletion of cellular EndoG by RNA interference (RNAi) makes previously sensitive cells become much more resistant to these apoptosis inducers, highlighting the central role of EndoG-mediated chromatin degradation in cell fate commitment to death.

Although constitutively expressed, EndoG expression can be transcriptionally induced during times of cellular stress and its responsiveness to various exogenous stimuli such as ischemia/reoxygenation, reactive oxygen species (ROS) or oxygen-glucose deprivation and apoptotic inducers such as cisplatin, curcumin, berberine or gallic acid has been observed (Li et al., 2004; Zhao et al., 2009; Zhang et al., 2009; Lee et al., 2008; Mercer et al., 2010; Papa and Germain, 2011; Apostolov et al., 2011; Wu et al., 2010; Mitra et al., 2012; Ho et al., 2009; Yeh et al., 2011). The increase in cellular levels of EndoG shortly precedes the onset of apoptotic cell death, characterized by chromatin condensation and degradation.

1.1.2 Evidence for a vital role of EndoG

Apart from its pro-death role in programmed cell death, EndoG has been implicated as having vital functions in the cell, which merit further investigation. Namely EndoG has been linked to DNA repair, recombination and/or replication and also as an enzyme

involved in cellular defence against foreign nucleic acids (Huang et al, 2002; Huang et al, 2006; Buttner et al., 2007a,b; Buzder et al., 2009; Zan et al., 2011).

EndoG was first identified in nuclei of cells that were not undergoing apoptosis (Côté and Ruiz-Carrillo, 1993; Gerschenson et al., 1995). Nuclear localization of EndoG in healthy cells is important in the context of its proposed vital functions in DNA repair, recombination and/or replication. First evidence for a role of this enzyme in DNA repair comes from *in vitro* assays that showed EndoG has strong affinity for sites of oxidative damage or sites distorted by DNA crosslinking agents (Ikeda and Ozaki, 1997). Specifically, susceptibility of DNA to nucleolytic attacks by EndoG is greatly enhanced after treatments with L-ascorbic acid or peplomycin, which introduce single-stranded breaks in the substrate *via* active oxygen radicals, with EndoG cleaving the substrate at or near these sites in the opposite strand. In addition, EndoG recognized and cleaved at sites of DNA distortions caused by cis-diamminedichloroplatinum(II), which induces intrastrand crosslinking. Further, EndoG may act with other co-factors in DNA repair as was suggested by findings that it immunoprecipitates with flap endonuclease 1 (FEN-1), an enzyme that is involved in long-patch base excision repair (Guo et al., 2008).

Involvement of EndoG in recombination was first reported by Huang et al. (2002), who showed that it was the only enzyme isolated from HeLa cell nuclei that was able to cleave the herpes simplex virus 1 (HSV-1) α sequence and thereby initiate the recombinational event that is responsible for HSV-1 genome inversion. A follow-up study by the same group also showed that a knockdown of EndoG in Vero cells resulted in a decrease of HSV-1 α sequence recombination, further implicating EndoG in this process (Huang et al, 2006). Recently, EndoG has been identified as one of the enzymes involved in

immunoglobulin class switch DNA recombination (CSR) in mouse B cells (Zan et al., 2011). The action of EndoG to induce dsDNA breaks in switch regions of the upstream and downstream C_H genes is required for efficient CSR, as it was shown that this process is decreased by two-fold in B cells of EndoG null mice. It is important to note that the lowered efficiency of CSR in EndoG null mice was not related to any changes in B cell apoptosis.

Indirect evidence of EndoG involvement in homologous recombination comes from observations that decreased or attenuated expression of this enzyme results in near complete elimination of polyploidy in both yeasts and mammalian cells (Diener et al., 2010; Buttner et al., 2007a). Polyploidization is associated with genomic instability and is recognized as a precursor to aneuploidy in cancer (Buttner et al., 2007a). Survival of polyploidy cells is much more dependent on homologous recombination than that of diploid or haploid cells, as has been demonstrated by screening knockouts of genes involved in this process. Interestingly, deletion of NUC1, the yeast EndoG homologue (42% identity, 62% similarity), decreases the abundance of the polyploid phenotype from a starting 20% of the growing yeast population to less than 1% (Buttner et al., 2007a). Similarly, EndoG knockdown in both human endothelial cells and human colon cancer cell lines results in specific killing of tetraploid cells (Diener et al., 2010; Buttner et al., 2007a). These observations imply that EndoG participates in genome maintenance by homologous recombination, however, there is not enough evidence currently for a definitive call.

EndoG also appears to be important for cellular proliferation in both yeasts and mammalian cells (Buttner et al., 2007b; Huang et al, 2006). EndoG deletion in yeasts

growing on fermentable media sensitizes cells to cell death by apoptotic stimuli like hydrogen peroxide and, importantly, leads to a significant decrease in cell survival even in the absence of these stimuli (Buttner et al., 2007b). Exogenous expression of EndoG at low levels can rescue this phenotype, but only if the enzyme retains its nuclease activity. Reduction of proliferation by EndoG depletion is characterized by an increase of cells in the G2/M phase of the cell cycle, suggesting a delay in G2/M (Buttner et al., 2007a,b). Similarly, knockdown of EndoG in human endothelial, colon cancer, Vero and 293T cells results in a decrease in cellular proliferation (Diener et al., 2010; Huang et al, 2006; Buttner et al., 2007a). These cells also become arrested in the G2/M phase of the cell cycle (Huang et al, 2006). Exogenous expression of EndoG as a fusion protein with GFP is able to reverse the phenotype (Huang et al, 2006). Because EndoG compromised yeast and mammalian cells become arrested in the G2/M phase of the cell cycle, which is consistent with an accumulation of damaged DNA, EndoG could function in DNA repair, recombination and/or replication (Huang et al, 2006; Buttner et al., 2007a). Additionally, despite EndoG's characterization as a pro-apoptotic factor, its expression is elevated in colorectal and gastric carcinomas (relative to normal mucosal cells of these tissues), also suggesting a pro-life role for the enzyme.

1.1.3 A role for EndoG in cellular defence against foreign nucleic acids

Uptake of exogenous DNA occurs during normal tissue growth, tumour growth, viral and bacterial infections, and as a result of intentional genetic manipulations in experimental animals and cultured cells (Buzder et al., 2009). It is also the core principle of gene therapy applications, where efficient delivery of exogenous DNA is required for sustained expression of therapeutic genes in target cells and tissues (Ochiai et al., 2006a).

However, intracellular double stranded DNA fragments (from infectious agents or transfection experiments) trigger innate antiviral immune responses *via* a signaling pathway that involves extrachromosomal histone H2B (Kobiyama et al., 2010). Further, it has been experimentally demonstrated that entry of exogenous DNA is harmful to the host cell and that it can trigger p53-dependent apoptotic cell death (Li et al., 1999; Nur et al., 2003). Another detrimental effect of exogenous DNA is the possibility for insertional mutagenesis due to homologous or non-homologous recombination (Torchilin, 2006). Therefore, the cell depends on an active mechanism to restrict DNA uptake and attenuate these deleterious effects (Buzder et al., 2009). Unfortunately, the activity of this defence mechanism also presents a barrier for intentional genetic manipulations and is an impediment to successful gene therapy applications.

Keeping in mind that entry of exogenous DNA into the host cell is followed in large part by its degradation (even when protected by lipid or viral packaging), the main effectors of this defence mechanism must be DNA degrading enzymes (Buzder et al., 2009). The first line of defence against exogenous DNA is in the cytosol, where, as of yet, unidentified DNases actively reduce the amount of DNA available for entry into the nucleus. This effect occurs within 50-90 minutes following microinjection of naked DNA into the cytoplasm or after it is released from endosomes following transfection with cationic lipids (Chu et al., 2006). Although cytosolic degradation of exogenous DNA is a major hurdle for successful gene delivery, it is not the only barrier for efficient and prolonged gene expression, as intranuclear disposition of non-integrating vectors, following DNA entry into the nucleus, is also a key factor (Ochiai et al., 2006a).

Silencing of genes encoded on non-integrating exogenous DNA, such as pDNA, has been observed *in vitro* and *in vivo*, resulting in the reduction of both the level and the duration of transient transgene expression (Chu et al., 2006; Ochiai et al., 2006a; Yamada et al., 2005; Berraondo et al., 2009; Ochiai et al., 2006b). Accordingly, highest levels of transient transgene expression in mammalian cells from non-viral plasmid vectors are observed early after pDNA delivery (24-48 hours) and dissipate shortly thereafter (72 hours). Transgene expression decreases over time with respect to plasmid copy number, suggesting that transgene copies are inactivated even after nuclear entry (Chu et al., 2006; Ochiai et al., 2006a; Yamada et al., 2005; Berraondo et al., 2009; Ochiai et al., 2006b). Part of the observed phenomenon may be attributed to *de novo* CpG methylation of exogenous DNA and/or deactivation by modification of DNA bound histones in addition to chromatin remodeling events. However, there is increasing evidence which suggests that much of the silencing occurs as a result of intranuclear exogenous DNA degradation, which occurs in parallel to other silencing mechanisms (Chu et al., 2006; Ochiai et al., 2006a; Yamada et al., 2005; Berraondo et al., 2009; Ochiai et al., 2006b). It is still unclear whether pDNA degradation is a specific action aimed at exogenous DNA clearance, or a byproduct of endogenous nuclease activities required for normal cellular DNA replication, recombination and repair, which are abundantly present in mammalian nuclei (Ochiai et al., 2006a).

Since EndoG has indirectly been implicated in DNA replication/repair and recombination, all of which would require its nuclease action in the nuclei of healthy, non-apoptotic, cells, a valid hypothesis is that it may be involved in intranuclear disposition of exogenous DNA, whether as consequence of non-specific action on DNA

substrates or a specific defence role. EndoG has already been implicated as a defence nuclease in experiments in primary tubular epithelial (PTE) cells of EndoG null mice. Transfection efficiency of EndoG null mouse PTE cells is more than two-fold higher than that of wildtype control PTE cells, as measured by a fluorescence reporter assay (facilitated by expression of CFP from the transfected plasmid) (Buzder et al., 2009).

Although the above finding argues that EndoG presents a block to transfection in its suggested defence role, it fails to explain how an enzyme with a nuclear/mitochondrial localization and not cytoplasmic could effectively prevent plasmid DNA (pDNA) from entering the nucleus. In addition, the effect of EndoG knockout on transgene expression was more pronounced at 48 than at 24 hours post transfection, and transfection efficiency was not assayed by pDNA copy number, but rather by transgene expression (Buzder et al., 2009). This opens up the possibility that EndoG may have degraded pDNA in the nucleus over time, rather than in the cytoplasm to prevent its entry.

Therefore the aim of our study was to investigate whether EndoG is a defence enzyme involved in intranuclear disposition of exogenous DNA in replicating mammalian cells. The hypothesis was that EndoG targeting by RNAi would augment pDNA stability and transgene expression in the cervical carcinoma HeLa cells. Our experimental approach was to compare the stability of pDNA and encoded transgene expression, with respect to time, between pDNA that could facilitate a knockdown of EndoG and control pDNA in HeLa cells. For this purpose, we engineered a short-hairpin RNA (shRNA) expression pDNA vector, pDC-CG-U6, and armed it with templates for the expression of shRNAs targeting six unique regions of EndoG mRNA. In addition to these six pDNA vectors, we constructed a negative control vector based on the same backbone but encoding a non-

targeting shRNA. These vectors were independently transfected into HeLa cells and their cellular levels as well as the expression of an encoded transgene were monitored over a four day time course at 24 hour intervals. By design, we avoided transfection of pDNA into HeLa cells that had differential EndoG levels at outset of experiment because of the previously reported effect of EndoG on pDNA uptake (Buzder et al., 2009).

1.2 Materials and Methods

1.2.1 Selection of targets within EndoG mRNA

Invitrogen's BLOCK-iT™ RNAi Designer tool (http://rnaidesigner.invitrogen.com/rnaiexpress/) was used to identify suitable regions within EndoG mRNA for targeting by shRNAs. In step 1, full length EndoG mRNA was used as input. In step 2, targeting was limited to the open reading frame (ORF) of the gene. In step 3, BLAST was used to filter targeting to sequences which are unique to EndoG mRNA using the Human – *Homo sapiens* database for reference (May 1, 2008 update). In step 4, default settings were used for target G/C content, minimum 35% and maximum 55%. In step 5, unique regions within EndoG mRNA, suitable for RNAi targeting, were identified (Table 1.1).

Table 1.1 - Sequences within the EndoG mRNA chosen for targeting by RNAi.

Start position of target seq. on EndoG mRNA (nt)	Target sequence (5`- 3`)
644	**GGCCAUGGACGACACGUUCUA**
653	**CGACACGUUCUACCUGAGCAA**
704	**GAAUGCCUGGAACAACCUGGA**
805	**CTGAUGGGAAAUCCUACGUAA**
809	**UGGGAAAUCCUACGUAAAGUA**
1009	**GGCUGCUCUUUGUGCCAAACA**

1.2.2 Construction of pDC-CG-U6, a shRNA expression vector

To express shRNAs directed against EndoG mRNA we constructed the plasmid vector pDC-CG-U6. The pDC-CG shuttle vector contained a GFP expression cassette under the control of the cytomegalovirus immediate/early (CMVie) promoter/enhancer and a small multi-cloning site (MCS) upstream of the cassette. We cloned the RNA Pol III promoter U6 at the *Eco* RI restriction site, while preserving the downstream MCS for insertion of shRNA DNA templates. Therefore, pDC-CG-U6 contained two adjacent transgene expression cassettes in the same orientation, one of which was used to express shRNA, driven by the U6 promoter, and the other to express green fluorescent protein (GFP), driven by the CMVie promoter/enhancer. The U6 promoter was chosen for shRNA expression because it regulates expression of small RNAs in its endogenous context and also because it requires a very short transcription termination signal (stretch of 4-6 T nucleotides). The cloning steps in the construction of pDC-CG-U6 are outlined below.

The RNA Pol III promoter U6 was amplified by PCR using *Pfu* DNA Pol, which has proofreading ability, using the p*Silencer* 2.1-U6 neo vector as a template (Ambion). Primers used for PCR were: U6 F: 5`AGCATGCAATTGCCCCCAGTGGAAAGACG3` and U6 R: 5`CGAATTCGGATCCCGCGTCCTTTCC3`. The forward primer had a 5` flanking sequence corresponding to the recognition site of *Mfe* I restriction enzyme and the reverse primer had a 5` flanking sequence corresponding to the recognition sequence of *Eco* RI restriction enzyme, which were not in the template sequence, but were required for downstream cloning. The PCR amplicon of U6 was cleaned and concentrated using a commercially available kit (PCR Purification Kit, Norgen Biotek).

In the next step, the U6 promoter, flanked by sequences of *Mfe* I and *Eco* RI recognition sites (5` to 3`), was ligated into a pUC19 vector previously digested with restriction enzyme *Hinc* II, which produced blunt ends. This step was necessary before cloning into pDC-CG due to the severely reduced activity of *Mfe* I on PCR products. The resultant vector, pUC19-U6 was amplified in *Escherichia coli* (*E. coli*) DH5α and purified by a commercial pDNA isolation kit (Plasmid MiniPrep DNA Kit, Norgen Biotek). Subsequently, the pUC19-U6 was digested with *Mfe* I and *Eco* RI restriction endonucleases and agarose gel electrophoresis was used to separate the U6 fragment from the pUC19 backbone. The band corresponding to U6 was excised from the agarose gel and purified using a commercially available kit (DNA Gel Extraction Kit, Norgen Biotek).

The shuttle vector pDC-CG was digested by *Eco* RI and the purified U6 promoter was incorporated into the vector by the T4 DNA ligase reaction (New England Biolabs). The sticky ends generated by *Mfe* I and *Eco* RI are compatible, but when annealed they produce a sequence that cannot be cleaved by either of the enzymes. Therefore the uniqueness of the *Eco R*I recognition site was preserved in pDC-CG-U6, directly downstream of the U6 promoter, which was important for subsequent insertions of various shRNA DNA templates.

1.2.3 Confirmation of sequence fidelity of pDC-CG-U6

The U6 promoter insert had the potential to form concatemers and also to ligate in either orientation into the pDC-CG shuttle vector, due to the compatibility of its sticky ends, making identification of *E. coli* DH5α clones harboring the correct version of pDC-CG-

U6 extremely tedious by conventional methods. To make the process more efficient, we screened bacterial colonies by an end-point PCR protocol that was sensitive as well as specific. Each bacterial colony that was screened was first resuspended in 20 µL of water, 2 µL of which was used as a template for PCR without prior DNA isolation.

The primers used in the PCR were F: 5`AGCATGCAATTGCCCCCAGTGGAAAG-ACG3` and R: 5`GATGTTGCCATCCTCCTTGA3`. The forward primer annealed to a region within the U6 promoter and the reverse primer annealed to a sequence in the pDC-CG backbone and only a single U6 insert in the proper orientation yielded a 1660bp amplicon. Of the 94 colonies screened by this method, only one clone, number 46, produced this specific amplicon after agarose gel electrophoresis of the PCR products. This clone was grown in ampicillin supplemented Luria- Bertani (LB) broth for 16 hours and pDC-CG was purified by a commercially available DNA isolation kit (Plasmid MaxiPrep DNA Kit, Norgen Biotek).

Purified pDC-CG-U6 was reconfirmed by restriction enzyme digestion in three separate reactions with enzymes: *Sph* I and *Pml* I double digestion, which produced expected fragments of 4992 and 316 bp; digestion with *Bam* HI, which produced expected visible fragments of 3570 bp, 809 bp, 635 bp, and 198 bp; and digestion with *Eco* RI which linearized the vector and produced a single band on the gel corresponding to 5308 bp, or the full length of the pDC-CG-U6.

Since the U6 promoter, inserted into pDC-CG-U6, was generated by PCR we sequenced this region of the vector to ensure the absence of any mutations. For this purpose, the purified vector was sent to a core facility (York University Core Molecular Biology and

DNA Sequencing Facility) along with the primer 5`AGCATGCAATTGCCCCCAGTG-GAAAGACG3`. The returned sequence encompassed the entire U6 promoter, as well as a region extending beyond the downstream MCS, and was an absolute match to the expected sequence of the U6 promoter.

1.2.4 Construction of shRNA DNA templates and cloning into pDC-CG-U6

The design of shRNAs, in the 5` to 3` orientation, was as follows: sense strand, which was homologous to the targeted region within EndoG mRNA; a short loop region (UUCAAGAGA); and the antisense strand, which was perfectly complementary to the target sequence. To facilitate shRNA expression we cloned corresponding DNA templates into the pDC-CG-U6 vector.

DNA templates for shRNA expression were constructed by annealing pairs of complementary oligomers (Integrated DNA Technologies) to create dsDNA molecules that encoded the following (5` to 3`): *Eco* RI recognition sequence, sense strand, loop region, antisense strand, RNA Pol III terminator sequence, and the *Pst* I recognition sequence. The dsDNA sequences were 63bp long with short single stranded overhangs on either end, which were homologous to *Eco* RI and *Pst* I-generated sticky ends.

Digestion of pDC-CG-U6 by *Eco* RI and *Pst* I restriction nucleases facilitated the subsequent ligation of shRNA DNA templates in the correct orientation, directly downstream of the U6 promoter. In total, seven pDC-CG-U6-based vectors were constructed in this manner, six of which contained unique DNA templates for the expression shRNAs directed against EndoG mRNA and one negative control vector that contained a DNA template for the expression of a shRNA without a complement in the

human transcriptome. The negative control shRNA target was 5`ACUACCGUUGUUA-UAGGUG3`. All of the pDC-CG-U6-shRNA vectors were sequenced, as described previously, to ensure template sequence fidelity.

The pDC-CG-U6-shRNA vectors were amplified in *E. coli* DH5α and subsequently purified by a commercially available plasmid isolation kit (Plasmid MaxiPrep DNA Kit, Norgen Biotek). To ensure compatibility of plasmid DNA preps for the transfection procedure, the protocol included an endotoxin removal component (as per manufacturer's instructions).

1.2.5 Cell culture

HeLa cells were maintained in 150 mm, 24-well or 6-well standard culture dishes, growing in a monolayer. Culture medium was Gibco's minimum essential medium (MEM) supplemented with 10% (v/v) foetal bovine serum (FBS) (PAA Labs), antimycotic-antibiotic (1X, Invitrogen), GlutaMAX^{TM} (1X, Invitrogen) and with sodium bicarbonate (3.7 g/l). Cultures were incubated in a 5% CO_2/air mixture at 37 °C.

1.2.6 Transfection of plasmids into subconfluent HeLa cells

HeLa cells were plated in 24-well plates so that they were 50% confluent on day of transfection. Individual plasmids (250 ng/well) were mixed with Opti-MEM I Reduced Serum Medium without serum to a final volume of 50 µL. Next, 1 µL of Lipofectamine 2000 (Invitrogen) was diluted in 50 µL Opti-MEM I Reduced Serum Medium. The diluted plasmids were then combined with the diluted Lipofectamine 2000 and left to incubate for 20 minutes at room temperature. The plasmid/lipofectamine mixture were

then added to each well and mixed into the medium by gentle rocking. Six hours after transfection, the medium was changed with fresh medium.

1.2.7 Transfection of plasmids into near-confluent HeLa cells

HeLa cells were plated in 6-well plates so that they were 90% confluent on day of transfection. Individual plasmids (4 µg/well) were mixed with Opti-MEM I Reduced Serum Medium without serum to a final volume of 250 µL. Next, 5 µL of Lipofectamine 2000 (Invitrogen) was diluted in 250 µL Opti-MEM I Reduced Serum Medium. The diluted plasmids were then combined with the diluted Lipofectamine 2000 and left to incubate for 20 min at room temperature. The plasmid/lipofectamine mixture were then added to each well and mixed into the medium by gentle rocking. Six hours after transfection medium was changed with fresh medium.

1.2.8 DNA/RNA isolation

Medium was aspirated and HeLa monolayers were washed twice with 1X phosphate buffered saline (PBS), pH7.4. A solution from a commercially available kit (RNA/DNA/Protein Purification Kit, Norgen Biotek) was used to lyse cells directly on the plate. Entire lysate was collected and applied to a purification column supplied by the manufacturer and recommended protocol was followed as specified. DNA and RNA were eluted in separate fractions and examined for quality and quantity by agarose gel electrophoresis and spectrophotometry, respectively.

1.2.9 Quantitative PCR analysis

Quantitative PCR (qPCR) was performed with the Bio-Rad iCycler thermocycler on 3 µL of each DNA elution using the iQ SYBR Green Supermix (Bio-Rad) with 300 nM of primers specific for the GFP gene encoded on the plasmid, F 5`GATCACATGAAGC-AGCACGA3` and R 5`GATGTTGCCATCCTCCTTGA3`. The human 5S gene (Fwd primer 5`GCCATACCACCCTGAACG3` and Rev primer 5`AGCCTACAGCACCCG-GTATT3`) was used for normalization and the comparative threshold method was used to assess the relative abundance of the plasmids at each time point. The total reaction volume per sample was 20 µL, and the PCR protocol was as follows: 15 minutes at 95^{o}C for enzyme activation, then 40 cycles of 15 seconds at 95^{o}C, 30 seconds at 60^{o}C and 45 seconds at 72^{o}C. Melt curve analysis was performed by relative fluorescence assessment at 0.5^{o}C increments with a 10 second duration, starting at 57^{o}C and continuing for 80 increments.

1.2.10 Reverse transcription followed by qPCR

Three µL of the total RNA elution was used in the reverse transcription (RT) reaction using the Superscript III system (Invitrogen). In the first step, RNA was mixed with 0.5 µL of 100 mM oligo(dT) 18-mer primer (IDT) and the reaction volume was completed to 10 µL using DNase/RNase free water. Denaturing at 70^{o}C for 5 minutes was followed by cooling at 4^{o}C for five minutes. At this step, 0.1 µL of the reverse transcriptase Superscript III (SSIII, Invitrogen) was added to the reaction in a mixture with 4 µL of the 5X First Strand Buffer, 2 µL of 0.1 M Dithiothreitol, 1 µL of 10 mM dNTPs and 2.9 µL of water. After the reaction mixture was completed, temperature was increased to 25^{o}C

for five minutes and then increased again to 42°C for 60 minutes, followed by 15 minutes at 70°C and an indefinite hold at 4°C.

The qPCR detection of GFP transgene expression levels was carried out using the human S15 for normalization and the comparative threshold method was used to assess the relative abundance of GFP mRNA at each time point. The primers used for detection of GFP copy DNA were F 5`GATCACATGAAGCAGCACGA3` and R 5`GATGTTGCCATCCTCCTTGA3` and for S15 copy DNA F 5`TTCCGCAAGTTCA-CCTACC3` and R 5`CGGGCCGGCCATGCTTTACG3`. The iQ SYBR Green Supermix (Bio-Rad) was used for the qPCR with 300 nM of primers, as described above for DNA analysis. Levels of EndoG mRNA were also interrogated at each time point using the primers: F 5`GACGACACGTTCTACCTGAGCAACGT3` and R 5`CCAGGATCAG-CACCTTGAAGAAGTG3`. The qPCR protocol for EndoG cDNA amplification varied slightly to protocol described previously due to the requirement of a higher primer annealing temperature, which was set at 65°C.

1.2.11 EndoG activity assay

Cultured HeLa cells, transfected with test and control pDC-CG-U6-shRNA vectors, were grown to near confluence in 6-well standard tissue culture plates. Medium was aspirated and cells were washed three times with ice-cold 1X PBS. Two-hundred µL of the single detergent buffer (50 mM Tris-CI pH 8.0, 150 mM NaCI, 0.02% sodium azide, 100 µg/mL PMSF, 1 µg/mL aprotinin and 1% Nonidet P-40) was added directly to cell monolayers and plates were incubated at 4°C for 20 minutes. Lysates were collected by pipetting into a chilled Eppendorf tube, followed by centrifugation at 12,000g for 2 minutes at 4°C. Soluble proteins from the supernatant were collected and stored at -70°C.

Total protein concentration was determined using the Pierce 660 nm Protein Assay Kit (Thermo Scientific) by mixing 1.5 mL of reagent to 0.1 mL of diluted samples, followed by incubation at room temperature for five minutes and spectrophotometry at 660 nm. Quantification was facilitated by standard curve analysis, using the BSA protein as a standard.

One µg of linearized plasmid target (pDC-CG-U6 digested with *Eco R*I) was incubated with 20 µg of total protein from cell extracts for 0, 30, 90, or 180 minutes at 37^{o}C. Each reaction was supplemented with 1 mM $MgCl_2$ to select for EndoG activity (Kieper et al., 2010). Ten µL of each 50 µL reaction was loaded on a 1% DNA agarose gel and examined after electrophoresis.

1.2.12 Cell counting

Medium was aspirated from HeLa cells cultured in 24-well standard tissue culture plates and monolayers were washed three times with 1X PBS. Cells were lifted with 200 µL of Gibco's 0.05% Trypsin-EDTA (1x) and counted on the haemocytometer counting chamber using the Olympus CK 2 inverted microscope for magnification.

1.3 Results

1.3.1 – Strategy of EndoG Knockdown by RNAi

1.3.1.1 Selection of RNAi targets within EndoG mRNA

To select appropriate regions on the EndoG mRNA for targeting by RNAi a proprietary algorithm (Invitrogen's BLOCK-iT™ RNAi Designer tool) was used. Six regions of EndoG mRNA were identified as possible targets (Fig. 1.1). Targeting was limited to the open reading frame (ORF) of EndoG, with a minimum and maximum G/C content of candidate sequences set at 35% and 55%, respectively. Basic Local Alignment Search Tool (Human – *Homo sapiens* database) was used to ensure only unique regions of EndoG were targeted. The control targeted sequence was not encoded in the human genome: 5`-ACUACCGUUGUUAUAGGUG-3`.

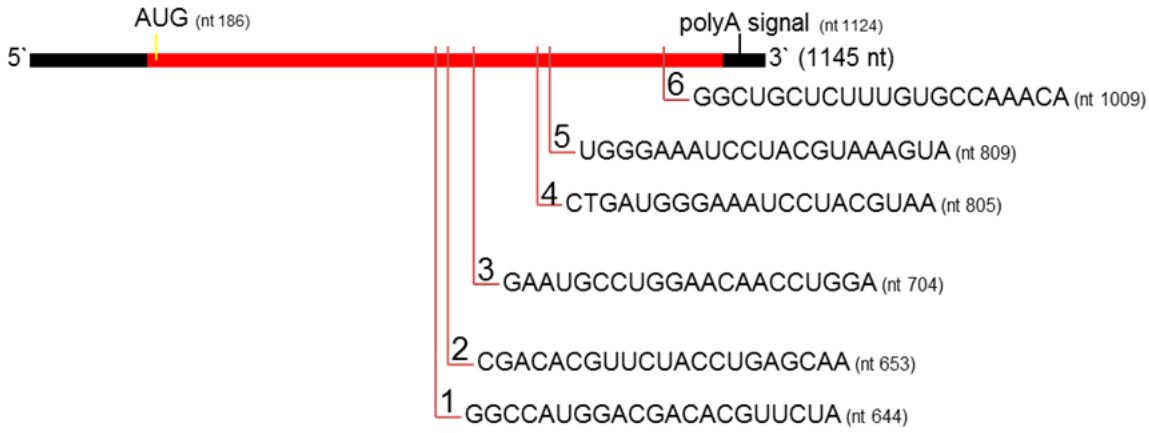

Figure 1.1: Full length EndoG mRNA (1145 nt). The coding sequence (in red) spans from nucleotides 186 to 1079 (894 nt). Relative positions of RNAi targets are indicated, along with the target sequences (and nucleotide positions in parentheses, in the 5` - 3` direction).

1.3.1.2 Design of RNAi effectors for EndoG knockdown

Identification of suitable targets within EndoG mRNA (Fig. 1.1) enabled us to design short-hairpin RNAs (shRNAs) that specifically antagonized these regions. Six shRNAs targeting EndoG mRNA, plus a negative control shRNA, were designed based on the following scheme, in the 5` to 3` direction: sense strand (identical to target sequence), loop region (9 nt), antisense strand (perfectly complementary to target sequence) (illustrated in Fig. 1.2, using target sequence at nt 644 of EndoG mRNA as a representative example).

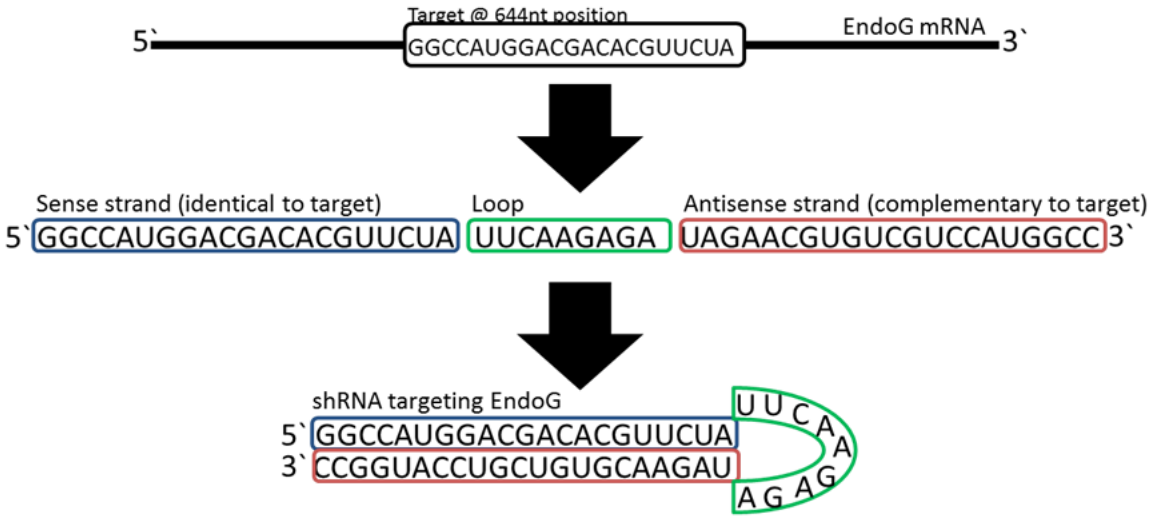

Figure 1.2: Construction design of a representative shRNA targeting EndoG mRNA at nucleotide position 644 (5` to 3` direction). The sense strand (blue border) is identical to the selected targeting site (black border), while the antisense strand (red border) is its perfect complement. Annealing between sense and antisense strands results in a hairpin structure, characterized by a single stranded loop region (green border).

1.3.2 – Construction of Plasmids for Expression of shRNAs Directed Against EndoG

1.3.2.1 Engineering the U6 (RNA Pol III) promoter into assay plasmid pDC-CG

The assay plasmid pDC-CG encoded a GFP reporter gene under the control of the cytomegalovirus immediate-early (CMVie) promoter/enhancer (Fig. 1.3). To drive expression of shRNAs directed against EndoG (or control shRNA), we inserted the U6 RNA Pol III promoter into our assay plasmid, pDC-CG, directly upstream of the GFP expression cassette. This was accomplished in several steps, as outlined in Figure 3, and resulted in the creation of pDC-CG-U6, an shRNA expression vector.

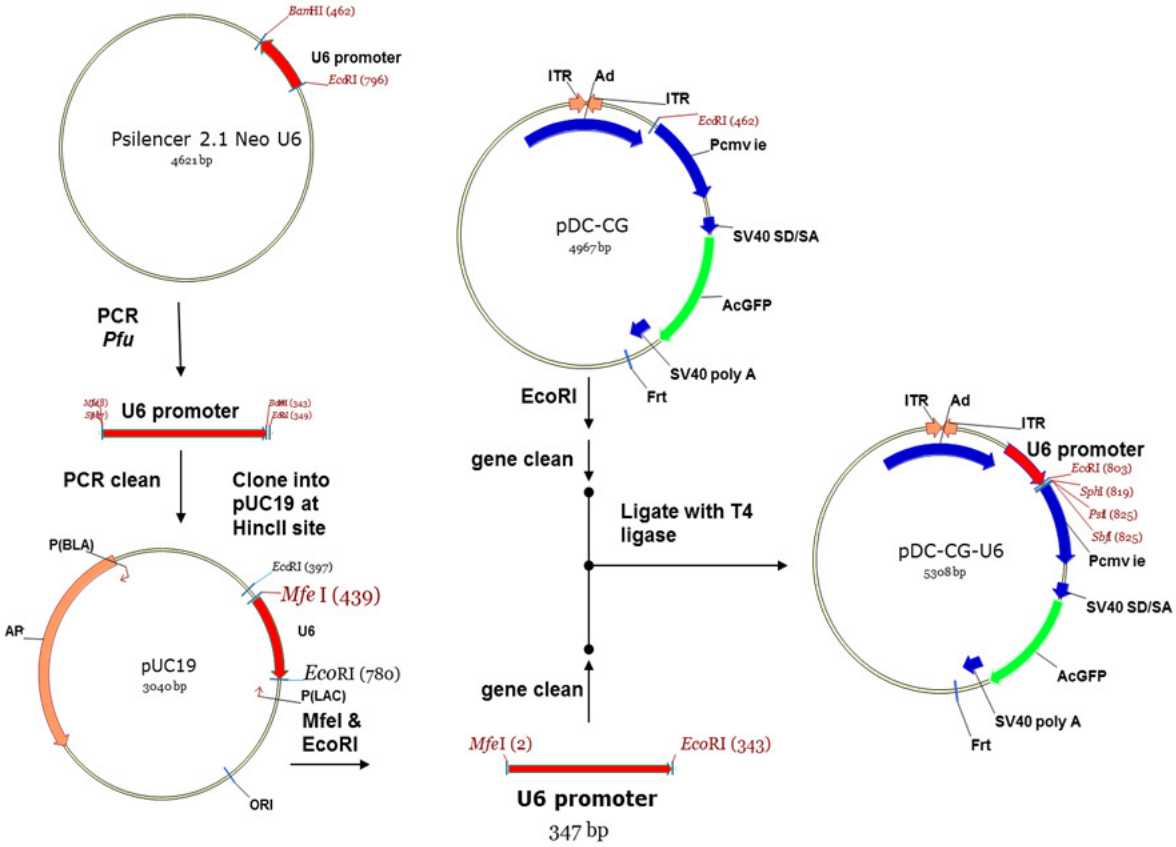

Figure 1.3: Design scheme used for the construction of the pDC-CG-U6 vector for expression of shRNAs and AcGFP. The RNA Pol III promoter, U6, was amplified by PCR from a commercially available vector (pSilencer 2.1 Neo U6, Ambion) and subsequently cloned into the pUC19 vector. Primers were flanked by recognition sequences for *Mfe* I and *Eco* RI (5` to 3`) which facilitated excision of the promoter from pUC19 and its insertion into an *Eco* RI site in the pDC-CG vector.

The resultant vector pDC-CG-U6 was confirmed by PCR (Fig. 4A), restriction enzyme digestion (Fig. 4B) and sequencing (Fig. 5).

A

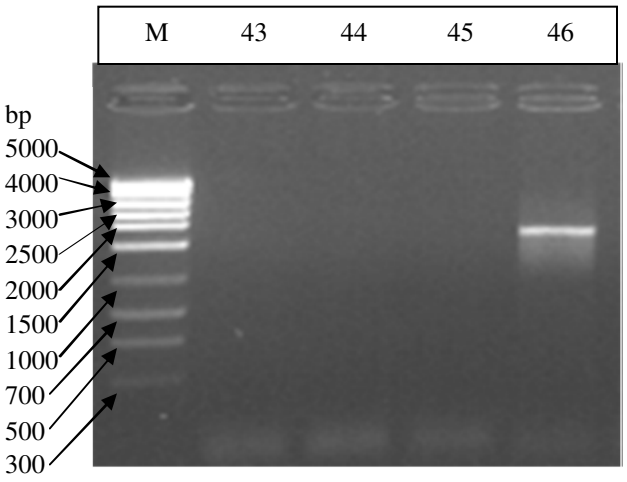

B

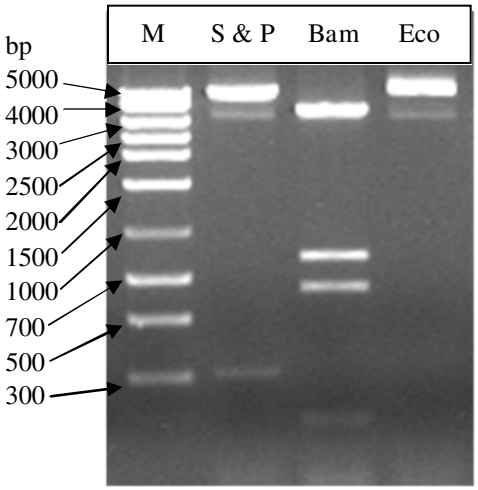

Figure 1.4: A) Screening for U6 promoter in the pDC-CG vector from *E. coli* DH5α colonies by end point PCR. Amplicon size from clone 46 was 1660 bps, confirming a single insertion of the promoter in the correct orientation. B) Confirmation of pDC-CG-U6 by restriction enzyme digestion. *Sph* I and *Pml* I (S & P) double digestion produced expected fragments of 4992 and 316 bps; digestion with *Bam* HI (Bam) produced expected visible fragments of 3570 bps, 809 bps, 635 bps, and 198 bps; digestion with *Eco* RI (Eco) linearized the vector and produced a single band on the gel corresponding to 5308 bps, or full length of the pDC-CG-U6.

5`.ggcatgcaattgcccccagtggaaagacgcgcaggcaaaacgcaccaggtgacggagcgtgaccgcgcgccgagcgcgcgccaaggtcg
ggcaggaagagggcctatttcccatgattccttcatatttgcatatacgatacaaggctgttagagagataattagaattaatttgactgtaaaca
caaagatattagtacaaaatacgtgacgtagaaagtaataatttcttgggtagtttgcagttttaaaattatgttttaaaatggactatcatatgctt
accgtaacttgaaagtatttcgatttcttgggtttatatatcttgtggaaaggacgcgggatccgaattcg. 3`

Figure 1.5: Full length sequence of the U6 RNA Pol III promoter confirmed by sequence analysis to be 100% identical to the insert in pDC-CG-U6.

1.3.2.2 Design and incorporation of EndoG-targeting shRNA templates into pDC-CG-U6

We made use of *Eco* RI and *Pst* I recognition sites immediately downstream of the U6 promoter to insert templates for shRNA expression (Fig. 1.6A). In total, seven plasmids based on the same backbone of pDC-CG-U6 were constructed, but each of the plasmids encoded a different shRNAs (Fig. 1.6B). Six of these plasmids carried templates for shRNAs directed against EndoG mRNA (from Fig. 1.1) and one was a negative control that encoded a non-targeting shRNA. Plasmids that carried shRNAs targeting EndoG were named p1 through p6, reflecting the relative positions (5` to 3` direction) of the sequence they targeted on the EndoG mRNA and the negative control plasmid was named pNC. All of the constructed plasmids were confirmed by DNA sequencing.

A

B

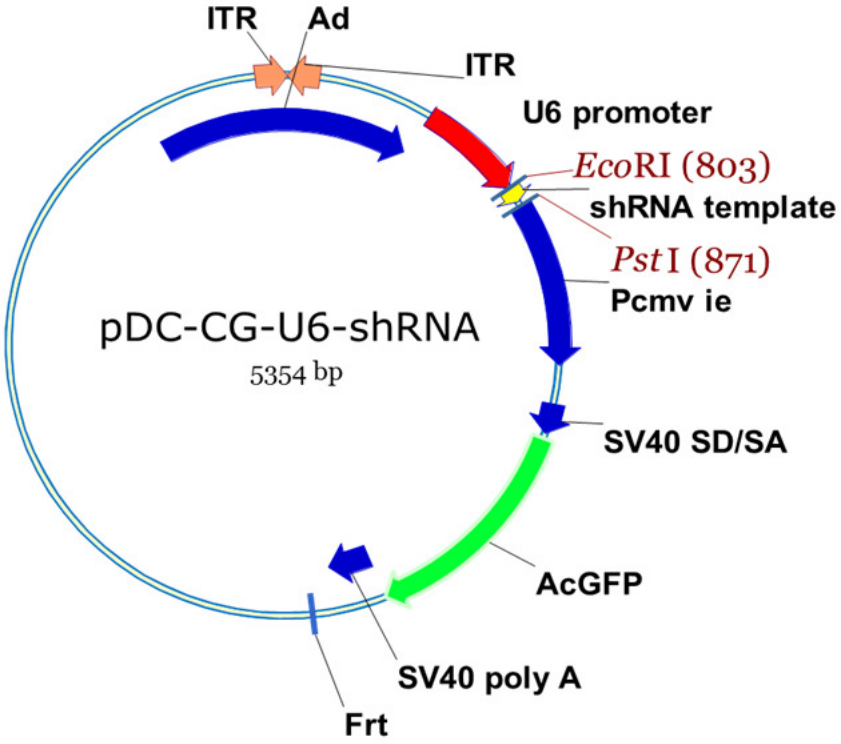

Figure 1.6: A) Representative shRNA template inserted between the *Eco* RI and *Pst* I sites of pDC-CG-U6, immediately downstream of the U6 promoter. In the example, shRNA is targeted at nucleotide 644 of EndoG mRNA. B) Representative map of pDC-CG-U6 showing (in yellow) the position of the inserted shRNA template downstream of the U6 promoter (red). Seven plasmids (p1 – p6 and pNC) were made, six of which carried shRNAs targeting EndoG and one negative control.

1.3.3 – Evaluating stability of plasmid DNA carrying shRNAs directed against 6 regions of EndoG mRNA

1.3.3.1 Relative cellular abundance of pDNA over time after transfection of sub-confluent HeLa cells

As described in the previous section, seven plasmids that were based on the pDC-CG-U6 backbone were constructed, six of which encoded a unique shRNA targeting EndoG mRNA (p1 through p6) and a negative control plasmid (pNC), which encoded an shRNA without a complement in the human transcriptome. In order to assess their relative stability in replicating mammalian cells, we transfected these plasmids into sub-confluent HeLa cells and then monitored their levels at 24-hour intervals over the next four days. We used a cationic liposome transfection reagent (Lipofectamine 2000, Invitrogen) and replaced the medium 6 hours after starting transfection. For the transfection, we used 200 ng of each plasmid per well of 40-50% confluent HeLa cells, cultured in 24-well standard tissue culture plates. Each plasmid was transfected into 15 well of cells in order to assay triplicate samples at each time point tested: 2, 24, 48, 72, and 96 hours post-transfection. In total, 105 individual samples were assayed.

The DNA that was isolated from each sample was analyzed by qPCR in two separate reactions. In one, primers specific for the backbone of the transfected pDNA were used, whereas in the other primers for the cellular 5S rRNA gene were used. Relative pDNA abundances were inferred using the equation 2^(Ct, 5S – Ct, pDNA), where Ct, 5S represents the threshold cycle of the PCR using 5S-specific primers and Ct, pDNA represents the threshold cycle of the PCR using pDNA-specific primers from a single

sample. The relative pDNA abundances, normalized with the 5S gene were plotted in Figure 1.7, allowing for inter-sample comparison.

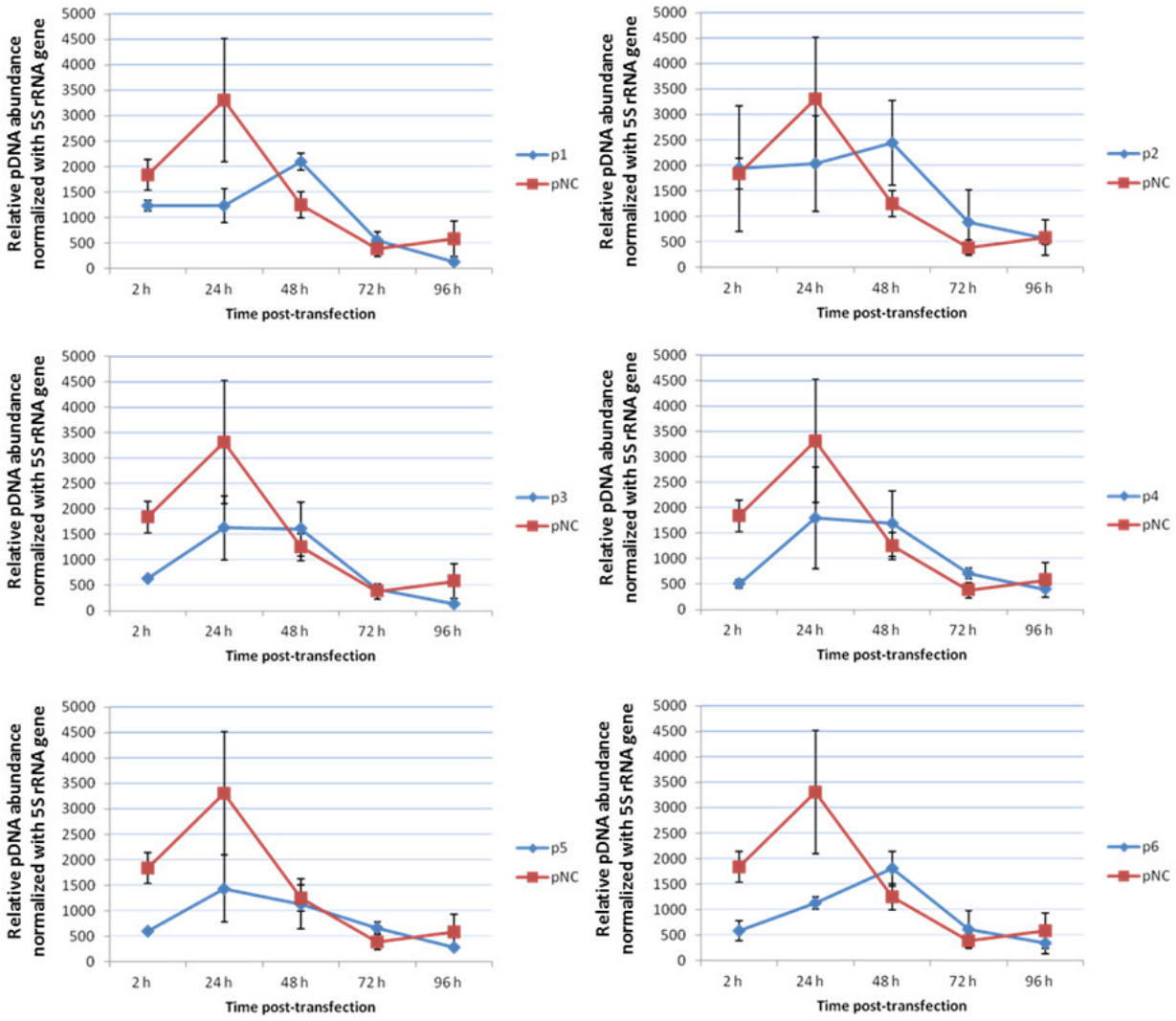

Figure 1.7: Effect of EndoG targeting on pDNA stability. Relative cellular abundance of test plasmids (p1 through p6, in blue) and the negative control plasmid (pNC, in red) at 2, 24, 48, 72 and 96 hours after transfection of 40-50 % confluent HeLa cells (cultured in 24-well plates) with 200 ng of each plasmid. Levels were measured by quantitative PCR using the cellular 5S rRNA gene for normalization. Values on x-axis are not indicative of actual pDNA copies, as they were inferred based on the equation 2^(Ct, 5S – Ct, pDNA), where Ct, 5S represents the threshold cycle of the PCR using 5S-specific primers and Ct, pDNA represents the threshold cycle of the PCR using pDNA-specific primers from a single sample. Therefore, the x-axis represents relative values of normalized plasmid abundances that allowed for inter-sample comparison. Error bars indicate SD.

The control vector (pNC) showed a time-dependent decrease with respect to cellular DNA (5S gene) after reaching peak levels at 24 hours post-transfection (Fig. 1.7). This indicated a loss of pDNA copy number from transfected cells, assuming that 5S rRNA gene content was correlated to cell number. It is important to note that cellular gene content may not have correlated exactly to the cell number due to the possibility of unequal cellular DNA replication rates.

The observed decrease of relative pNC abundance was greatest between 24 and 48 hours post-transfection (Table 1.2). In contrast, test plasmids did not show an equivalent drop in copies, relative to cellular DNA, between these two time points (24 and 48 hours) (Fig. 1.7, Table 1.2). Relative plasmid abundance for test plasmids either did not change during this window (p2, p3, p4, and p5) or actually increased (p1 and p6) (Table 1.2).

Table 1.2 – Ratios of relative cellular abundances of test and control pDNA vectors between 48 and 24 hours post transfection (p.t.) of sub-confluent HeLa cells. The greatest difference was observed for pNC, where the ratio is 0.38 compared to ~1 for the test pDNA vectors (p1 through p6).

pDNA vector	Relative cell. abundance of pDNA at 48 h p.t./Relative cell. abundance of pDNA at 24 h p.t.
p1	1.70
p2	1.20
p3	0.99
p4	0.94
p5	0.79
p6	1.60
pNC	**0.38**

Differences between the relative pDNA abundances of test and control vectors were also observed at 2 at 24 hours post-transfection. Due to the time-frame required for shRNA

expression and action it is unlikely these effects were related to EndoG-targeting and they were most likely the result of variable transfection efficiencies (not assayed) between individual plasmids, which was expected considering the transfection procedure used.

1.3.3.2 Abundance of pDNA over time after transfection of sub-confluent HeLa cells without cellular normalization

The relative pDNA abundance in each sample of transfected cells was also examined without normalizing with the 5S rRNA cellular gene in order to eliminate any effects that unequal replication of cellular DNA may have on the perceived pDNA stability. In addition, this eliminated the effects of dilution by mitosis on perceived pDNA stability and allowed for examining the "absolute" plasmid abundance per well of transfected HeLa cells (Fig. 1.8).

Briefly, for each sample, regardless of condition or time-point assayed, DNA was extracted from the entire population of HeLa cells growing in a single well. Equal proportions of each DNA sample were interrogated by qPCR using primers specific for the transfected pDNA backbone and the relative abundance of pDNA in each sample was inferred by the equation 2^-Ct, pDNA, where Ct, pDNA represents the threshold cycle of the reaction. The calculated pDNA abundance for each sample was representative of the absolute amount of pDNA in a single well of HeLa cells. Therefore, the values generated were used to compare relative pDNA abundance per well of transfected cells between different conditions and time-points.

We observed that the abundance per well (or the absolute quantity) of the negative control plasmid (pNC, in red) decreased between 24 and 48 hours, whereas it remained

constant for all of the test plasmids (p1 through p6, in blue) (Fig. 1.8, Table 1.3). These results indicated that pNC was lost from the transfected HeLa cells, rather than diluted, whereas the EndoG-targeting plasmids were neither diluted nor lost between 24 and 48 hours post-transfection of sub-confluent HeLa cells (Table 1.2, Table 1.3).

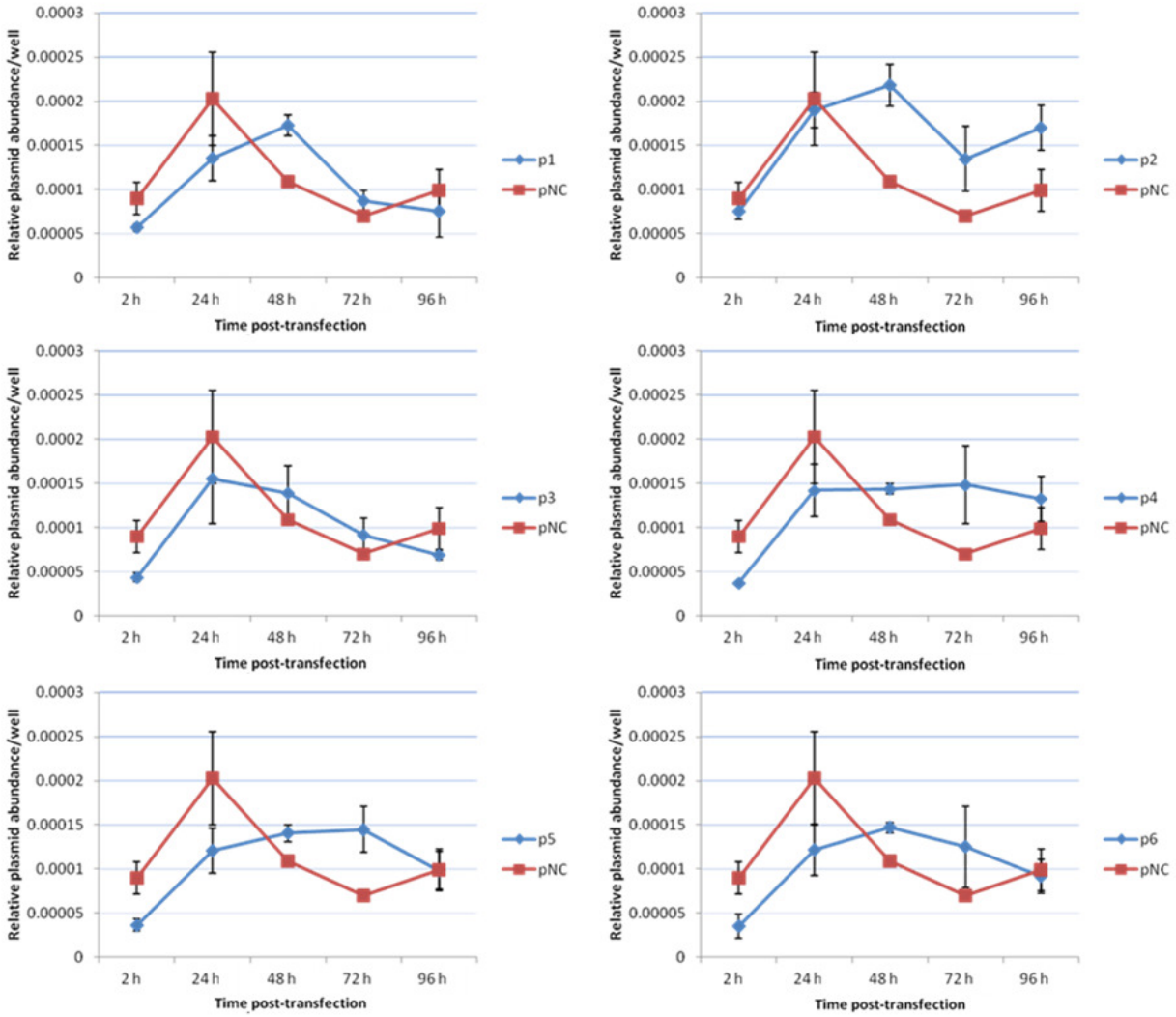

Figure 1.8: Effect of EndoG targeting on pDNA stability disregarding normalization of data against cellular DNA. PCR quantification of plasmid DNA in each well of transfected cells (p1 through p6, in blue and pNC, in red), disregarding normalization with cellular DNA, at 2, 24, 48, 72 and 96 hours after transfection of 40-50 % confluent HeLa cells (cultured in 24-well plates) with 200 ng of each plasmid. The abundance of pDNA in each sample was inferred by the equation 2^-Ct, pDNA, where Ct, pDNA represents the threshold cycle of the PCR using pDNA-specific primers. The calculated pDNA abundance for each sample was representative of the absolute amount of pDNA in a single well of HeLa cells, although the values on x-axis are relative and not indicative of actual pDNA copies. Error bars indicate SD.

Table 1.3 - Ratios of absolute abundances of test and control pDNA vectors between 48 and 24 hours post transfection (p.t.) of sub-confluent HeLa cells. The greatest difference was observed for pNC, where the ratio is 0.54 compared to ~1 for the test pDNA vectors (p1 through p6).

pDNA vector	Abs. pDNA abundance at 48 h p.t./Abs. pDNA abundance at 24 h p.t.
p1	1.28
p2	1.15
p3	0.89
p4	1.01
p5	1.16
p6	1.21
pNC	**0.54**

1.3.3.3 Relative cellular abundance of pDNA over time after transfection of near-confluent HeLa cells

To test whether the observed difference in stability between plasmids carrying shRNAs directed against EndoG and the negative control plasmid was dependent on initial cell density at the time of transfection reagent exposure, we repeated the above described experiment in near-confluent HeLa cells. Also, for this experiment we reduced the pool of plasmids carrying shRNAs against EndoG to two (p2 and p6), while using the same negative control plasmid (pNC), in order to reduce sample handling (from 105 samples to 36). Plasmids p2 and p6 were chosen because they encoded shRNAs against discrete regions of EndoG mRNA that were separated by 344 nucleotides. In addition, we did not assay past 72 hours to avoid excessive necrotic cell death.

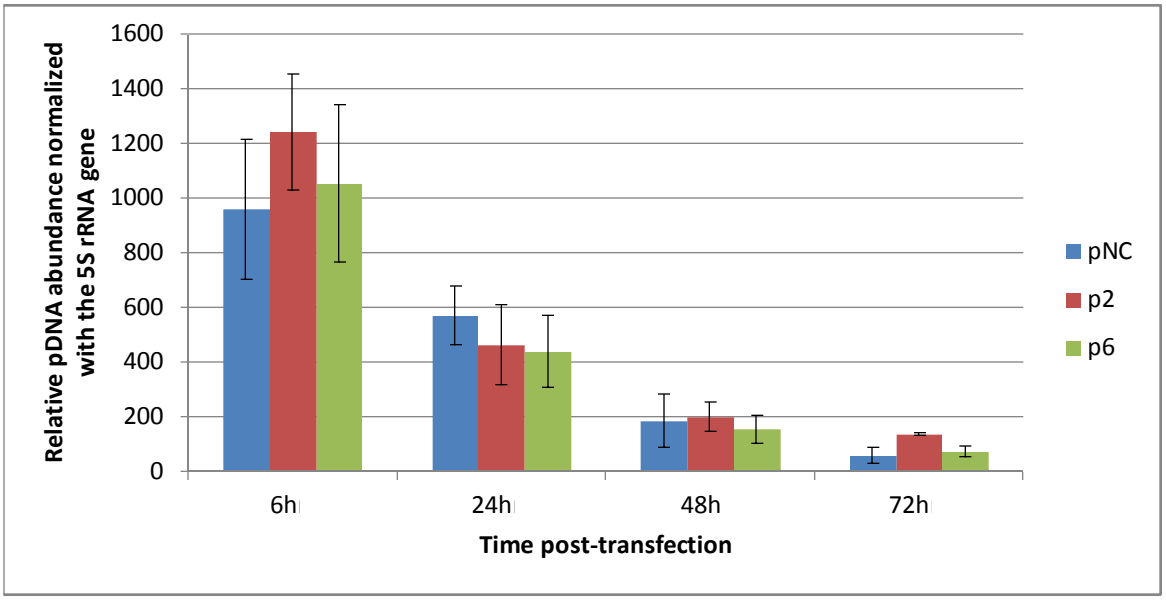

Figure 1.9: Effect of EndoG targeting on pDNA stability following transfection of near-confluent cells. Relative abundance of plasmids pNC, p2 and p6 at 2, 24, 48 and 72 hours after transfection of near-confluent HeLa cells (cultured in 6-well plates) with 4 µg of each plasmid. Levels were measured by quantitative PCR using the 5S gene for normalization. All plasmids showed similar abundance levels at each time point assayed. All plasmids showed a time dependent decrease in copy number. Error bars indicate SD.

The reasoning for repeating the experiment in HeLa cells that were near-confluent at time of transfection, as opposed to sub-confluent, was the observation that cells seeded at a lower density at the outset of the experiment were more sensitive to the cytotoxicity of the cationic liposome transfection reagent (Lipofectamine2000, Invitrogen). These effects are illustrated in Figure 1.16, where it is clear that sub-confluent HeLa cells do not proliferate normally up to 48 hours following treatment with the transfection reagent.

As we can see from Figure 1.9, when near-confluent cells were transfected, the plasmid abundances, relative to the cellular 5S rRNA gene, were similar between all three vectors (pNC, p2 and p6), regardless of encoded shRNAs, and decreased in a time-dependent fashion. No differences in pDNA stability between test and control pDNA vectors were observed during the period between 24 and 48 hours following transfection (Table 1.4). This result was in direct contrast to the previous observation made from the experiment on HeLa cells that were sub-confluent at time of transfection. This indicated that cell density was an important factor in determining whether targeting of EndoG had a positive or neutral effect on pDNA stability.

Table 1.4 – Ratios of relative cellular abundances of test (p2 and p6) and control pDNA vectors between 48 and 24 hours post transfection (p.t.) of near-confluent HeLa cells. The test vector p6 and the control pNC showed equivalent decreases between 24 and 48 hours following transfection.

pDNA vector	Relative cell. abundance of pDNA at 48 h p.t./Relative cell. abundance of pDNA at 24 h p.t.
p2	0.43
p6	0.35
pNC	0.33

1.3.4 – Evaluating transgene expression from plasmids carrying shRNAs directed against EndoG mRNA in HeLa cells sub-confluent at time of transfection

1.3.4.1 *Relative expression of GFP reporter gene normalized with cellular mRNA*

To evaluate reporter gene GFP expression in cells transfected with test and negative control plasmids, RNA that was isolated from HeLa cell monolayers was subjected to a reverse transcriptase (RT) reaction to generate cDNA and subsequently amplified by qPCR, using primers specific for the GFP transcript. GFP expression was normalized with the expression of the ribosomal protein S15 cellular gene in each sample, using the equation 2^(Ct, S15 – Ct, GFP) and the resultant values plotted in Figure 1.10.

Reporter gene expression was higher in cells transfected with test plasmids (p1 – p6) at 24 and 48 hours post transfection, relative to cells transfected with the negative control plasmid (pNC) when expression was normalized with the expression of a cellular housekeeping gene (S15) (Fig. 1.10).

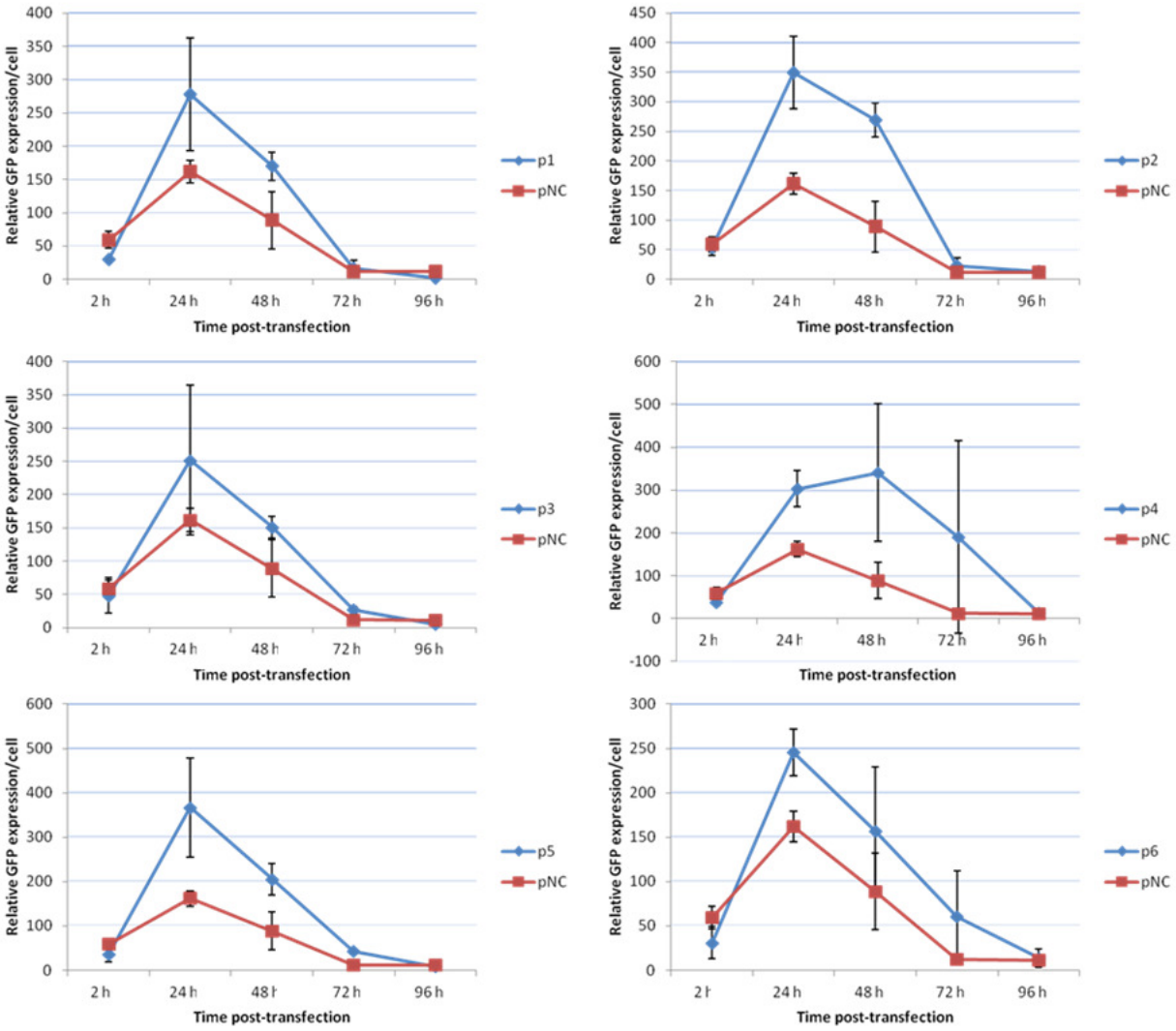

Figure 1.10: Effect of EndoG targeting on reporter gene expression. Relative GFP expression in cells transfected with the negative control plasmid (pNC) and test plasmids (p1 - p6) assayed at 24 hour intervals over four days. Levels of GFP mRNA were measured by RT-qPCR and normalized with the expression of the S15 gene using the equation 2^(Ct, S15 – Ct, GFP). Error bars indicate SD.

1.3.4.2 Relative expression of GFP reporter gene normalized with cellular mRNA and against cellular pDNA abundance

To compare the levels of GFP expression with respect to the levels of intracellular pDNA that encoded the transgene, GFP mRNA expression was normalized with pDNA abundance using matched RNA and DNA samples isolated from a single well of transfected HeLa cells. The equation used for calculating relative GFP mRNA expression values was 2^[(Ct, S15 – Ct, GFP) – (Ct, 5S – Ct, pDNA)], where Ct, "sequence name" represents the threshold cycle of each qPCR using primers specific for S15 and GFP cDNAs, the transfected pDNA backbone and the cellular 5S rRNA gene.

As we can see from Figure 1.11, all test plasmids (in blue) expressed more GFP mRNA per plasmid copy relative to the negative control plasmid (in red) at 24 hours post transfection. Furthermore, GFP mRNA expression with respect to plasmid copy number reached its peak at 24 hours post transfection in cells transfected with plasmids carrying shRNA against EndoG, which was not the case in cells transfected with the negative control plasmid (pNC). It is also important to note that GFP expression did not differ between EndoG-targeting plasmids, p2 or p6, and the negative control plasmid, pNC, at any of the assessed time-points following transfection of near-confluent HeLa cells (data not shown).

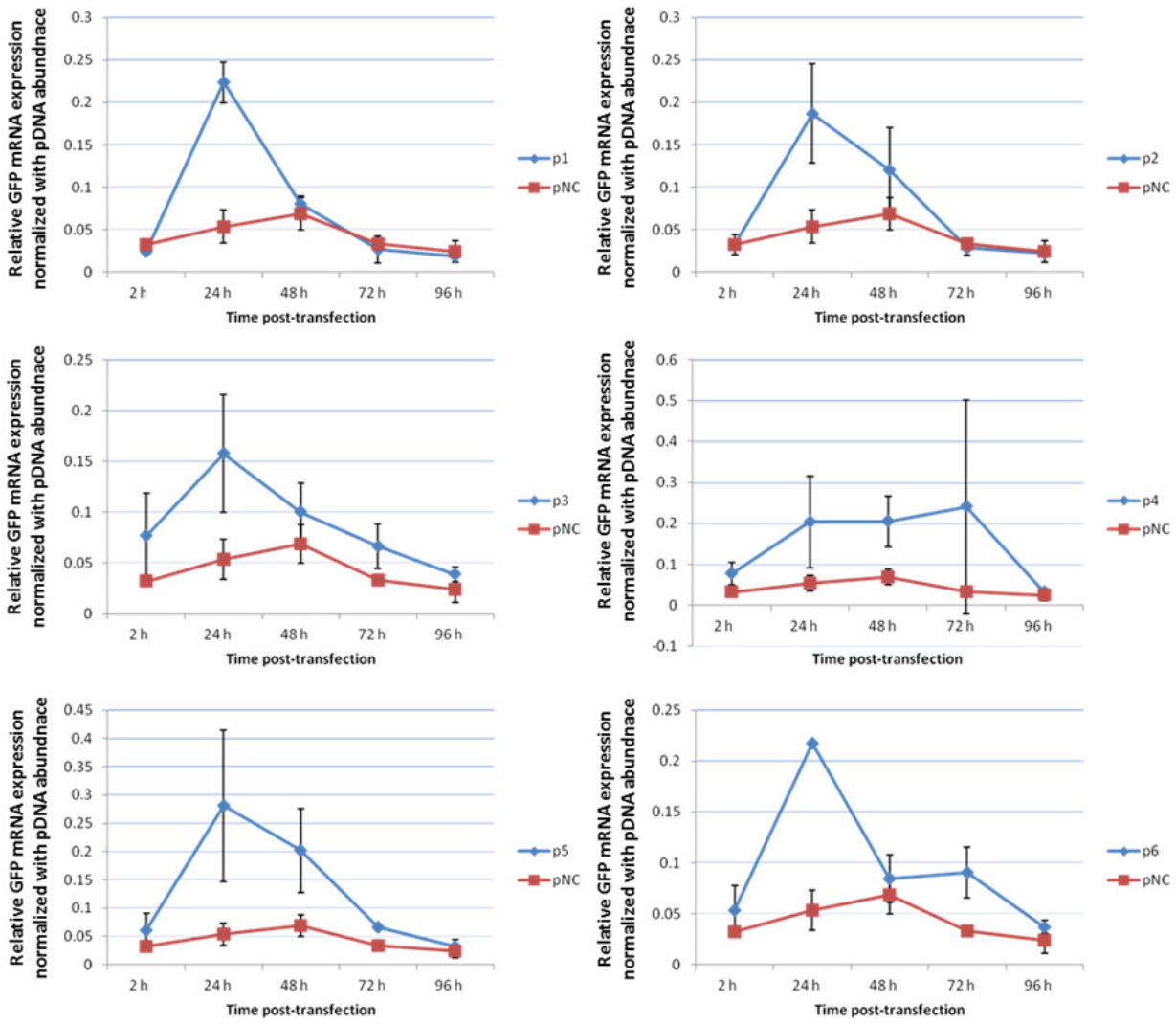

Figure 1.11: Effect of EndoG targeting on reporter gene expression normalized against pDNA abundance. Relative GFP mRNA expression normalized against plasmid abundance for the negative control plasmid (pNC) and test plasmids (p1 - p6) assayed at 24-hour intervals over four days. Levels of GFP mRNA were measured by RT-qPCR and normalized using the expression of the S15 gene and plasmid abundance was normalized using the 5S gene. The equation used for calculating relative GFP mRNA expression values was 2^[(Ct, S15 – Ct, GFP) – (Ct, 5S – Ct, pDNA)]. Error bars indicate SD.

1.3.5 – Evaluating EndoG levels in cells transfected with plasmids carrying shRNAs targeting EndoG

1.3.5.1 Measuring cellular levels of EndoG mRNA in sub-confluent HeLa cells following transfection

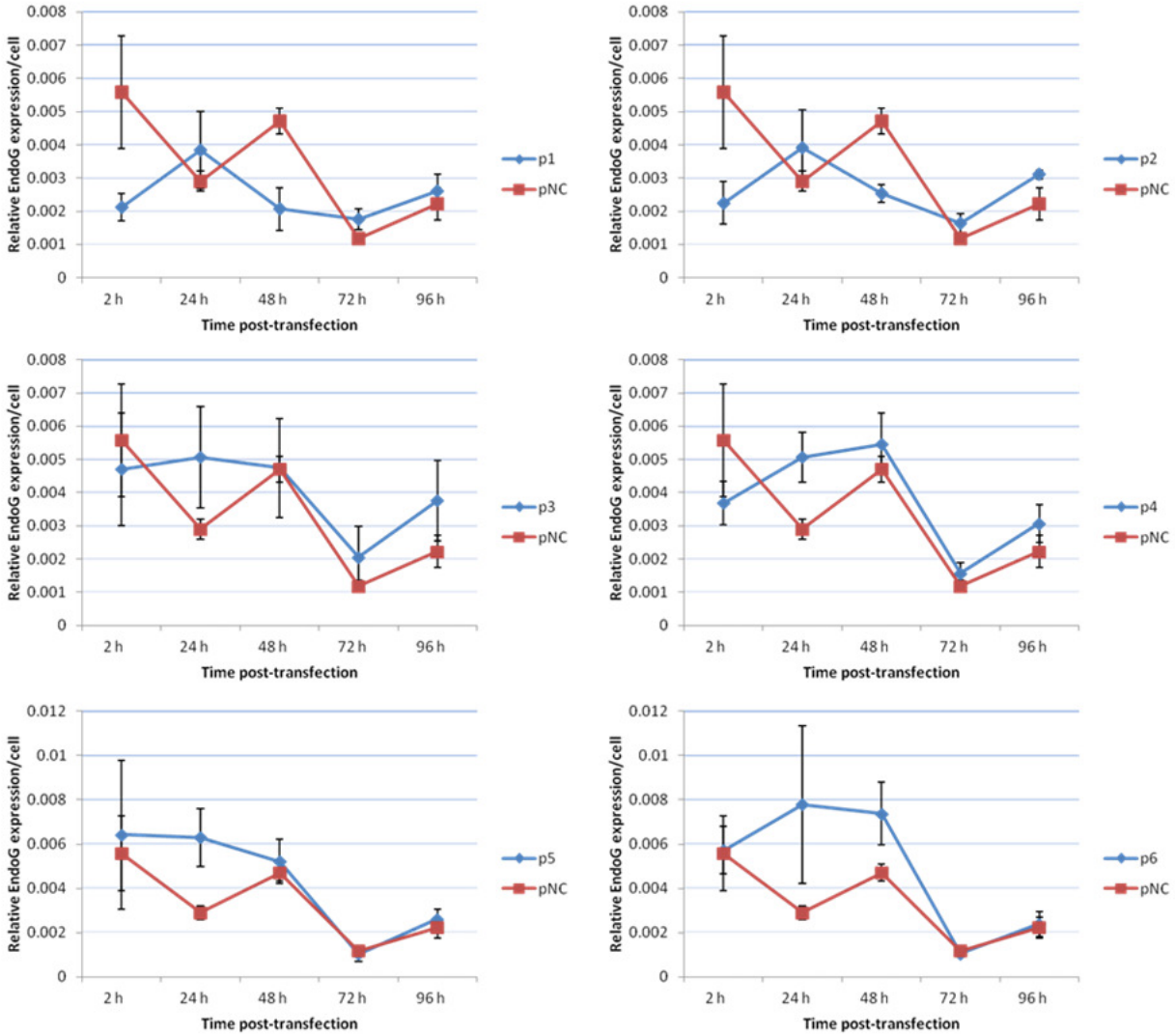

Figure 1.12: Effect of EndoG targeting on cellular EndoG mRNA expression levels. Relative EndoG mRNA expression per cell in cells transfected with the negative control plasmid (pNC) and test plasmids (p1 – p6). Levels of EndoG mRNA were measured by RT-qPCR and normalized with the expression of the S15 gene using the equation 2^(Ct, EndoG – Ct, S15). Error bars indicate SD.

Looking at Figure 1.12, specifically at cells transfected with the negative control plasmid (pNC) it is obvious that EndoG mRNA levels fluctuate somewhat and importantly that they increased between 24 and 48 hours after transfection (Table 1.5). Conversely, EndoG levels decreased during that same period (below those observed for the negative control) in cells transfected with test plasmids p1 and p2, confirming the EndoG knockdown (Fig. 1.12). Interestingly, in cells transfected with test plasmids p3, p4, p5 and p6 the levels of EndoG mRNA appeared to be higher than in cells transfected with the negative control at 24 hours post transfection and they were more or less equal subsequently. However, even in cells transfected by these test plasmids, EndoG levels did not change between 24 and 48 hours post-transfection, whereas they increased in cells that were transfected with the negative control plasmid (Table 1.5). Therefore, EndoG mRNA was upregulated following transfection of pNC into sub-confluent HeLa cells.

Table 1.5 - Ratios of EndoG mRNA expression between 48 and 24 hours post transfection (p.t.) of sub-confluent HeLa cells with test (p1 through p6) and control pDNA vectors. Cells transfected pNC show upregulation of EndoG between these time points, an effect that is absent from cells transfected with EndoG-targeting vectors.

pDNA vector	EndoG mRNA exp. at 48 h p.t./EndoG mRNA exp. at 24 h p.t.
p1	0.53
p2	0.64
p3	0.93
p4	1.07
p5	0.82
p6	0.94
pNC	**1.62**

1.3.5.2 Measuring cellular levels of EndoG mRNA in near-confluent HeLa cells following transfection

Levels of EndoG mRNA decreased in near-confluent HeLa cells transfected with plasmids carrying EndoG targeting shRNAs (p2 and p6) relative to control, which started at 24 hours and continued until the end of the experiment (Fig. 1.13). Importantly, transfection of the negative control plasmid into near-confluent HeLa cells did not result in an associated increase in EndoG mRNA between 24 and 48 hours post-transfection, which was observed following transfection of sub-confluent HeLa cells. Therefore, EndoG mRNA upregulation was specific to the transfection of pNC into sub-confluent HeLa cells.

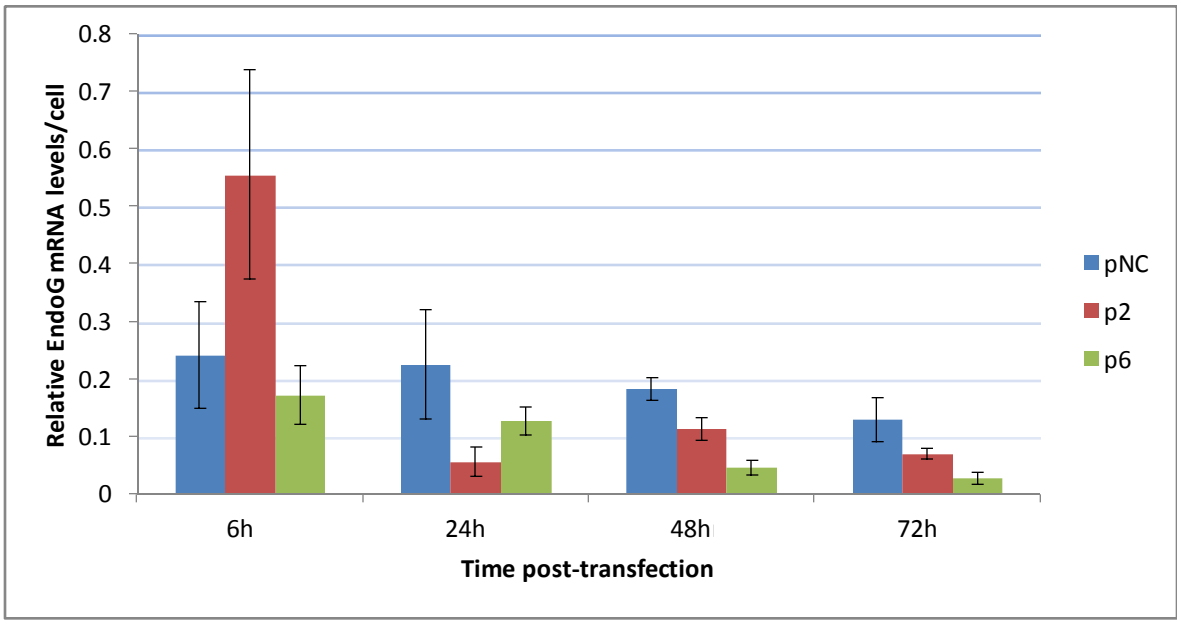

Figure 1.13: Effect of EndoG targeting on cellular EndoG mRNA expression levels following transfection of near-confluent cells. Relative EndoG expression in cells transfected with pNC, p2, and p6 assayed at 24 hour intervals over three days. Levels of EndoG mRNA were measured by RT-qPCR and normalized using the expression of the S15 gene. EndoG mRNA levels in cells transfected p2 and p6 are detectably lower at 24, 48 and 72 hours post-transfection. Error bars indicate SD.

1.3.5.3 Measuring EndoG activity in cells transfected with plasmids carrying shRNAs against EndoG mRNA

Incubation of plasmid DNA target (linearized pDNA sequence) with cell extracts of cells transfected with either of the p6 (Figure 1.14) or p2 (Figure 1.15) test plasmids resulted in a decrease in target DNA degradation relative to cell extracts isolated from cells transfected with the negative control plasmid (pNC). This showed that nuclease activity was suppressed in cell extracts transfected with p6 or p2.

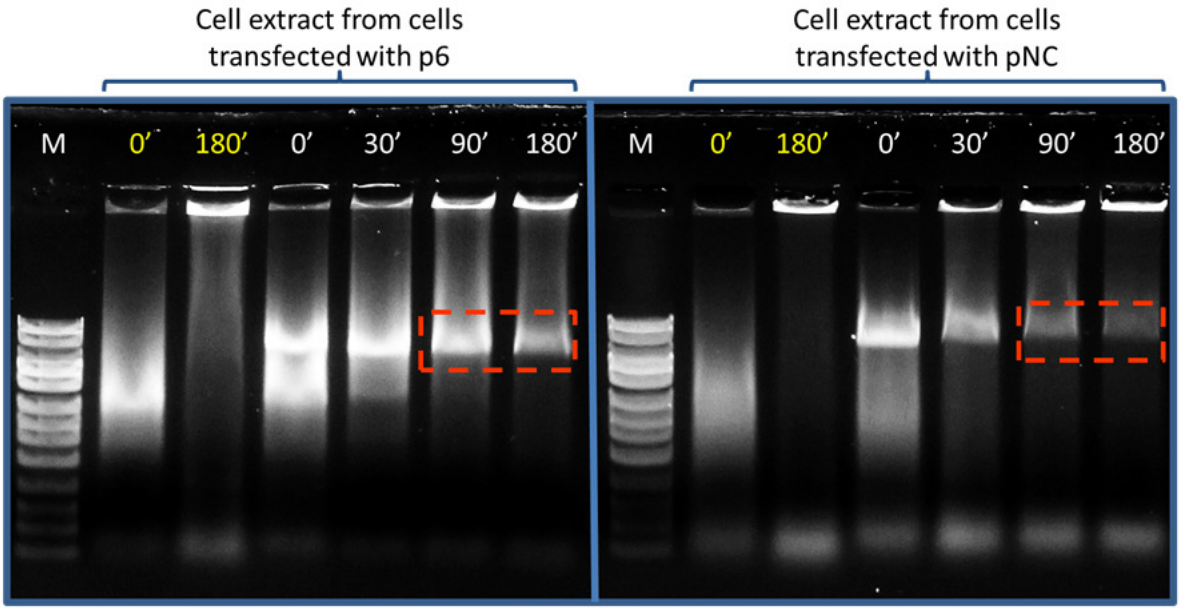

Figure 1.14: Effect of EndoG targeting on nuclease activity in cell extracts. One µg of linearized plasmid target was incubated with 20 µg of total protein from cell extracts of cells transfected with p6 (left) or pNC (right) for 0, 30, 90, or 180 minutes at 37°C. Ten uL of each 50 µL reaction was loaded on a 1% DNA agarose gel. Each reaction was supplemented with 1mM $MgCl_2$. Target pDNA is more intact after incubation with cell extracts from cells transfected with p6 than pNC. Samples not spiked with plasmid target (in yellow) were also incubated for 180 minutes, showing similar results.

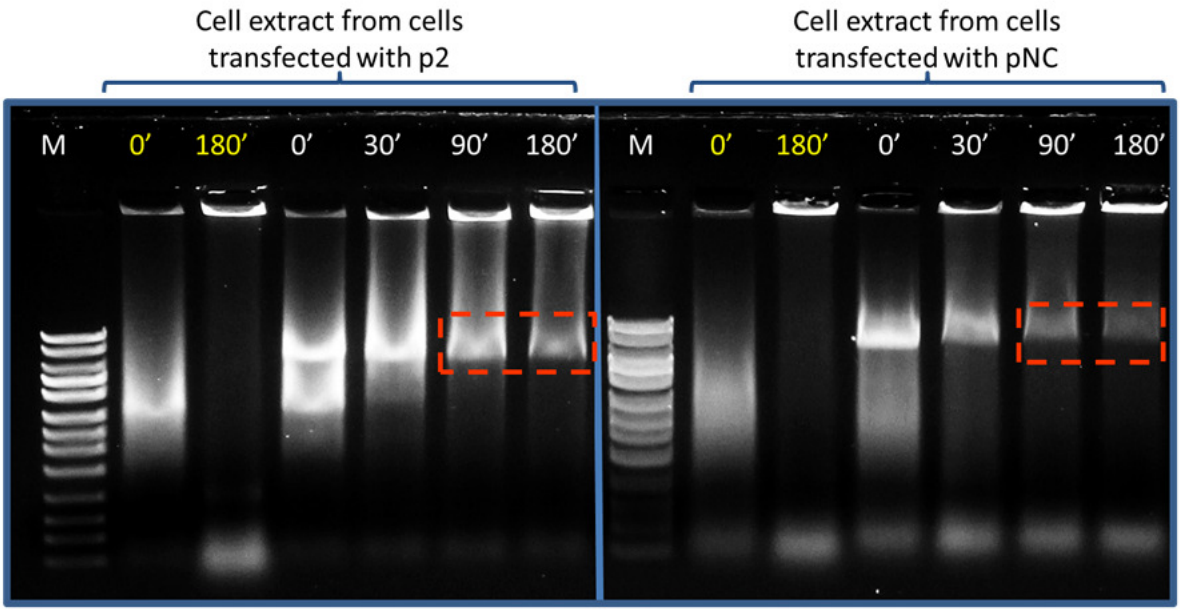

Figure 1.15: Effect of EndoG targeting on nuclease activity in cell extracts. One µg of linearized plasmid target was incubated with 20 µg of total protein from cell extracts of cells transfected with p2 (left) or pNC (right) for 0, 30, 90, or 180 minutes at 37°C. Ten uL of each 50 µL reaction was loaded on a 1% DNA agarose gel. Each reaction was supplemented with 1mM $MgCl_2$. Target pDNA is more intact after incubation with cell extracts from cells transfected with p2 than pNC. Samples not spiked with plasmid target (in yellow) were also incubated for 180 minutes, showing similar results.

1.3.6 – Measuring cellular growth rate following transfection of sub-confluent HeLa cells

To assess whether targeting of EndoG protected cells from the cytotoxicity of the cationic liposome transfection reagent, we measured HeLa cell proliferation (Fig. 1.16) over a four day time course following transfection with the EndoG-targeting plasmid, p6, or the negative control plasmid pNC. In both transfection conditions the cell numbers did not increase between the start of the experiment and 48 hours after transfection, which differed from the climbing trajectory observed over the following two days. There were no significant differences in cell numbers at any of the points assayed, however it is important to note that results from Chapter II of this study showed that EndoG-silencing induced a cell proliferation defect in HeLa, which may have masked any protective effects.

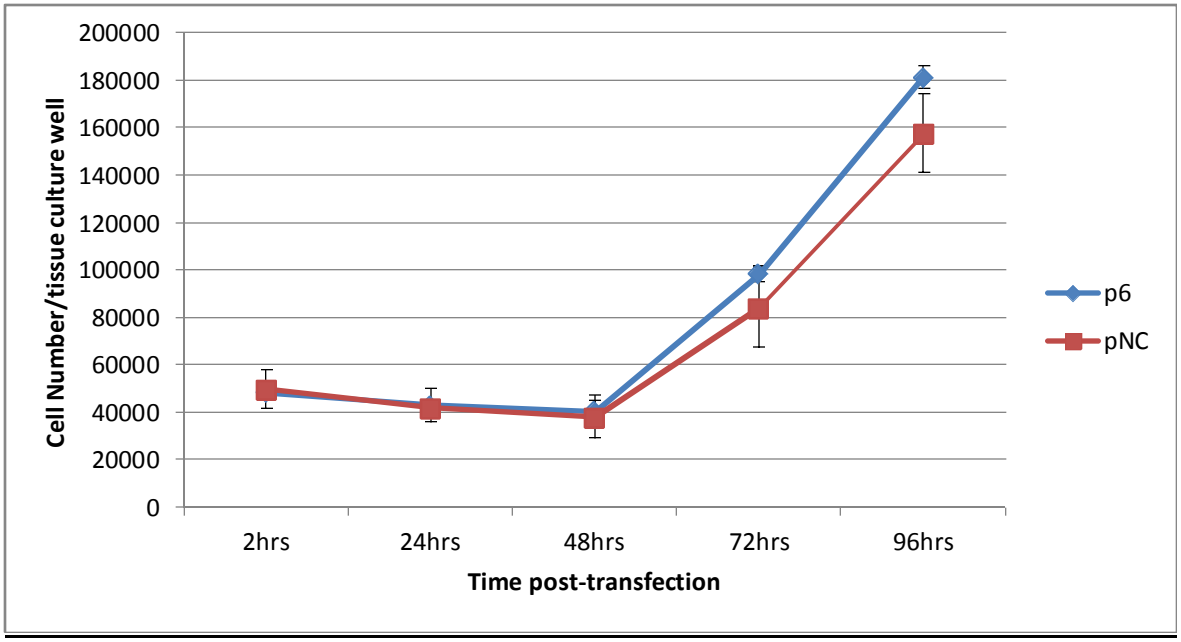

Figure 1.16: Effect of EndoG targeting on cellular growth following transfection of sub-confluent cells. Cell counts of HeLa cells cultured in triplicate wells of a 24-well tissue culture plate after transfection with 400ng of EndoG-targeting (p6) or negative control (pNC) plasmids using Lipofectamine 2000 as a transfection reagent.

1.4 Discussion

The mitochondrial enzyme EndoG has so far been investigated mostly in the context of its role in apoptotic cell death, although it has also been implicated in a number of vital biological functions (Huang et al, 2002; Huang et al, 2006; Buttner et al., 2007a,b; Buzder et al., 2009; McDermott et al., 2011; Zan et al., 2011). Most of the proposed vital functions of EndoG require its nuclease action inside nuclei of healthy, non-apoptotic cells. Since exogenous DNA occupies the same intranuclear environment as the host genomic DNA, the aim of this study was to investigate whether EndoG is a cellular defence enzyme, involved in exogenous DNA stability and hence expression of genes encoded on that DNA. Specifically, we tested the effects of EndoG depletion on plasmid DNA abundance and transgene expression in replicating mammalian cells (HeLa).

The strategy for this study was to assay plasmid stability within a four day time course in cellular backgrounds that either have wildtype (normal) or reduced levels of EndoG. Unfortunately, overexpression of EndoG was not an option due to the endogenous cytotoxicity of the mature form of EndoG, which non-specifically degrades genomic DNA and kills the cell (Winnard et al., 2008). In addition, transfection of pDNA into cellular backgrounds that have different EndoG levels at outset of experiment was also not considered since EndoG has previously been reported to reduce transfection efficiency of mammalian primary and epithelial cells (Buzder et al., 2009).

To avoid any effects that transfection efficiency, and hence initial cellular abundance of plasmid DNA, could have on its perceived longitudinal stability, the experimental design was appropriately tailored to synchronize delivery of pDNA with an effector of EndoG

silencing. For this purpose, templates for shRNAs that specifically target six distinct sequences in the coding region of EndoG mRNA were designed and separately engineered into the assay pDNA vectors, along with a template for an shRNA that did not have a complement in the human transcriptome. Probing of multiple target sites was done to ensure silencing, as there may be some heterogeneity with respect to silencing efficiencies based on sequence and location of target (Gavrilov and Saltzman, 2012).

Apart from shRNA cassettes, all assay pDNA vectors shared an identical backbone that included a cassette for the expression of a GFP reporter gene, under the control of the CMVie enhancer/promoter. All pDNA vectors were independently transfected into sub-confluent HeLa cells using a cationic liposome transfection reagent (Lipofectamine 2000, Invitrogen). Low initial seeding density ensured that cells could replicate for the entire duration of the four-day time course without constraints imposed by the surface area of the tissue-culture dish, as HeLa cells grow in a strict monolayer and are contact inhibited (Heacock et al., 1984).

At each time point (24 hour interval), plasmid stability was assayed by quantitative PCR and the comparative threshold method was used to infer relative plasmid abundance per cell, using a cellular gene for normalization. Although transfection efficiency was not assayed, it is probable that two subpopulations of cells were present in each tissue-culture well, regardless of plasmid used: cells that took up the plasmid and those that did not. Replication of both subpopulations of cells resulted in an increase in cell number over time, whereas plasmid vectors, which cannot replicate in HeLa, or any other mammalian cells, could not follow suit (Middleton and Sugden, 1994). Therefore, the ratio of plasmid

to cellular DNA was lowest at the conclusion of the four-day time-course due to simple dilution by mitosis for all plasmids, regardless of EndoG-targeting.

Interestingly, plasmids that encoded shRNAs targeting EndoG mRNA, showed a dissimilar pattern of time-dependent cellular abundance relative to non-targeting control plasmid at 24 and 48 hours post-transfection, but were similar thereafter. The relative cellular abundance of EndoG-targeting plasmids either stayed the same or slightly increased during this interval (24-48 hours post-transfection), while it sharply decreased in the case of the non-targeting control. This may have happened as a consequence of differential degradation of EndoG-targeting and non-targeting pDNA vectors during this time period, but did not exclude other explanations such as differences in replication rates of host cells and/or cell viability (Huang et al, 2006; Li et al., 2001).

If we consider the above described dilution effect, brought on by replication of both transfected and non-transfected cells in each well, as the only factor responsible for the decrease of the ratio between plasmid and cellular DNA, then only the relative number of plasmids should have decreased between time points, but the absolute number of plasmids in a single well should have stayed the same, regardless of cell number. On the other hand, if absolute plasmid abundance decreased between time points, this could not be explained by a dilution effect, but rather pDNA degradation.

In order to test for this, plasmid abundance per well over the entire time course of the experiment was assayed by uncoupling plasmid DNA quantification from normalization with a cellular gene. It was observed that the abundance per well (or the absolute quantity) of the non-targeting control plasmid decreased between 24 and 48 hours,

whereas it remained consistent for all of the EndoG-targeting plasmids. This meant that during this time interval the relative cellular abundance of the non-targeting control plasmid did not decrease as function of simple dilution by mitosis, but much more likely as a consequence of degradation. In contrast, during the same time period the absolute abundance of EndoG-targeting plasmids stayed the same, suggesting a protective effect. Interestingly, as mentioned previously the relative abundance of EndoG-targeting plasmids normalized with cellular DNA also stayed consistent during this window, which implies that the plasmid was not diluted by cellular replication, which would be expected since doubling time of HeLa cells is one day (Meck et al., 1976).

Although EndoG knockdown produced a measurable effect on plasmid stability in HeLa cells, the mechanism behind the observation required further testing. It would have been convenient to assume that EndoG had an effect on plasmid DNA levels by specifically targeting exogenous DNA with its nuclease action, but this assumption failed to consider additional factors. Namely, the transfection reagent used to introduce pDNA into HeLa cells was a cationic liposome (Lipofectamine 2000) the use of which has been experimentally shown to increase cellular levels of reactive oxygen species (ROS), lead to mitochondrial membrane depolarization and release of proapoptotic factors from the mitochondrial intermembrane space (Kongkaneramit et al., 2008; Takano et al., 2003; Aramaki et al., 2000; Aramaki et al., 1999; Iwaoka et al., 2006; Takano et al., 2001).

The main cellular localization of EndoG is in the mitochondrial intermembrane space, from which it is released following apoptotic triggers, such as ROS, that collapse mitochondrial membrane potential (Arnoult et al., 2003; Zhao et al., 2009; Marzetti et al.,

2008; Higgins et al., 2009). Apoptotic triggers also upregulate gene expression of several mitochondria associated proapoptotic factors, including EndoG (Li et al., 2004; Zhao et al., 2009; Zhang et al., 2009; Lee et al., 2008; Mercer et al., 2010; Papa and Germain, 2011; Apostolov et al., 2011; Wu et al., 2010; Mitra et al., 2012; Ho et al., 2009; Yeh et al., 2011). Upon its release from mitochondria, EndoG quickly translocates to the nucleus and degrades DNA in a non-specific fashion (Arnoult et al., 2003; Bahi et al., 2006; Strauss et al., 2008). Therefore, low cell density at the outset of the experiment, which exaggerated cytotoxic effects of Lipofectamine 2000, could have triggered EndoG-dependent cell death in cells that took up plasmid DNA.

Supporting this explanation is the EndoG mRNA expression pattern observed for cells transfected with the EndoG-targeting and non-targeting control plasmids. Namely, between 24 and 48 hours post-transfection, EndoG is upregulated in cells transfected with the non-targeting control plasmid, suggesting a response to an apoptotic trigger, while in cells transfected with EndoG-targeting plasmids this upregulation was not observed, presumably as a consequence of RNAi targeting. This is consistent with previously reported upregulation of EndoG expression as a marker of apoptotic cell death (Li et al., 2004; Zhao et al., 2009; Zhang et al., 2009; Lee et al., 2008; Mercer et al., 2010; Papa and Germain, 2011; Apostolov et al., 2011; Wu et al., 2010; Mitra et al., 2012; Ho et al., 2009; Yeh et al., 2011). At time points after 48 hours post-transfection, these effects dissipated (most likely because surviving cells normalized their gene expression) and EndoG expression pattern was similar at 72 and 96 hours post-transfection in all transfected cells.

This would explain why absolute copy number (plasmid abundance per well) of the non-targeting plasmid was reduced at 48 hours, relative to 24 hours after transfection. The cells that took up the plasmid most likely succumbed to apoptosis due to the associated uptake of the cationic liposome, as the increase in EndoG mRNA expression implied (Kongkaneramit et al., 2008; Takano et al., 2003; Aramaki et al., 2000; Aramaki et al., 1999; Iwaoka et al., 2006; Takano et al., 2001). This would also explain why EndoG-targeting plasmids showed increased stability relative to the non-targeting control, as the shRNA they encoded could have attenuated EndoG-dependent cell death by reducing cellular levels of EndoG (Li et al., 2004; Wang et al., 2008; Basnakian et al., 2006).

A similar effect was reported for both aggressive prostate and breast cancer cells, where low expression levels of EndoG correlated with resistance of these cancer cell lines to chemotherapeutic agents cisplatin and etoposide, both of which induce cell death in part by increasing intracellular levels of ROS (Wang et al., 2008; Basnakian et al., 2006). Furthermore, both reports showed experimentally that silencing of EndoG by siRNA in expressing cell lines could attenuate cell death after exposure to these chemotherapeutics (Wang et al., 2008; Basnakian et al., 2006). The central role of EndoG in mitochondria associated apoptosis has been well documented and several studies have shown that EndoG silencing can make cultured cells refractive to apoptosis triggers (Apostolov et al., 2011; Kim et al., 2008; Higgins et al., 2012). Therefore, the differential loss of copies observed between EndoG-targeting and non-targeting vectors could be due to the non-specific nuclease action of EndoG on chromatin (and all other nucleic acids in the nucleus) as a result of programmed cell death, rather than targeted action against exogenous DNA.

In order to test whether the observed difference in plasmid stability between the non-targeting control and EndoG-targeting vectors was a result of specific targeting of exogenous DNA by EndoG, or simply a byproduct of the cytotoxic nature of the transfection reagent used in the experiment, a new experimental design was devised. Namely, proapoptotic effect of Lipofectamine 2000 was minimized by increasing the starting cell density of HeLa to near confluence, which was specifically recommended in the manufacturer's user manual.

In this experiment, plasmid abundance, relative to cellular DNA, was similar between EndoG-targeting and non-targeting plasmids and decreased in a time-dependent fashion. This result suggested that the observed effect of EndoG on plasmid stability in the previous experiment was not due to specific targeting of exogenous DNA by EndoG. Importantly, transfection of nearly-confluent cells, where cytotoxic effects of Lipofectamine 2000 were minimized, did not bring about a measurable response in EndoG expression upregulation between 24 and 48 hours post-transfection, also suggesting that apoptosis was not initiated *via* an EndoG-dependent pathway in these cells. Therefore, silencing of EndoG did not result in differential cell death between cells transfected with the EndoG-targeting and non-targeting plasmids and hence failed to produce the outcome observed in the previous experiment in sub-confluent HeLa cells.

Another possible contributing factor to the observed differences in relative plasmid abundance per cell between EndoG-targeting and non-targeting vectors observed in sub-confluent HeLa cells could also be differential replication of cells transfected with these vectors. Namely, silencing of EndoG has been reported to slow down cellular replication

of mammalian and other eukaryotic cells (this effect was also observed and reported in Chapter II of our study), but the mechanism behind this phenomenon has not been well described other than the observation that EndoG-deficient cells become disproportionally arrested in the G2/M phase of the cell cycle (Buttner et al., 2007a,b; Huang et al, 2006; Diener et al., 2010). This may have decreased effects of plasmid dilution by mitosis and could explain why relative abundance of EndoG-targeting plasmids with respect to cell number did not decrease between 24 and 48 hours post-transfection.

However, we could not demonstrate this effect experimentally using raw cell count data, which was similar for cells transfected with EndoG-targeting and non-targeting vectors. In addition, EndoG-targeting plasmids were similarly diluted with respect to cellular DNA as the non-targeting control plasmid at time points assayed after 48 hours post-transfection. However, we cannot exclude this possibility as raw cell counts are not representative of cell viability, apoptosis status or replication potential, and the protective effect of EndoG-silencing with regard to cationic liposome treatment may have concealed replication deficiencies with respect to cells transfected with the non-targeting control plasmid.

In sub-confluent HeLa cells, reporter gene (GFP) expression was higher in cells transfected with most of the EndoG-targeting plasmids at 24 and 48 hours post transfection, relative to cells transfected with the non-targeting control plasmid when expression was normalized with the expression of a cellular housekeeping gene. Although this may be an effect associated with differences in molecular integrities between EndoG-targeting and the non-targeting control plasmids, this cannot be

concluded based on the data, as quality of pDNA isolated from HeLa cells was not assayed.

However, GFP expression data was normalized with plasmid DNA abundance for each EndoG-targeting and the non-targeting control plasmid. All EndoG-targeting plasmids expressed more GFP mRNA per plasmid copy relative to the non-targeting control plasmid at 24 hours post transfection. This would imply that EndoG-targeting plasmids were better preserved relative to the non-targeting control plasmid, but cannot be concluded with certainty as plasmid copy number does not correlate to transgene expression in a linear manner (Glover et al., 2010). Specifically, once a certain threshold of plasmid copies is reached, transgene expression remains unaffected by further increases (Takahashi et al., 2011). Another possible explanation for the observed effect is that triggering of cell death by transfection reagent cytotoxicity activated the proposed apoptotic RNase function of EndoG thereby reducing the amount of the GFP reporter gene transcript in HeLa cells that were sub-confluent at time of transfection with the negative control vector (Kalinowska et al., 2005). Interestingly, transfection of nearly-confluent cells, where transfection reagent cytotoxicity was minimized, did not result in greater GFP mRNA expression from EndoG-targeting plasmids relative to non-targeting control.

1.5 Conclusion:

In conclusion, EndoG silencing was not found to increase exogenous DNA stability and transgene expression under physiological circumstances. Therefore, it is unlikely that EndoG is a mediator of intranuclear plasmid DNA disposition. However, protective

effects of EndoG silencing on exogenous DNA stability may be perceived to occur in cells if additional EndoG expression is induced by an extrinsic stimulus. This does not reflect a role for EndoG in defence against exogenous DNA, but most likely its role in non-specific degradation of all nuclear DNA following induction.

Chapter II

EndoG depletion may improve efficiency of first generation adenovirus vector replication

2.1 Introduction

The high efficiency of gene transfer into a wide variety of dividing and non-dividing mammalian cells, coupled with a relatively low risk of transformation, have made adenovirus type 5 (Ad5) derived vectors a staple tool for successful gene delivery *in vitro* and *in vivo* (reviewed in Yao et al., 2011). In particular, the first generation Ad5 vectors, which have the entire E1 region of the viral genome deleted (Ad5 ΔE1), have been used extensively for the transduction of therapeutic and cytotoxic genes into carcinoma cells.

An important consideration for the use of Ad5 ΔE1 vectors is that they are considered replication incompetent, owing to the dependence of Ad5 on the products of E1 genes for the initiation of events that lead to productive viral replication (Jones and Shenk, 1979). However, a number of studies have demonstrated that Ad5 ΔE1 DNA is replicated in human tumour cells, which may be important in the context of their application in treatment of human malignancies (Lieber et al., 1996; Nelson and Kay, 1997; Goldsmith et al., 1998; Brand et al., 1999; Steinwaerder et al., 2000; Steinwaerder et al., 2001; Bernt et al., 2002; Ghosh and Duigou, 2005). Namely, replication of viral DNA is correlated with increased expression of virally encoded genes that mediate cytotoxicity (Brand et al., 1999; Wersto et al., 1998). Furthermore, viral DNA replication can lead to productive replication of the virus, which results in host cell death and the production of new virions with the ability to repeat this process (Steinwaerder et al., 2000; Bernt et al., 2002). Therefore, it is important to study factors that may enhance this process, as Ad5 ΔE1 could potentially have oncolytic properties that may be applied for treatment of human malignancies.

2.1.1 First generation adenovirus vectors

Several generations of Ad5 based vectors have been developed and they differ with respect to the sequence deletions made in the viral genome, which result in differences in the size of recombinant DNA they can accommodate, their immunogenicity, as well as their replicative potential in different cellular backgrounds (reviewed in Benihoud et al., 1999). In the first generation Ad5 vector (Ad5 ΔE1), the early genes 1A and 1B (E1A and E1B) are completely deleted and usually replaced with a transgene expression cassette under the control of the cytomegalovirus immediate early (CMVie) promoter/enhancer element. The E1A encodes two major proteins, E1A 13S (or E1A-289R) and E1A 12S (or E1A-243R), produced by differential splicing of the same transcription unit, which are the first viral products expressed upon wildtype Ad5 infection (reviewed in Shenk, 1996). The E1A 13S mainly transactivates other viral genes, notably those encoded in the E2 and E4 regions, which are important for Ad5 DNA replication. The major function of the E1A 12S is to drive cell cycle progression and to induce cellular DNA synthesis, doing so by directly transactivating cellular genes and by physically interacting with cell cycle regulatory proteins. In particular, the binding of the retinoblastoma (Rb) tumour suppressor proteins, results in the release of the E2F transcription factors, which in turn upregulate the expression of S phase proteins involved in DNA synthesis (Dyson, 1998). Therefore, quiescent cells are made to progress to S phase, which creates a favourable environment for viral DNA replication (Vousden, 1995).

In normal cells, expression of E1A gene products also triggers G1 arrest or apoptosis, which occurs as a result of tumour suppressor p53 stabilization (Xiong et al., 1993;

Miyashita and Reed, 1995). Since premature cell death would reduce viral yield, the Ad 5 encodes two E1B proteins, the E1B 19k and 55k, which specifically attenuate p53-mediated apoptosis and extend the time-frame available for viral replication (Rao et al., 1992; Debbas and White, 1993). Both proteins are encoded by the same mRNA, however due to differentially positioned AUG translation initiation codons, they do not have homology in amino acid sequence (Esche et al., 1980; Bos et al., 1981; Montell et al., 1984). The E1B 55k binds p53 directly to block it, while the E1B 19k works downstream of p53 in an analogous role to the Bcl-2 anti-apoptotic proteins, binding to Bax and preventing the release of pro-apoptotic factors from mitochondria (Sarnow et al., 1982; Roth et al., 1998; Han et al., 1996; Sabbatini et al., 1997). Deletion of the E1B 19k gene from Ad5 results in reduced viral yields with increased degradation of both cellular and viral DNA (Pilder et al., 1984; White et al., 1984). In addition to opposing E1A triggered apoptosis, the E1B 55k is important for preferential transport of late viral mRNA from the nucleus to the cytoplasm, a role it fulfils in co-operation with the E4 orf6 protein (Leppard and Shenk, 1989; Bridge and Ketner, 1990).

In lieu of the importance of the E1 region for viral growth, Ad5 ΔE1 is considered replication incompetent in normal cells and can only be propagated in the permissive human embryonic kidney 293 (HEK293) cell line, which has been transformed with the adenovirus E1 region and provides its products *in trans* (Graham et al., 1977). However, transcription of late viral mRNA and synthesis of encoded late proteins, in addition to Ad5 DNA replication have been observed in cultured cells that have not been transformed with adenovirus (Brand et al., 1999). In particular, many human tumour-derived cell lines support Ad5 ΔE1 DNA replication to various degrees, depending

greatly, but not exclusively, on the multiplicity of infection (MOI) (Lieber et al., 1996; Nelson and Kay, 1997; Goldsmith et al., 1998; Brand et al., 1999; Steinwaerder et al., 2000; Steinwaerder et al., 2001; Bernt et al., 2002; Ghosh and Duigou, 2005). In some tumour cells, replication of viral DNA leads to observable cytopathic effects (CPE), which is a hallmark event of productive viral replication (Steinwaerder et al., 2000; Steinwaerder et al., 2001; Bernt et al., 2002).

2.1.2 Replication of viral DNA in Ad5 ΔE1 infected cells

Infection of mouse livers *in vivo* with Ad5 ΔE1 does not lead to *de novo* synthesis of viral DNA, which is in contrast to highly efficient viral DNA replication in isolated, cultured hepatocytes (Nelson and Kay, 1997). Since cells in the mouse liver are quiescent, while isolated hepatocytes replicate in culture, it is likely that active cell cycling is important for Ad5 ΔE1 DNA replication (Steinwaerder et al., 2000). As stated previously, the genes encoded in the E1 region are responsible for driving quiescent cells to progress through the cell cycle in order to make available cellular factors that are required for virus DNA replication and whose expression is cell cycle regulated. Since tumour cells do not need to be induced to progress through the cell cycle, Ad5 ΔE1 DNA replication may occur as a result of availability of cellular proteins and transcription factors that would otherwise be absent from normal quiescent cells (Steinwaerder et al., 2000; Bernt et al., 2002).

Several cellular proteins, such as NF-IL6, heat shock proteins, and some transcription factors, have the ability to transactivate E1A regulated viral genes (Spergel and Chen-Kiang, 1991; Imperiale et al., 1984; La Thangue and Rigby, 1987). In HeLa cells, which have been transformed with the human papilloma virus 18 (HPV-18), this function may

be performed by "endogenous" expression of HPV E6 and E7 genes, which bind to p53 and pRb (Steinwaerder et al., 2001). In particular, E7 shares some homology with the adenovirus E1A 12S, which could lead to transactivation of Ad5 encoded viral genes when the E1 region is deleted (Phelps et al., 1988). However, even tumour cells that have not been transformed by oncogenic viruses support Ad5 ΔE1 DNA replication and the efficiency of this process does not correlate with the statuses of the tumour suppressors, p53 and pRb (Brand et al., 1999; Steinwaerder et al., 2000). Hence, the most important factor for efficient Ad5 ΔE1 DNA replication appears to be progression of the cell cycle to a favourable phase that can support both high rates of virus internalization and also provide cellular proteins required for viral DNA replication (Steinwaerder et al., 2000; Bernt et al., 2002).

In the case of infection with wildtype Ad5, quiescent cells are made to progress to the S phase, however, Ad5 ΔE1 may require different cellular factors to replace the transactivating properties of adenovirus E1A proteins and hence require a different cellular environment that can provide them. This is supported by the observation that infection of cultured cells with Ad5 ΔE1 causes a partial G2/M arrest or delay in cell cycle progression, which becomes more apparent in later stages of infection, due to the inappropriate expression of cyclin A, cyclin B1, cyclin D and cyclin-dependent kinase $p34^{cdc2}$ which is induced by viral E4 genes (other than orf6) (Wersto et al., 1998; Brand et al., 1999; Steinwaerder et al., 2000; Bernt et al., 2002). In fact, Steinwaerder *et al.* (2000) and Bernt et al. (2002) demonstrated that highest levels of Ad5 ΔE1 DNA replication occur in the G2/M phase and that prolongation of G2/M leads to increased efficiencies of Ad5 ΔE1 DNA replication in the human cervical carcinoma HeLa cells. Importantly,

cells artificially arrested in the G2/M phase at time of infection with Ad5 ΔE1 exhibit the most efficient virus internalization and viral DNA replication, relative to other points in the cell cycle, and exhibit MOI dependent CPE.

2.1.3 Maximizing Ad5 ΔE1 DNA replication in tumour cells

Endonuclease G (EndoG), a nuclear-encoded mitochondrial endonuclease, is a conserved apoptosis regulator in eukaryotic organisms (Diener et al., 2010). Apart from its role in programmed cell death, EndoG has been implicated in vital roles in the cell, including mitochondrial DNA replication, DNA recombination and cell proliferation (McDermott et al., 2011; Huang et al., 2002; Huang et al., 2006; Buttner et al., 2007a; Zan et al., 2011). Importantly, reduction of cellular levels of EndoG by RNA interference (RNAi) leads to the accumulation of both yeast and mammalian cells in the G2/M phase of the cell cycle without any additional stimulus (Huang et al, 2006; Buttner et al., 2007a,b; reviewed in Galluzzi et al., 2012). Since exogenous expression of EndoG-GFP can rescue this phenotype, the delay in G2/M transition is a specific effect of EndoG silencing (Huang et al, 2006). Therefore, depletion of EndoG may prolong the G2/M delay associated with Ad5 ΔE1 infection of tumour cells and thus increase viral DNA replication in a similar manner to what has been observed when tumor cells are chemically arrested in the G2/M phase (Steinwaerder et al., 2000; Bernt et al., 2002).

With respect to the application of Ad5 ΔE1 vectors for viral oncolytic therapy, maximizing replication of Ad5 ΔE1 DNA should enhance cytotoxicity of these vectors and result in higher efficacy with respect to cancer cell killing. Therefore, we tested whether an Ad5 ΔE1 vector which encodes an RNAi effector against EndoG expression

would exhibit augmented viral DNA replication and CPE in the human cervical carcinoma HeLa cells.

2.2 Materials and Methods

2.2.1 Construction of Ad5 ΔE1 vectors

First generation (Ad5 ΔE1) adenovirus vectors, AdsiEndoG and AdsiCAD, were constructed by the FLP-frt recombination system, which is based on the co-transfection of two plasmids with complementary viral DNA components into the E1-producing HEK 293 cells (Ng et al., 2000; Graham et al., 1977).

The pBHGfrtΔE1,3FLP vector (35,552bp) was a circularized human adenovirus type 5 (Ad5) genome with the following modifications: a substitution in the viral E1 region that encoded the yeast site specific recombinase FLP under the control of the CMVie promoter/enhancer and a *frt* recombination sequence; a deletion of the viral E3 region; and a deletion of the viral packaging sequence (Ψ).

The pDC-CG-U6-EndoGshRNA and pDC-CG-U6-CADshRNA shuttle vectors (5,354bp) were pUC19-based plasmids that contained Ad5 inverted terminal repeats (ITRs), Ad5 packaging sequence, U6 promoter-regulated shRNA expression cassette (vector specific), CMVie promoter/enhancer-regulated AcGFP expression cassette with SV40 poly A signal, and a *frt* recombination sequence.

Construction of pDC-CG-U6-EndoGshRNA vector has been described in Chapter I Materials and Methods and Results sections. This plasmid is the EndoG targeting vector p3. The pDC-CG-U6-CADshRNA vector was engineered in an analogous manner to pDC-CG-U6-EndoGshRNA (Chapter I), except the shRNA expressed by this vector

targeted the caspase activated DNase (CAD) mRNA at the following sequence: 5`GAGAAGUGGACUGGGAGUA3`.

Transfection of HEK293 cells was carried out using Lipofectamine 2000 (Invitrogen) as per manufacturer's instructions. The pBHGfrtΔE1,3FLP and pDC-CG-U6-shRNA vectors were mixed to a final quantity of 5 µg of DNA, at equal molar ratios, and co-transfected into nearly confluent HEK293 cells. Cultures were maintained for 10-15 days following transfection until visible plaques formed in the monolayer.

Homologous recombination mediated by the site specific recombinase FLP between *frt* sequences on the pBHGfrtΔE1,3FLP and pDC-CG-U6-shRNA vectors resulted in the generation of Ad5 ΔE1 DNA vectors, which contained all the viral elements required for replication, except genes encoded in the viral E1 region. The E1 region was replaced by the U6 promoter-regulated shRNA expression cassette (vector specific) and a CMVie promoter/enhancer-regulated AcGFP expression cassette. The HEK293 cells provided the E1 gene products *in trans* facilitating production of infectious virions, detected by the onset of cytopathic effects (CPE).

When ~70% of cells exhibited visible CPE, a rubber policeman was used to scrape cells of the surface of the culture dish. The culture medium (~2 mL) that contained infected cells was collected and sequentially frozen and thawed three times to release virions from cells that were still intact. The cell suspensions were centrifuged at 12,000g for five minutes to settle cell debris. The supernatant was collected and stored at -70^{o}C.

A control Ad5 ΔE1 vector, AdGFP, was also used in this study, which contains the same CMVie promoter/enhancer regulated GFP expression cassette as AdsiEndoG and AdsiCAD, but is missing the U6 promoter regulated shRNA expression cassette.

2.2.2 Confirmation of Ad5 ΔE1 vectors

To confirm the sequences of Ad5 ΔE1 vectors, viral DNA was isolated and following digestion with a restriction endonuclease it was analyzed by agarose gel electrophoresis. In addition, PCR was used to confirm absence of wild type Ad5 contamination.

One hundred µL of viral suspensions were mixed with an equal volume of a 1.2% SDS solution supplemented with 20 µL of 20 mg/mL Proteinase K. The mixtures were incubated at 55^{o}C for one hour. The resulting lysates were mixed with the binding solution of a commercially available DNA purification kit (Norgen Biotek) and processed on a spin column assembly, as per manufacturer's instructions.

Five µL of eluted DNA was mixed with 1 µL of *Hind* III restriction endonuclease (NEB), 2 µL of appropriate buffer (50 mM NaCl, 10 mM Tris-HCl, 10 mM $MgCl_2$, 100 µg/ml BSA, pH 7.9) and 12 µL of DNase/RNase-free water. Reaction was incubated at 37^{o}C for three hours and subsequently examined by 1% agarose gel electrophoresis. The resultant bands were sized by comparison to a DNA sizing ladder (Norgen Biotek). The digestion patterns matched with theoretical predictions based on an *in silica* model (Vector NTI, Invitrogen).

PCR on 2 µL of eluted DNA was performed using E1 region specific primers F 5`ATTCACGTAGCCAGCCACTC3` and R 5`TCGGTCACATCCAGCATCAC3.

Absence of amplification confirmed that Ad5 ΔE1 vector preps were free of contamination with wild type Ad5.

2.2.3 Amplification of infectious Ad5 ΔE1 vectors

Nearly-confluent HEK293 cells, cultured in 150 mm standard tissue culture plates were independently infected with AdsiEndoG, AdsiCAD and AdGFP. Infection was carried out by aspirating culture medium and overlaying the monolayer with the Ad5 ΔE1 vector of choice diluted in 2 mL of 1X PBS++ (1X PBS, supplemented with 1 mM of $MgCl_2$ and $CaCl_2$). After 45 minutes of incubation in a 5% CO_2-air mixture at 37^{o}C, medium (18 mL) was resupplied to the cells.

When ~70% of cells exhibited visible CPE (usually 48 hours post-infection), the cells were scraped by a rubber policeman and the medium was collected and pooled. The cell suspension was centrifuged at 2000g for 10 minutes and supernatant removed. One ml of PBS++ was added to the cell pellet for every 150 mm dish scraped and the cells were resuspended by vortexing. Three cycles of freezing with liquid nitrogen and thawing at 37^{o}C in a water bath were sequentially carried out to lyse the cells and release virions. The cell suspension was centrifuged at 12,000g to pellet cellular debris and supernatant was collected.

2.2.4 Determining titer of Ad5 ΔE1 vectors

Viral titer was determined using the plaque assay standard protocol. Medium was aspirated from confluent HEK293 cells growing in a monolayer and cultured in 6-well culture dishes. Ad5 ΔE1 vectors were serially diluted in 500 µL of PBS++ and several

dilutions in the expected titer range were used to infect HEK293 cells cultured in 6-well tissue culture dishes. After 45 minutes of incubation in a 5% CO_2-air mixture at 37°C, PBS++ was aspirated and cells were overlaid with a liquid medium mixture of 0.6% UltraPure™ Agarose (Invitrogen) and MEM supplemented with 5% FBS. Plates were left at room temperature for 15 minutes to allow agar medium to solidify and they were subsequently incubated in a 5% CO_2-air mixture at 37°C. Visible plaques in the cell monolayer developed within 5 to 10 days and were counted. Viral titer was determined by multiplying the visualized plaque forming units (p.f.u.) in a given well by the dilution factor of the initial viral suspension.

2.2.5 Infection of HeLa cells

HeLa cells were seeded at a density of 50,000 cells/well of a 24-well tissue culture plate one day before infection. On day of infection, medium was aspirated and 100 µL of PBS++ -diluted Ad5 ΔE1 vector was added to the monolayer. After 45 minutes of incubation in a 5% CO_2-air mixture at 37°C, 500 µL of medium was added per well of cells. Next day, medium was replaced by fresh medium.

2.2.6 DNA/RNA isolation

Medium was aspirated and HeLa monolayers were washed twice with 1X phosphate buffered saline (PBS), pH7.4. A solution from a commercially available kit (RNA/DNA/Protein Purification Kit, Norgen Biotek) was used to lyse cells directly on the plate. Entire lysate was collected and applied to a purification column supplied by the manufacturer and recommended protocol was followed as specified. DNA and RNA were

eluted in separate fractions and examined for quality and quantity by agarose gel electrophoresis and spectrophotometry, respectively.

2.2.7 Quantitative PCR analysis

Quantitative PCR (qPCR) was performed with the Bio-Rad iCycler thermocycler on 3 µL of each DNA elution using the iQ SYBR Green Supermix (Bio-Rad) with 300 nM of primers specific for the E2A gene encoded on the viral vector, F 5`ACACTCAGCGGGTTCATCAC3` and R 5`AGATGTGGCGCTACAAATGG3`. The human 5S gene (Fwd primer 5`GCCATACCACCCTGAACG3` and Rev primer 5`AGCCTACAGCACCCGGTATT3`) was used for normalization and the comparative threshold method was used to assess the relative abundance at each time point. The total reaction volume per sample was 20 µL, and the PCR protocol was as follows: 15 minutes at 95^{o}C for enzyme activation, then 40 cycles of 15 seconds at 95^{o}C, 30 seconds at 60^{o}C and 45 seconds at 72^{o}C. Melt curve analysis was performed by relative fluorescence assessment at 0.5^{o}C increments with a 10 second duration, starting at 57^{o}C and continuing for 80 cycles.

2.2.8 Reverse transcription followed by qPCR

Three µL of the total RNA elution was used in the reverse transcription (RT) reaction using the Superscript III system (Invitrogen). In the first step, RNA was mixed with 0.5 µL of 100 mM oligo(dT) 18-mer primer (IDT) and the reaction volume was completed to 10 µL using DNase/RNase free water. Denaturing at 70^{o}C for five minutes was followed by cooling at 4^{o}C for five minutes. At this step, 0.1 µL of the reverse transcriptase Superscript III (SSIII, Invitrogen) was added to the reaction in a mixture with 4 µL of the

5X First Strand Buffer, 2 µL of 0.1 M Dithiothreitol, 1 µL of 10 mM dNTPs and 2.9 µL of water. After the reaction mixture was completed, temperature was increased to 25^{o}C for five minutes and then increased again to 42^{o}C for 60 minutes, followed by 15 minutes at 70^{o}C and an indefinite hold at 4^{o}C.

The qPCR detection of GFP transgene expression levels was carried out using the human β-actin gene for normalization and the comparative threshold method was used to assess the relative abundance of GFP mRNA at each time point. The primers used for detection of GFP cDNA were F 5`GATCACATGAAGCAGCACGA3` and R 5`GATGTTGCC-ATCCTCCTTGA3` and for β-actin F 5`GCCGAGGACTTTGATTGCAC3` and R 5`ACCAAAAGCCTTCATACATCTCA3`. The iQ SYBR Green Supermix (Bio-Rad) was used for the qPCR with 300 nM of primers, as described above for DNA analysis. Levels of EndoG mRNA were also interrogated at each time point using the primers: F 5`GACGACACGTTCTACCTGAGCAACGT3` and R 5`CCAGGATCAGCACC-TTGAAGAAGTG3`. The qPCR protocol for EndoG cDNA amplification varied slightly to protocol described previously due to the requirement of a higher primer annealing temperature, which was set at 65^{o}C.

2.2.9 Cell counting

Medium was aspirated from HeLa cells cultured in 24-well standard tissue culture plates and monolayers were washed three times with 1X PBS. Cells were lifted with 200 µL of Gibco's 0.05% Trypsin-EDTA (1x) and counted on the haemocytometer counting chamber using the Olympus CK 2 inverted microscope for magnification.

2.3 Results

2.3.1 – Construction of recombinant Ad 5 vector for EndoG-silencing

In order to test whether targeting of EndoG by RNAi would augment viral DNA replication in HeLa cells, we constructed AdsiEndoG, an Ad5 ΔE1 vector carrying an expression cassette for a shRNA directed against EndoG mRNA. In addition, a control Ad5 ΔE1 vector with the same backbone sequence was constructed, but encoding a shRNA against CAD, which is an apoptotic nuclease with no known roles outside of apoptosis and which is not functional in non-apoptotic cells by way of chaperone-mediated inhibition (AdsiCAD).

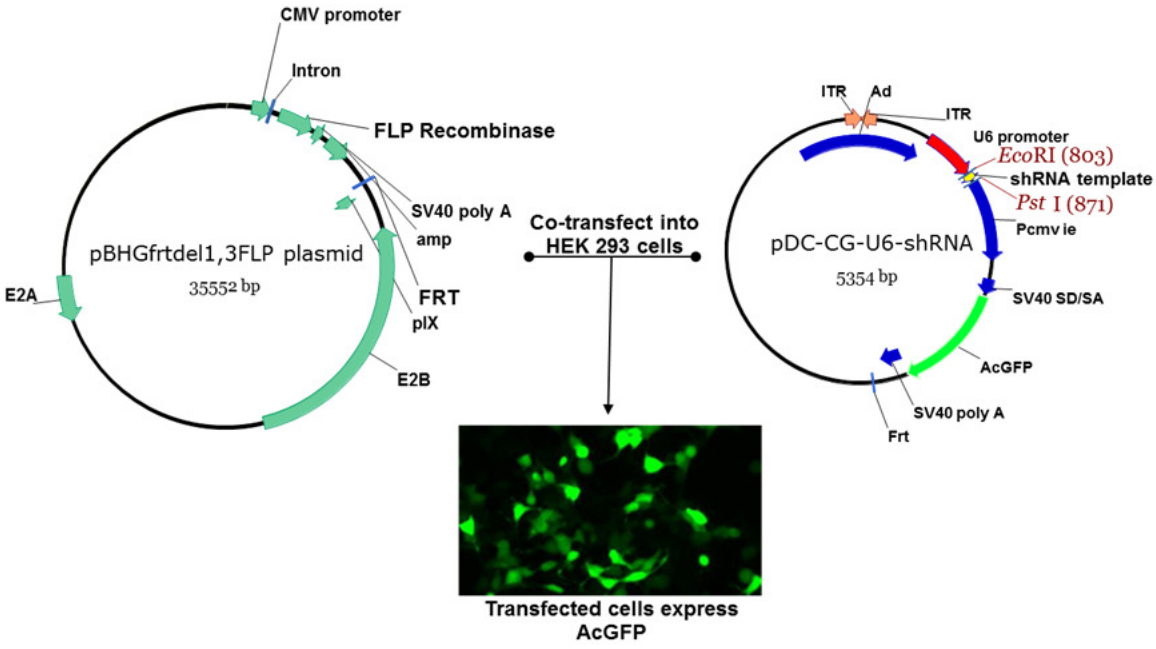

Figure 2.1: FLP recombinase dependent generation of subE1 Ad 5 vectors. HEK 293 cells were co-transfected with the shuttle plasmid, pDC-CG, which encoded a cassette for shRNA expression and a GFP reporter gene, and with the pBHGfrtdel1,3FLP plasmid, which encoded the FLP recombinase as well as the entire Ad 5 sequence, without viral E1 and E3 genes.

The FLP recombinase system was employed to generate Ad5 ΔE1 vectors with substitutions in the E1 gene region. The pBHGfrtdel1,3FLP plasmid encoded the FLP recombinase as well as the entire Ad 5 sequence, without viral E1 and E3 genes, and the Frt recombination site. This plasmid was co-transfected with a shuttle plasmid pDC-CG-U6-shRNA into HEK 293 cells, which have been transformed with the Ad E1 gene (Fig. 2.1). Recombinations between the two plasmids at Frt and Ad5 ITR sites, created recombinant adenoviruses with the EndoG- or CAD-directed shRNA and GFP expression cassettes subbed in at the E1 position (Fig. 2.2).

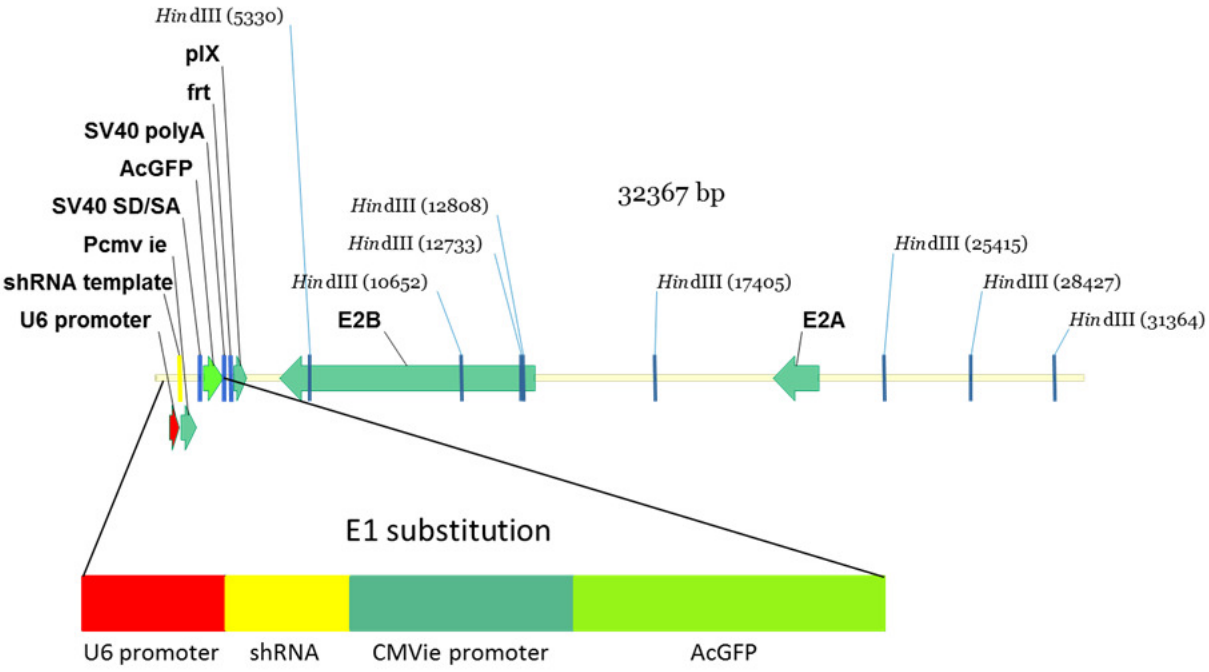

Figure 2.2: Recombinant Ad 5 vector encoding discrete shRNA and reporter gene expression cassettes. Recombination between the two plasmids generated a recombinant Ad 5 (Ad5 ΔE1) vector that encoded both the shRNA template and the GFP reporter gene and which replicated in HEK 293 cells producing observable cytopathic effects.

Since HEK 293 cells have been transformed with the E1 gene of Ad 5 and provide its product *in trans*, the recombinant viruses were allowed to replicate and produced observable cytopathic effects (CPE) in the cellular monolayer. The Ad5 ΔE1 vectors were harvested and confirmed by *Hind* III restriction enzyme digestion, which produced an expected pattern of fragment lengths when visualized on an agarose gel after electrophoresis (Fig. 2.3). In addition, PCR was used to confirm absence of the E1 gene in both Ad5 ΔE1 vectors, which ensured that the preparations were not contaminated with WT Ad 5 (Figure 2.4A).

In this chapter of the study, we characterized the effects of EndoG targeting on Ad5 ΔE1 infection in HeLa cells. However, the constructed Ad5 ΔE1 vectors were also used to test the effects of EndoG silencing on homologous recombination between plasmids, as well as transfection efficiency in Chapter III of this study.

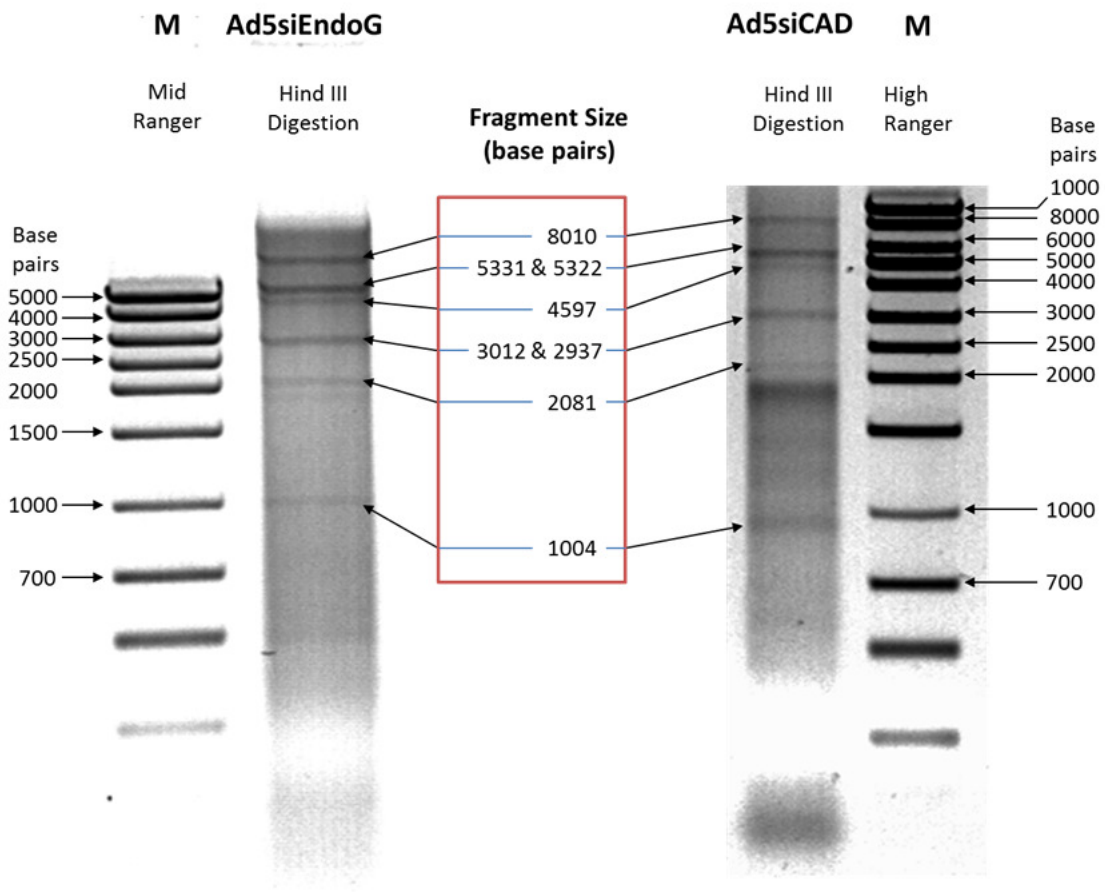

Figure 2.3: Confirmation of recombinant Ad 5 (Ad5 ΔE1) vector by *Hind* III restriction enzyme digestion. Obtained fragment lengths corresponded to the predicted pattern based on sequence analysis and were different than those expected for wildtype Ad 5.

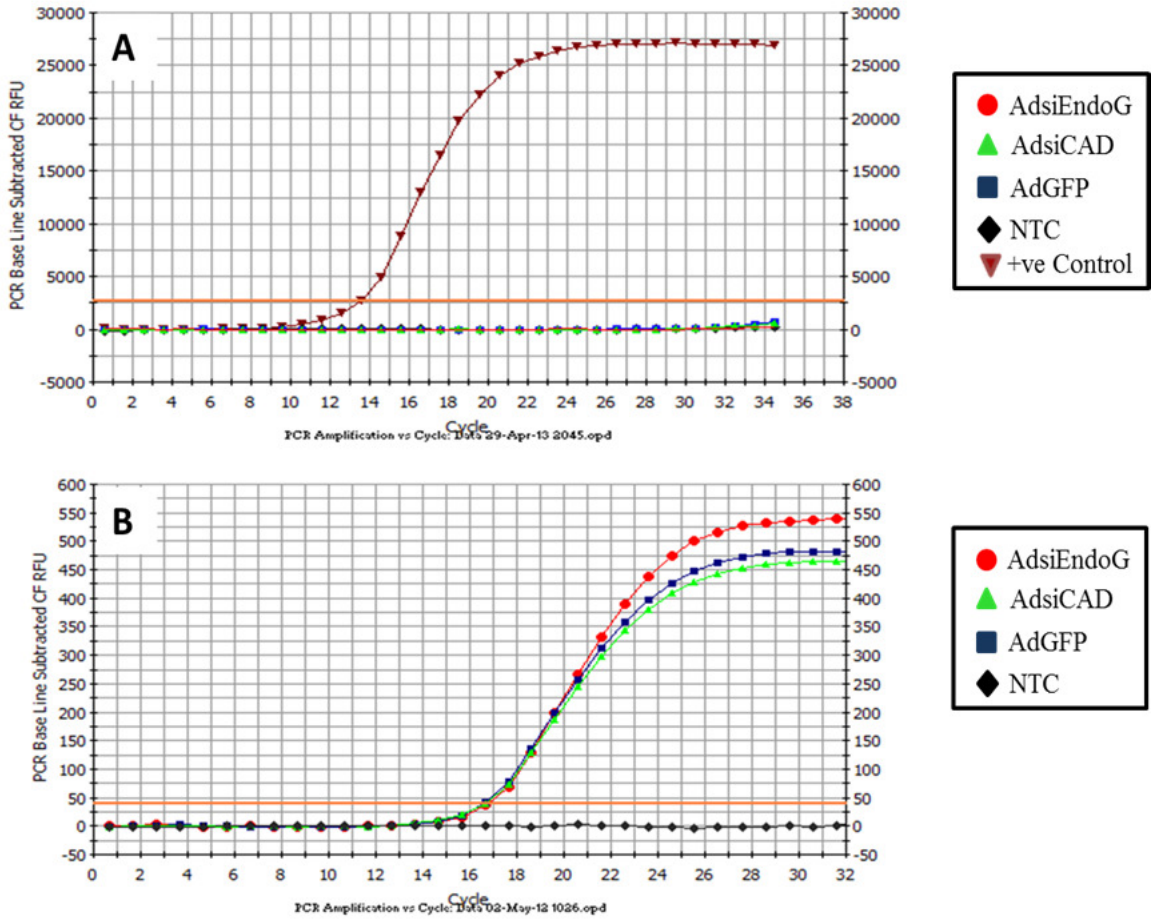

Figure 2.4: A) The qPCR analysis of DNA isolated from AdsiEndoG, AdsiCAD and AdGFP using primers specific for the E1 region of the wild type Ad5 genome confirmed the absence of this region in all of the Ad5 ΔE1 preparations. The positive control (+ve control) was a plasmid that contained the entire E1 Ad5 region. The negative control (NTC) did not contain any template for PCR. B) The qPCR analysis of DNA isolated from AdsiEndoG, AdsiCAD and AdGFP using primers specific for the GFP gene confirmed presence of the transgene in all Ad5 ΔE1 preparations. The negative control (NTC), which did not contain any template sequence, did not amplify.

2.3.2 – Characterization of AdsiEndoG, an EndoG targeting Ad5 ΔE1

2.3.2.1 Replication of AdsiEndoG DNA in HeLa cells

To test whether knockdown of EndoG affects Ad5 ΔE1 DNA replication rates, HeLa cells were infected at MOI 10 p.f.u./cell with AdsiEndoG, an Ad5 ΔE1 encoding a shRNA expression cassette directed against EndoG and two control Ad5 ΔE1 vectors: AdsiCAD, targeting the caspase activated DNase, and AdGFP.

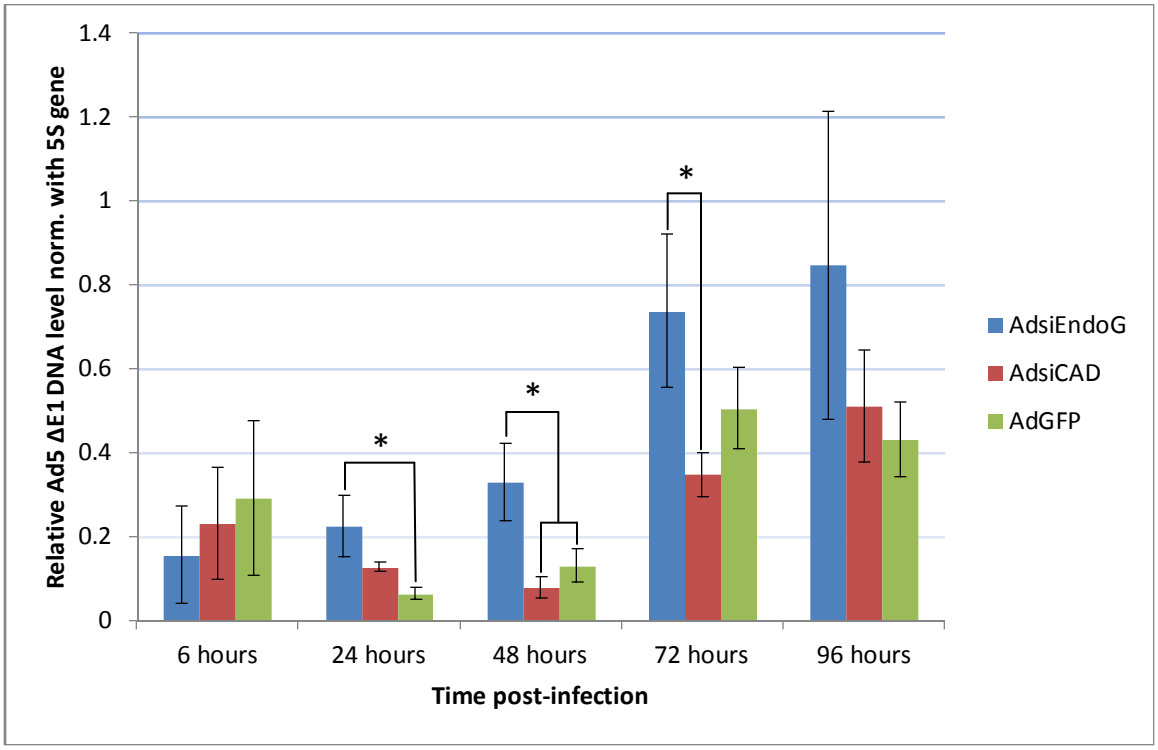

Figure 2.5: Effect of Endog targeting on the replication efficiency of an adenovirus vector in HeLa cells. Relative levels of AdsiEndoG, AdsiCAD and AdGFP DNA over a 4 day time-course in HeLa cells infected at MOI of 10 p.f.u./cell (N=3). Ad5 ΔE1 DNA level was inferred by qPCR analysis of the Ad5 E2A gene and normalized by the amplification of the cellular 5S gene, using the equation 2^(Ct, 5S – Ct, E2A). Significant differences were observed at 24, 48 and 72 hours between AdsiEndoG and one or both of the control vectors (Student's *t* test, p values <0.05). HeLa cells were seeded at a density of 40-50 000 cells/well prior to infection and allowed to replicate over the next four days. Error bars indicate SD.

Figure 2.5 is a summary of the relative Ad5 ΔE1 DNA levels, as assessed by qPCR, at five time points post-infection and normalized with the cellular 5S rRNA gene. It is important to note that normalizing with the 5S rRNA gene resulted in the determination of only approximate Ad5 ΔE1 DNA levels with respect to cell number, as differences in cell cycle distribution of the infected HeLa cells may have resulted in differences with respect to the number of 5S rRNA copies per individual cell. Nonetheless, differences in relative Ad5 ΔE1 DNA levels with respect to the 5S cellular gene were observed between AdsiEndoG and one of or both of the control Ad5 ΔE1 vectors at 24, 48 and 72 hours post-infection, with AdsiEndoG DNA being relatively higher compared to the control vectors at these time points. These results indicated enhanced AdsiEndoG DNA replication relative to control Ad5 ΔE1 vectors.

To examine if the same trend was observed when normalization with cellular DNA was disregarded, Ad5 ΔE1 DNA levels were examined per well of infected cells rather than per cell. Equal proportions of total DNA elutions were analyzed by qPCR and raw Ct values for the E2A gene were converted to relative values based on the equation 2^-Ct and the data was presented in Figure 2.6. The relative level of AdsiEndoG DNA per well of infected cells was statistically significantly higher than one or both of the control Ad5 ΔE1 vectors at 24, 48, 72, and 96 hours post-infection (24, 48, and 96 hours relative to AdsiCAD and 24, 72, and 96 hours relative to AdGFP, t test, p values <0.05). In absolute terms, at the conclusion of the experiment (96 hours post-infection), there was 50 times more viral DNA in cells infected with AdsiEndoG, relative to its initial amount at time of infection, compared to only 14 and 9 times more for AdsiCAD and AdGFP, respectively.

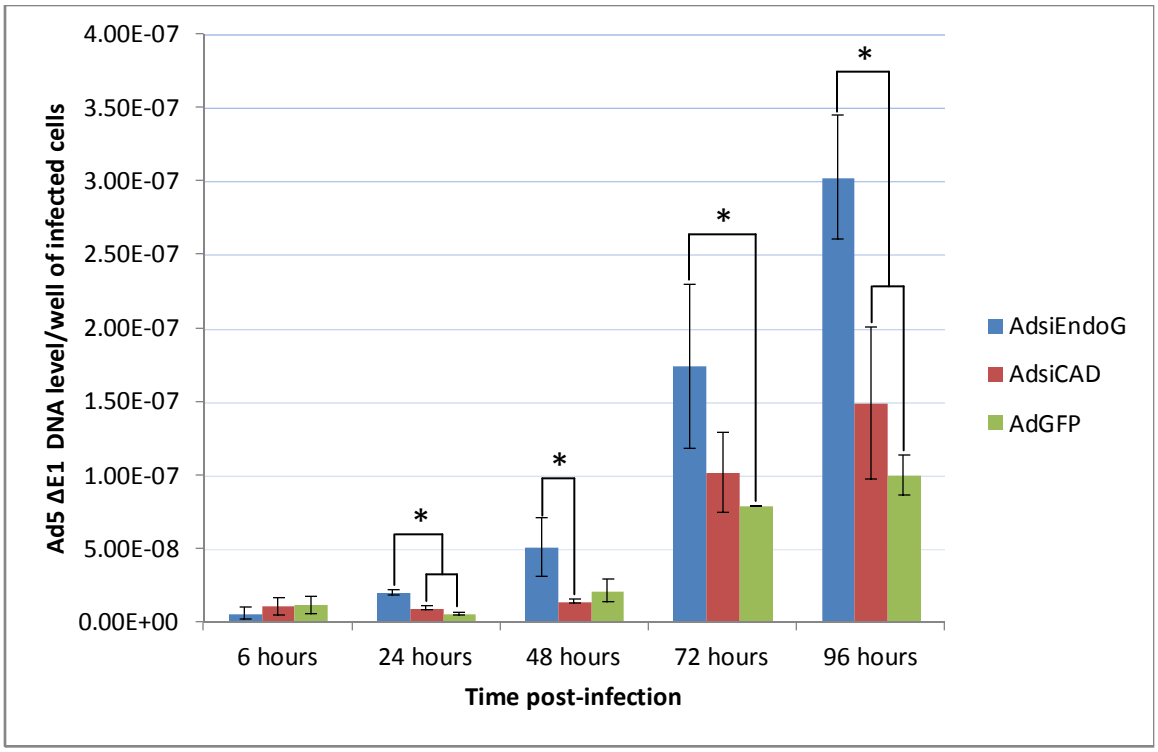

Figure 2.6: Effect of Endog targeting on the replication efficiency of an adenovirus vector in HeLa cells disregarding normalization of data against cellular DNA. Relative content of AdsiEndoG, AdsiCAD and AdGFP over a four day time-course in HeLa cells infected at MOI of 10 p.f.u./cell (N=3). Ad5 ΔE1 DNA content was inferred by qPCR analysis of the Ad5 E2A gene (2^-Ct). Significant differences were observed at 24, 48 and 72 and 96 hours between AdsiEndoG and one or both of the control vectors (Student's *t* test, p values <0.05). HeLa cells were seeded at a density of 40-50 000 cells/well prior to infection and allowed to replicate over the next four days. Error bars indicate SD.

2.3.2.2 Effect of AdsiEndoG infection on HeLa cell proliferation

A technical repeat of the above experiment was done in order to assess replication rates of infected cells over the same four day time-course (Fig. 2.7). Cells were washed with PBS twice and subsequently lifted by trypsinization and counted by haemocytometer. At each time point after the initial assessment at 6 hours post-infection, there were significantly fewer cells in wells infected with AdsiEndoG relative to the mock infected control (Student's *t* test, p values <0.05).

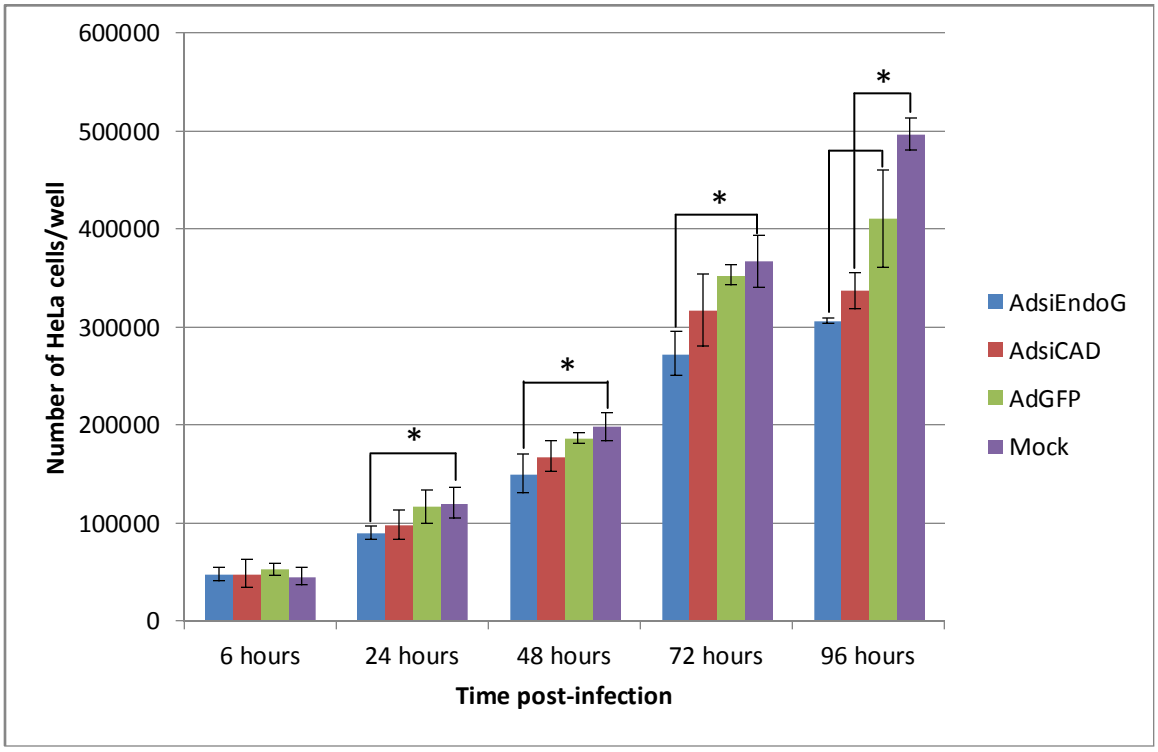

Figure 2.7: Effect of EndoG targeting on HeLa cell proliferation. Average number of HeLa cells infected with AdsiEndoG, AdsiCAD and AdGFP at MOI of 10 p.f.u./cell (N=3) or mock-infected over a four day time-course. HeLa cells were seeded at a density of 40-50 000 cells/well prior to infection and allowed to replicate over the next four days. At each time point, cells were washed twice with PBS and lifted by trypsin. Cell counting was done on the haemocytometer. Error bars indicate SD.

Conversely, the only time point where the difference in cell number reached statistical significance between the other infection conditions, with AdsiCAD and AdGFP, and the mock infected control was at 96 hours post-infection. CPE was not observed in any of the wells at any time point after infection with all of the Ad5 ΔE1 vectors, suggesting that differences in cellular abundances were not a result of virus-associated lysis, but due to unequal cell replication rates. Therefore, targeting of EndoG resulted in a HeLa cell proliferation defect, which coincided with increased Ad5 ΔE1 DNA replication over the same time-course.

2.3.2.3 Infection of HeLa with AdsiEndoG at high MOI

Since replication of Ad5 ΔE1 DNA can lead to proportional CPE when HeLa cells are infected at high initial MOI, we tested whether previously observed differences in Ad5 ΔE1 DNA replication rates between AdsiEndoG and AdsiCAD or AdGFP would lead to differential CPE in cells infected with these vectors. Therefore, HeLa cells were infected at MOI of 50 p.f.u./cell, which was 5 times higher than in the initial experiment.

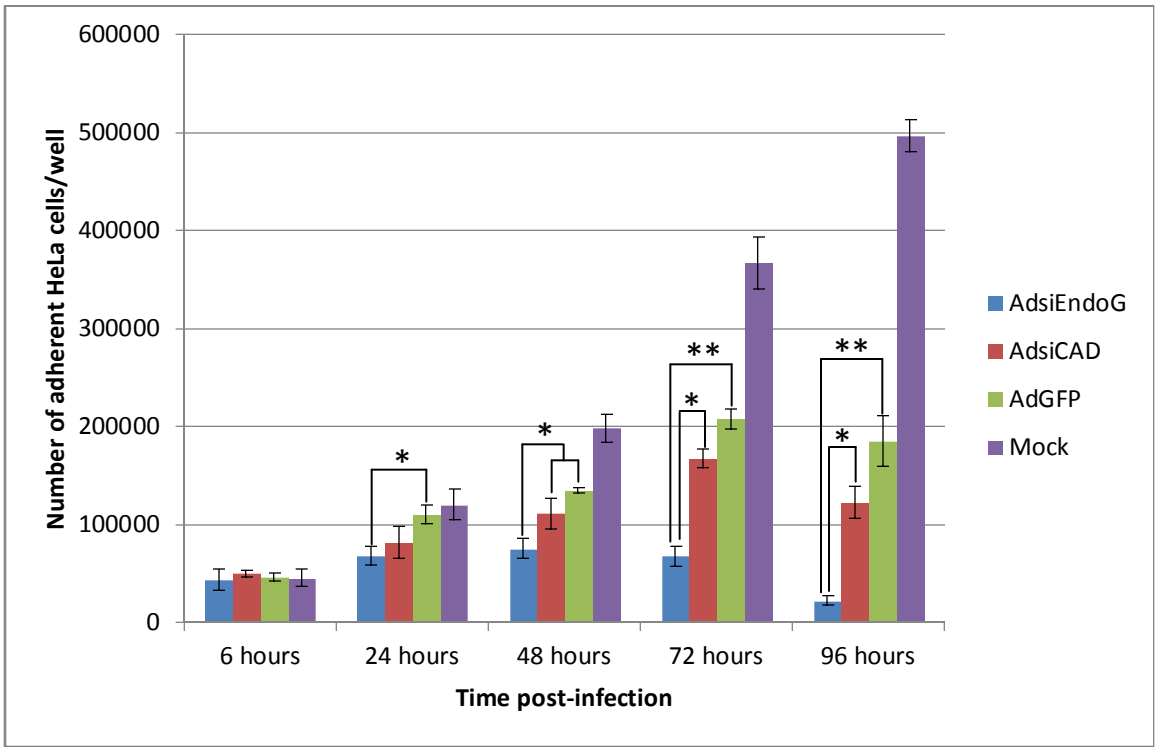

Figure 2.8: Effect of EndoG targeting on levels of adenovirus vector-induced CPE in HeLa cells. Average number of adherent HeLa cells infected with AdsiEndoG, AdsiCAD and AdGFP at MOI of 50 p.f.u./cell (N=3) or mock-infected over a four day time-course. HeLa cells were seeded at a density of 40-50 000 cells/well prior to infection and allowed to replicate over the next four days. At each time point, cells were washed twice with PBS and lifted by trypsin. Cell counting was done on the haemocytometer. Error bars indicate SD.

CPE resulted in a morphological change in cell shape that lead to the detachment of cells from the surface of the culture dish and only adherent cells were counted at each time point of the experiment. At MOI of 50 p.f.u./cell, CPE was observed in all of the Ad5 ΔE1 infection conditions, which reduced the amount of adherent cells per well compared to the mock infected control. The degree of observed CPE was highest in wells of HeLa cells infected with AdsiEndoG relative to AdsiCAD and AdGFP infected cells, which was reflected in the lowest adherent cell counts at 24, 48, 72 and 96 hours post-infection (Student's t test p values <0.05, Fig. 2.8). At 96 hours post infection, less than 5% of cells infected with AdsiEndoG were still adhered to the plate, relative to mock infected control, compared with 24.7% and 37.2% of cells infected with AdsiCAD and AdGFP, respectively (Table 2.1).

Table 2.1 – Percent of HeLa cells adhered to the culture dish at 48, 72, and 96 hours post-infection (p.i.) with AdsiEndoG, AdsiCAD and AdGFP at MOI of 50 p.f.u./cell, relative to mock infected control.

Ad5 ΔE1 vector at MOI of 50 p.f.u./cell	**% of adherent HeLa cells relative to mock**		
	48 hours p.i.	**72 hours p.i.**	**96 hours p.i.**
AdsiEndoG	37.8	18.4	4.4
AdsiCAD	56.1	45.5	24.7
AdGFP	67.6	56.6	37.2

2.3.2.4 Effect of EndoG targeting on Ad5 ΔE1-encoded transgene expression

As AdsiEndoG and AdsiCAD exhibited differences in replication levels in HeLa cells infected at MOI of 10 p.f.u./cell, while also showing different levels of induced CPE in cells infected at MOI of 50 p.f.u./cell, we tested whether these differences had an effect on the expression of a GFP transgene both of the vectors encoded. HeLa cells were infected with MOI of 10 p.f.u./cell and relative GFP mRNA expression assessed (Fig. 2.9). At 72 hours post-infection, cells infected with AdsiEndoG expressed significantly more GFP mRNA compared to cells infected with AdsiCAD (p value <0.05).

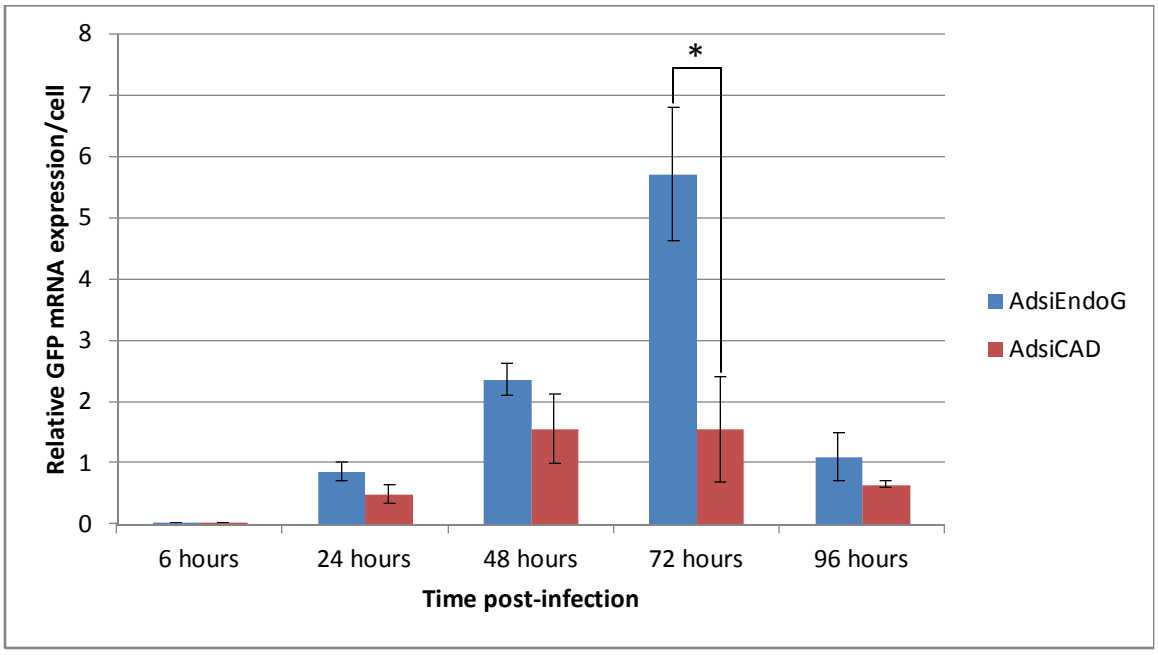

Figure 2.9: Effect of EndoG targeting on adenovirus vector-encoded reporter gene mRNA expression. Relative GFP mRNA expression over a four day time-course in HeLa cells infected with AdsiEndoG, AdsiCAD and AdGFP at MOI of 10 p.f.u./cell (N=3). GFP mRNA expression was inferred by RT-qPCR analysis and normalized with the expression of the cellular β-actin gene using the equation 2^(Ct, β-actin – Ct, GFP). Significant difference in GFP mRNA expression between AdsiEndoG and AdsiCAD was observed at 72 hours post-infection (Student's *t* test, p values <0.05). HeLa cells were seeded at a density of 40-50 000 cells/well prior to infection and allowed to replicate over the next four days. Error bars indicate SD.

2.3.2.5 Knockdown of EndoG mRNA by AdsiEndoG

Relative EndoG expression was also assessed by RT-qPCR in HeLa cells infected with AdsiEndoG, AdsiCAD and AdGFP at MOI of 10 p.f.u./cell (Fig. 2.10). At 48 hours post-infection EndoG mRNA abundance is statistically significantly lower in cells infected with AdsiEndoG relative to AdsiCAD and AdGFP infected cells (p value <0.05).

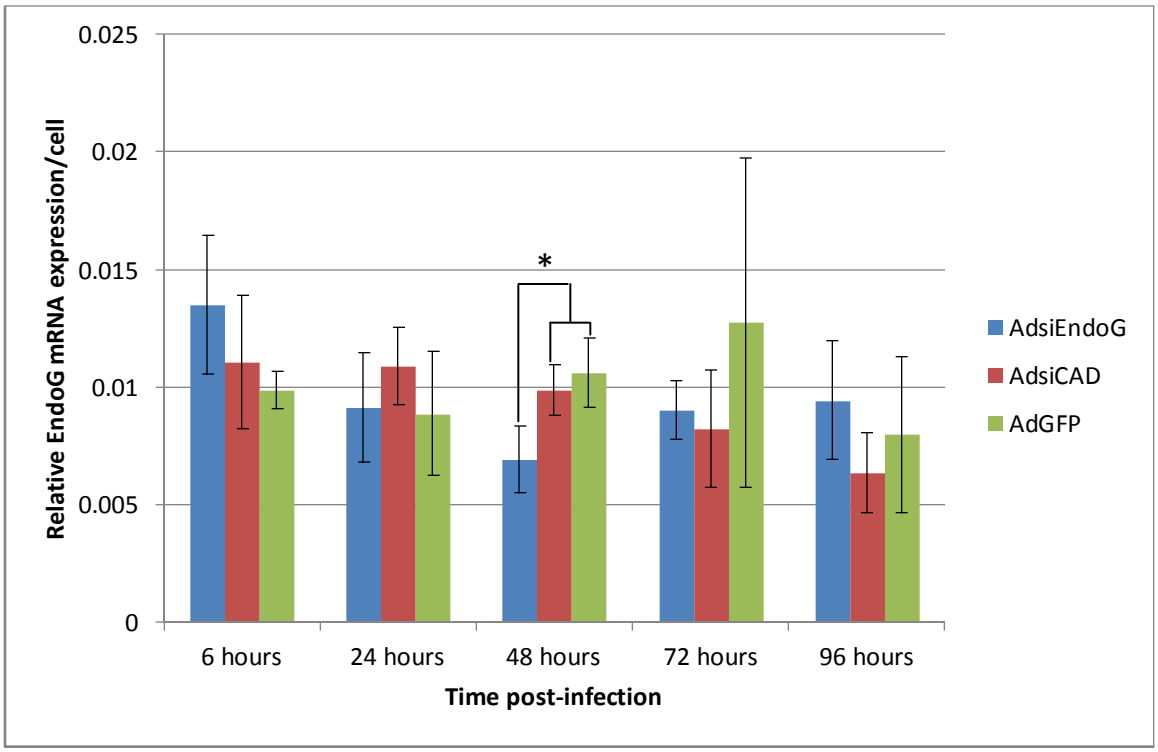

Figure 2.10: Effect of adenovirus vector-mediated EndoG targeting on cellular EndoG mRNA expression. Relative EndoG mRNA expression over a four day time-course in HeLa cells infected with AdsiEndoG, AdsiCAD and AdGFP at MOI of 10 p.f.u./cell (N=3). EndoG mRNA expression was inferred by RT-qPCR analysis and normalized the expression of the cellular β-actin gene using the equation 2^(Ct, β-actin – Ct, EndoG). Significant differences in EndoG mRNA expression between AdsiEndoG and AdsiCAD and AdGFP were observed at 48 hours post-infection (Student's *t* test, p values <0.05). HeLa cells were seeded at a density of 40-50 000 cells/well prior to infection and allowed to replicate over the next four days. Error bars indicate SD.

2.4 Discussion

Human adenovirus type 5 derived first generation vectors (Ad5 ΔE1) are routinely used for the transduction of exogenous genes into human tissues and cells, *both in vitro* and *in vivo* (reviewed in Yao et al., 2011). Owing to the deletion/substitution of the viral E1 region, which encodes the E1A and E1B genes, these vectors are considered replication incompetent in normal, quiescent cells (Jones and Shenk, 1979). However, Ad5 ΔE1 DNA replication has been demonstrated in some proliferating, cultured cells and in tumour derived cells lines (Lieber et al., 1996; Nelson and Kay, 1997; Goldsmith et al., 1998; Brand et al., 1999; Steinwaerder et al., 2000; Steinwaerder et al., 2001; Bernt et al., 2002; Ghosh and Duigou, 2005). The efficiency of Ad5 ΔE1 DNA replication has been positively correlated to the development of cytopathic effects (CPE) in infected cells, and higher intranuclear concentration of Ad5 ΔE1 DNA is related to increased expression of viral genes that mediate cytotoxicity (Steinwaerder et al., 2000; Holm et al., 2004; Brand et al., 1999; Wersto et al., 1998; reviewed in Benihoud et al., 1999). Enhanced cell killing ability of Ad5 ΔE1 vectors is desired for their potential use in viral oncolytic therapy, therefore it is important to develop strategies that can enhance their replication in tumour cells (reviewed in Guse and Hemminki, 2009; reviewed in Rein et al., 2006).

Other studies have established the importance of cell cycling for efficient Ad5 ΔE1 DNA replication and identified the G2/M transition in the cell cycle as the optimal cellular environment for this process (Wersto et al., 1998; Steinwaerder et al., 2000; Bernt et al., 2002). Prolongation of the G2/M transition or chemically induced cell cycle arrest in this phase results in enhanced Ad5 ΔE1 internalization, viral DNA replication and

development of CPE in the cervical cancer cell line HeLa (Steinwaerder et al., 2000; Bernt et al., 2002).

The mitochondrial apoptosis regulator EndoG exerts control of the cell cycle in physiological circumstances (Huang et al, 2006; Buttner et al., 2007; reviewed in Galluzzi et al., 2012). RNAi induced silencing of EndoG expression results in a cell proliferation defect that is characterized by an accumulation of cells in the G2/M transition without any additional stimuli (Huang et al, 2006). Therefore, we hypothesized that an Ad5 ΔE1 virus that encodes an RNAi effector against EndoG mRNA would exhibit augmented DNA replication and CPE in HeLa cells compared to control Ad5 ΔE1 vectors.

In Chapter I of this study we identified a suitable region within EndoG mRNA for targeting by RNAi. To facilitate the knockdown, a vector for shRNA expression was constructed, which also encoded an autonomous cassette for the expression of a GFP reporter gene. Using the FPL-frt recombination system in HEK 293 cells, we engineered AdsiEndoG, an Ad5 ΔE1 vector capable of knocking down EndoG levels in HeLa cells by RNA Pol III U6 promoter driven expression of shRNA. We also engineered the control vector AdsiCAD, which was homologous to AdsiEndoG, except it encoded a shRNA template directed against the caspase activated DNase (CAD). CAD is expressed in a completely inactive form in the cell and has no known functions outside of apoptosis, therefore its knockdown has no effect on cells under physiological circumstances. In addition we made use of a previously constructed Ad5 ΔE1, AdGFP, which did not code for any RNAi effectors, but encoded a homologous GFP expression cassette.

Infection of HeLa cells at MOI of 10 p.f.u./cell with AdsiEndoG and the control AdsiCAD and AdGFP vectors resulted in detectable viral DNA replication. This finding confirmed previous studies that demonstrated Ad ΔE1 DNA replication in HeLa even when cells are infected at a relatively low MOI (Steinwaerder et al., 2000; Bernt et al., 2002). Furthermore, low levels of Ad ΔE1 DNA replication did not result in cell killing, as CPE was not observed in any of the infected cells, which was, again, an expected outcome based on previous reports (Steinwaerder et al., 2000; Bernt et al., 2002). However, the levels of Ad ΔE1 DNA replication varied significantly between cells infected with the AdsiEndoG and the two controls. Despite similar levels of viral DNA internalization, measured at 6 hours post-infection, levels of AdsiEndoG DNA were significantly higher relative to control vectors at 24 hours post-infection and this trend continued to the conclusion of the experiment. In fact, at 96 hours post-infection, AdsiEndoG DNA accumulated to levels that were on average 50 folds higher than the initial concentration used to infect cells. In comparison, over the same time-frame, the DNA of the two control vectors, AdsiCAD and AdGFP, increased 14 and 9 folds, respectively, without showing a statistically significant difference between them. Therefore, AdsiEndoG DNA was replicated at the highest levels, relative to the two control vectors.

We hypothesized that differences in levels of Ad ΔE1 DNA replication rates between AdsiEndoG and the controls arose from cell cycle deregulation caused by EndoG depletion in AdsiEndoG infected HeLa cells. To test this claim, proliferation of HeLa cells infected with Ad ΔE1 or mock-infected cells was monitored over the entire course of the experiment. Cells infected with AdsiEndoG exhibited a cell proliferation defect,

unrelated to development of CPE, which was observed 24 hours following infection and at every time-point assayed thereafter. This finding is supported by previous reports which demonstrated a similar effect of EndoG knockdown on Vero, 293T and yeast cell proliferation, which is characterized by an accumulation of cells in the G2/M transition of the cell cycle (Huang et al, 2006; Buttner et al., 2007a,b). Therefore, increased rates of AdsiEndoG DNA replication, which coincided with a measurable decrease in EndoG mRNA levels and cellular proliferation, most likely resulted from a prolongation of the G2/M transition and, hence, the temporal extension of a favourable cellular environment for Ad ΔE1 DNA replication. This finding is in agreement with observations made from Ad ΔE1-infected HeLa cells chemically arrested at the G2/M transition phase of the cell cycle (Steinwaerder et al., 2000; Bernt et al., 2002).

In contrast, HeLa cells infected with the control Ad ΔE1 vectors, AdsiCAD and AdGFP, did not show augmented proliferation, relative to mock-infected cells, up to 72 hours post-infection. However, at the very end of the experiment time-course, at 96 hours post-infection, all of the Ad ΔE1 vectors induced a measurable cell proliferation defect, which was most apparent in cells infected with AdsiEndoG. This was expected since basal expression of viral E4 genes, other than orf6, can induce the inappropriate expression of cyclin A, cyclin B1, cyclin D and cyclin-dependent kinase $p34^{cdc2}$ which deregulate the cell cycle and cause a partial arrest at the G2/M transition (Wersto et al., 1998; Brand et al., 1999; Steinwaerder et al., 2000).

Since EndoG knockdown in HeLa produced a cell proliferation defect and resulted in enhanced replication of Ad ΔE1 DNA, we tested whether expression of the reporter gene

GFP, encoded by all the vectors, was similarly affected. At 72 hours post-infection, cells infected with AdsiEndoG expressed significantly more GFP mRNA than AdsiCAD-infected cells. The most obvious explanation for this result is that higher concentrations of vector DNA and, hence, DNA template availability, led to higher transcription rates of the reporter gene (Bourbeau et al., 2007). Although this would explain the bulk of the effect, differential expression rates per vector copy could also be responsible for the observation. In fact, when GFP mRNA expression was normalized with cellular Ad ΔE1 DNA content at 72 hours-post infection, cells infected with AdsiEndoG still showed higher reporter expression relative to AdsiCAD infected cells. A possible explanation for the observation may lie in the inherent property of the cytomegalovirus immediate/early (CMVie) promoter/enhancer element, which was used to drive GFP expression, to increase in activity following the activation of the cellular DNA damage response, especially in tumor derived cell lines (Zacal et al., 2005). In this case, knockdown of EndoG could have led to a higher accumulation of DNA damage, due to its proposed role in cellular DNA repair/recombination, which is consistent with a cell cycle arrest/delay at the G2/M transition (Bunz et al., 1998), and hence, higher transcription rates of a gene under the control of the CMVie promoter/enhancer.

Although replication of Ad ΔE1 DNA and encoded transgene expression were enhanced by EndoG targeting, the question still remained whether AdsiEndoG could induce higher levels of CPE in the cervical cancer HeLa cells. Since, initial vector copy number is a predetermining factor in Ad ΔE1 DNA replication and subsequent CPE development, we tested whether increasing the MOI to 50 p.f.u./cell would augment the cell killing ability of AdsiEndoG. All of the Ad ΔE1 vectors were able to reduce HeLa cell viability at this

high MOI, however infection with AdsiEndoG brought on the appearance of CPE sooner and to a much higher extent relative to the two control Ad ΔE1 vectors. At 96 hours post-infection, relative to the mock-infected condition, only 5% of cells infected with AdsiEndoG were still attached to the culture dish surface, compared to 25% and 37% of cells infected with AdsiCAD and AdGFP, respectively.

These results are in agreement with the study performed by Bernt *et al.* (2002), which demonstrated synergy between Ad ΔE1 infection and administration of cytostatic drugs on reducing viability of HeLa cells growing in culture or a HeLa xenograft established in mice. Importantly, the only chemotherapeutics that showed this effect were ones that arrested the cell cycle at the G2/M transition, whereas G0-G1 arrest did not produce an effect. Therefore, increased CPE upon infection with high MOI of AdsiEndoG, observed in our study, is most likely a result of G2/M transition arrest or delay induced by EndoG knockdown.

Another important consideration of the study performed by Bernt *et al.* (2002) is that cells were infected prior to administration of the cytostatic drugs, meaning that the virus was fully internalized upon drug treatment. Therefore, the observed effects of G2/M arrest on enhanced tumour cell killing ability were specific to increased rates of Ad ΔE1 DNA replication and not increased virus internalization. This is supported by our findings, since knockdown of EndoG, and hence the associated cell proliferation defect, occurred after transcription of AdsiEndoG-encoded shRNA, which required prior internalization of the virus. Thus, the positive effects of EndoG-knockdown on the ability of AdsiEndoG to induce CPE in HeLa cells were not the result of higher virus internalization rates, but occurred due to enhanced viral DNA replication.

2.5 Conclusion:

To summarize, the data showed that EndoG knockdown induced a cell proliferation defect in HeLa cells, which coincided with increased replication of Ad ΔE1 DNA and encoded transgene expression. In addition, at high MOI, an Ad ΔE1 vector encoding shRNA against EndoG induced higher levels of CPE in the HeLa cervical cancer cells relative to traditional Ad ΔE1 vectors. Taken together, targeting of EndoG or other cell cycle regulators may improve the utility of first generation adenovirus vectors in cancer therapy. Firstly, expression of therapeutic or cytotoxic genes may be increased even upon infection with relatively low Ad ΔE1 doses due to increased viral DNA replication and second, the oncolytic ability of Ad ΔE1 may be enhanced at higher doses.

Chapter III

EndoG depletion does not improve pDNA uptake in HeLa cells but does reduce levels of homologous recombination

3.1 Introduction

EndoG represents the most abundant nuclease activity in humans relative to the ubiquity of expression across all tissues and cells, albeit at low cellular concentrations (Irvine et al., 2005). It has mostly been investigated in the context of programmed cell death, as its translocation from mitochondria to the nucleus, following apoptosis induction, coincides with high molecular weight DNA degradation (Li et al., 2001; Arnoult et al., 2003; Bahi et al., 2006; Strauss et al., 2008). Interestingly, initial studies on its role in the cell pointed to a vital function, specifically in mitochondrial DNA (mtDNA) replication and/or maintenance (Côté and Ruiz-Carrillo, 1993). Doubts surrounding the exact localization of EndoG within mitochondria and whether it physically interacts with mtDNA, coupled with absence of any apparent mtDNA-related phenotypes in EndoG-null mice, led to a partial dismissal of this theory. However, a recent study by McDermott *et al.* (2011) has re-established the link between EndoG and mtDNA metabolism and demonstrated that deregulated expression of EndoG in mice leads to phenotypic changes in the left ventricular mass of the heart. The dual vital and lethal roles of EndoG are reminiscent of another mitochondrial protein, the apoptosis inducing factor (AIF).

Other vital functions of EndoG have also been proposed and include roles in genomic DNA (gDNA) recombination, as well as a role for the enzyme against uptake of foreign DNA (fDNA) (Buzder et al., 2009; Zan et al., 2011). Although EndoG is primarily localized within the mitochondrial intermembrane space, it has a putative nuclear localization signal at its amino end (within the same region that is cleaved off after mitochondrial targeting) and has been isolated from and identified by immunolocalization in nuclei of healthy non-apoptotic cells (Côté and Ruiz-Carrillo, 1993; Ikeda et al., 1997;

Huang et al., 2002; Varecha et al., 2007). Exogenous overexpression of EndoG can be cytotoxic, however evidence suggests that it requires other cofactors, such as other nucleases, and H2B phosphorylation in order to induce apoptotic DNA laddering at physiological concentrations (Varecha et al., 2007; Varecha et al., 2012).

3.1.1 Role of EndoG in defence

Uptake of fDNA by mammalian cells is restricted by cellular defence enzymes to prevent deleterious effects which include transformation and triggering of apoptosis (Buzder et al., 2009; Torchilin, 2006; Li et al., 1999; Nur et al., 2003). At the core of the defence network are cellular DNases which catalyze the destruction of exogenous DNA before it transverses the nuclear membrane (Ochiai et al., 2006a). Within the first hour after exogenous DNA microinjection, most of it is degraded in the cytoplasm by yet unidentified nucleases, which represent a major barrier to successful expression of encoded transgenes (Chu et al., 2006).

Experiments in primary tubular epithelial (PTE) cells of EndoG null mice have implicated EndoG as one of the defence enzymes (Buzder et al., 2009). In that study, EndoG silencing led to increased transfection efficiency of PTE cells relative to cells with normal levels of this enzyme. Transfection efficiency was determined by quantifying the expression of a fluorescent marker gene encoded on the test pDNA vector. The observed positive effect of EndoG silencing on the efficiency of transfection was more pronounced at 48 than at 24 hours post-transfection (Buzder et al., 2009). Although vector degradation by nuclease activity of EndoG could explain the observed results, differential transgene expression between the two conditions may have occurred through other

silencing mechanisms, such as epigenetic changes, which do not depend on pDNA degradation (Hong et al., 2001).

Considering that successful delivery of exogenous DNA encoding therapeutic genes is at the core of gene therapy applications, it would be worthwhile to investigate the utility of EndoG knockdown for the improvement of this process. Therefore our objective was to knockdown expression of EndoG in the cervical carcinoma HeLa cells and then quantify the resultant effect on pDNA uptake. In this study, the levels of intracellular pDNA were measured directly by qPCR, rather than associated gene expression. Also, a human cervical cancer cell line, HeLa, was assayed in order to test whether the defence function of EndoG is conserved between species and different tissues/cells.

3.1.2 Role of EndoG in homologous recombination

Involvement of EndoG in recombination was first reported by Huang et al. (2002), who showed that it was the only enzyme isolated from HeLa cell nuclei that was able to cleave the herpes simplex virus 1 (HSV-1) α sequence and thereby initiate the recombinational event that is responsible HSV-1 genome inversion. A follow-up study by the same group also showed that a knockdown of EndoG in Vero cells resulted in a decrease of HSV-1 α sequence recombination, further implicating EndoG in this process (Huang et al, 2006). Recently, EndoG has been identified as one of the enzymes involved in immunoglobulin class switch DNA recombination (CSR) in mouse B cells (Zan et al., 2011). The action of EndoG to induce dsDNA breaks in switch (S) regions of the upstream and downstream C_H genes is required for efficient CSR, as it was shown that this process is decreased two-

fold in B cells of EndoG null mice. It is important to note that the lowered efficiency of CSR in EndoG null mice was not related to any changes in B cell apoptosis.

Indirect evidence of EndoG involvement in homologous recombination comes from observations that decreased or attenuated expression of this enzyme results in near complete elimination of polyploidy in both yeasts and mammalian cells (Diener et al., 2010; Buttner et al., 2007). Polyploidization is associated with genomic instability and is recognized as a precursor to aneuploidy in cancer (Buttner et al., 2007a). Survival of polyploidy cells is much more dependent on homologous recombination than that of diploid or haploid cells, as has been demonstrated by screening knockouts of genes involved in this process. Interestingly, deletion of NUC1, the yeast EndoG homologue (42% identity, 62% similarity), decreases the abundance of the polyploid phenotype from a starting 20% of the growing yeast population to less than 1% (Buttner et al., 2007a). Similarly, EndoG knockdown in both human endothelial cells and human colon cancer cell lines results in specific killing of tetraploid cells (Diener et al., 2010; Buttner et al., 2007a). These observations imply that EndoG participates in genome maintenance by homologous recombination, however, there is not enough evidence currently for a definitive call. Therefore we sought to investigate the role of EndoG in homologous recombination using exogenous DNA substrates.

3.2 Materials and Methods

3.2.1 Infection of HeLa cells

HeLa cells were seeded at a density of 150,000 cells/well of a 24-well tissue culture plate one day before infection. On day of infection, medium was aspirated and 100 µL of PBS++ -diluted Ad5 ΔE1 vector was added to the monolayer. After 45 minutes of incubation in a 5% CO_2-air mixture at 37°C, 500 µL of medium was added per well of cells. Next day, medium was replaced by fresh medium.

3.2.2 Transfection of HeLa cells

Two days after infection, 0.1 µg of pUC19 plasmid was mixed with Opti-MEM I Reduced Serum Medium without serum to a final volume of 50 µL. Next, 1 µL of Lipofectamine 2000 (Invitrogen) was diluted in 50 µL Opti-MEM I Reduced Serum Medium. The diluted plasmid was then combined with the diluted Lipofectamine 2000 and left to incubate for 20 minutes at room temperature. The plasmid/lipofectamine mixture were then added to each well and mixed into the medium by gentle rocking. Six hours after transfection medium was changed with fresh medium.

3.2.3 DNA isolation

Medium was aspirated and HeLa monolayers were washed twice with 1X phosphate buffered saline (PBS), pH7.4. A solution from a commercially available kit (RNA/DNA/Protein Purification Kit, Norgen Biotek) was used to lyse cells directly on the plate. Entire lysate was collected and applied to a purification column supplied by the manufacturer and recommended protocol was followed as specified. DNA was eluted and

examined for quality and quantity by agarose gel electrophoresis and spectrophotometry, respectively.

3.2.4 Quantitative PCR analysis

Quantitative PCR (qPCR) was performed with the Bio-Rad iCycler thermocycler on 3 µL of each DNA elution using the iQ SYBR Green Supermix (Bio-Rad) with 300 nM of primers specific for the LacZ gene encoded on the plasmid, F 5`TAGCGGTGATGTT-GAACTG3` and R 5`ACTATCCCGACCGCCTTACT3`. The human 5S gene (Fwd primer 5`GCCATACCACCCTGAACG3` and Rev primer 5`AGCCTACAGCAC-CCGGTATT3`) was used for normalization and the comparative threshold method was used to assess the relative abundance of the plasmids at each time point. The total reaction volume per sample was 20 µL, and the PCR protocol was as follows: 15 minutes at 95^{o}C for enzyme activation, then 40 cycles of 15 seconds at 95^{o}C, 30 seconds at 60^{o}C and 45 seconds at 72^{o}C. Melt curve analysis was performed by relative fluorescence assessment at 0.5^{o}C increments with a 10 second duration, starting at 57^{o}C and continuing for 80 cycles.

3.2.5 Homologous recombination Kit

The Homologous Recombination Assay Kit (Norgen Biotek) was used as per manufacturer's instructions. Briefly, HeLa cells cultured in 24-well tissue culture plates were transfected with 0.5 µg of each deletion plasmid (referred to as dl1 and dl2 in the manufacturer's manual) using Lipofectamine 2000, as described above. The two "dl" plasmids, which were based on the pUC19 cloning vector, contained non-overlapping deletions within the LacZ gene. Forty-eight hours after transfection, DNA was isolated

using a commercially available DNA isolation kit (RNA/DNA/Protein Purification Kit, Norgen Biotek).

The eluted DNA was used for qPCR analysis using 2 µL of recombination-specific Assay Primers Mixture (proprietary sequence) in a 20 µL total reaction volume. In addition, same DNA was used for qPCR analysis using 2 µL of the plasmid backbone-specific Universal Primers Mixture (proprietary sequence) for normalization by the comparative threshold method. Additional normalization was performed using the human 5S gene, as described above.

The qPCR protocol was as follows: 15 minutes at 95^{o}C for enzyme activation, then 40 cycles of 15 seconds at 95^{o}C, 30 seconds at 58^{o}C and 1 minute at 72^{o}C. Melt curve analysis was performed by relative fluorescence assessment at 0.5^{o}C increments with a 10 second duration, starting at 57^{o}C and continuing for 80 cycles.

The expected amplicon size using the recombination-specific Assay Primers Mixture was 420bp.

3.3 Results

3.3.1 – Effect of EndoG silencing on plasmid DNA uptake in HeLa cells

To test the effect of EndoG on fDNA uptake into mammalian cells, recombinant adenoviruses (Ad5 ΔE1 vectors), encoding effectors of RNAi, were used to establish different backgrounds in HeLa cells with respect to EndoG levels. A test plasmid (pUC19) was transfected into HeLa with low or wildtype EndoG expression and intracellular pDNA levels were assayed by quantitative PCR at 24 and 48 hours after transfection.

The AdsiEndoG, an Ad5 ΔE1 recombinant adenovirus, encoded a U6 driven cassette for the expression of shRNA directed against EndoG mRNA, whereas AdsiCAD encoded shRNA directed against the caspase activated DNase (CAD), while otherwise being completely homologous to AdsiEndoG. Silencing CAD, another apoptotic nuclease, was chosen as a control condition for two reasons: first, CAD is expressed in a completely inactive form in the cell and is not activated unless the cell has already committed to caspase-dependent apoptosis; and second, unlike EndoG, CAD has not been implicated to participate in any biological functions that are outside of the apoptotic program. Therefore, silencing CAD expression should not have reduced overall nuclease activity of HeLa cells, as it is inactive in non-apoptotic cells, and importantly should not have produced any phenotypes that are not related to apoptosis.

These Ad5 ΔE1 vectors were used to infect HeLa cells at an MOI of 10 p.f.u./cell 48 hours prior to transfection with 0.1 μg pUC19, as previous characterization of their

effects on HeLa cells identified this time-point as the period were cellular abundance of EndoG mRNA diverged between the two conditions (Fig. 3.1). In addition, a mock infection was also performed using a PBS++ solution devoid of any infectious material. The transfection was done on confluent cells using a cationic liposome transfection reagent (Lipofectamine2000, Invitrogen) following the manufacturer's recommendations.

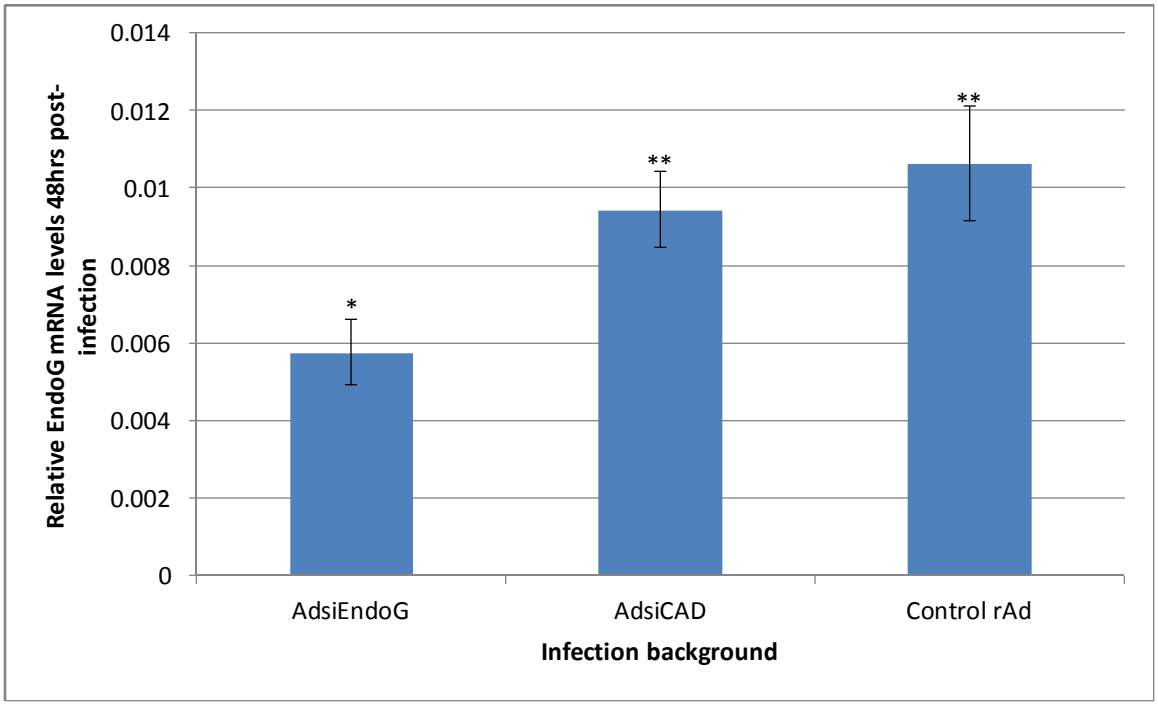

Figure 3.1: Relative EndoG mRNA levels 48 hours after infection of HeLa cells at MOI of 10 p.f.u./cell (N=3). Relative levels were measured by RT-qPCR and normalized with the expression of the human β-actin gene using the equation 2^(Ct, β-actin – Ct, EndoG). EndoG mRNA levels were ~45% lower in AdsiEndoG infected cells than in cells infected with a control Ad5 ΔE1 vector or AdsiCAD (Student's *t* test, p values <0.05).

At 24 hours after transfection with 0.1 µg of pUC19, there were no statistically significant differences in relative pDNA abundance between AdsiEndoG and AdsiCAD infected HeLa cells or the mock infected control HeLa cells (Fig. 3.2). However, at 48 hours post transfection, pDNA levels were higher in cells infected with the two Ad5 ΔE1

vectors relative to the mock-infected cells, reaching statistical significance (Student's *t* test, two tailed, p values <0.05).

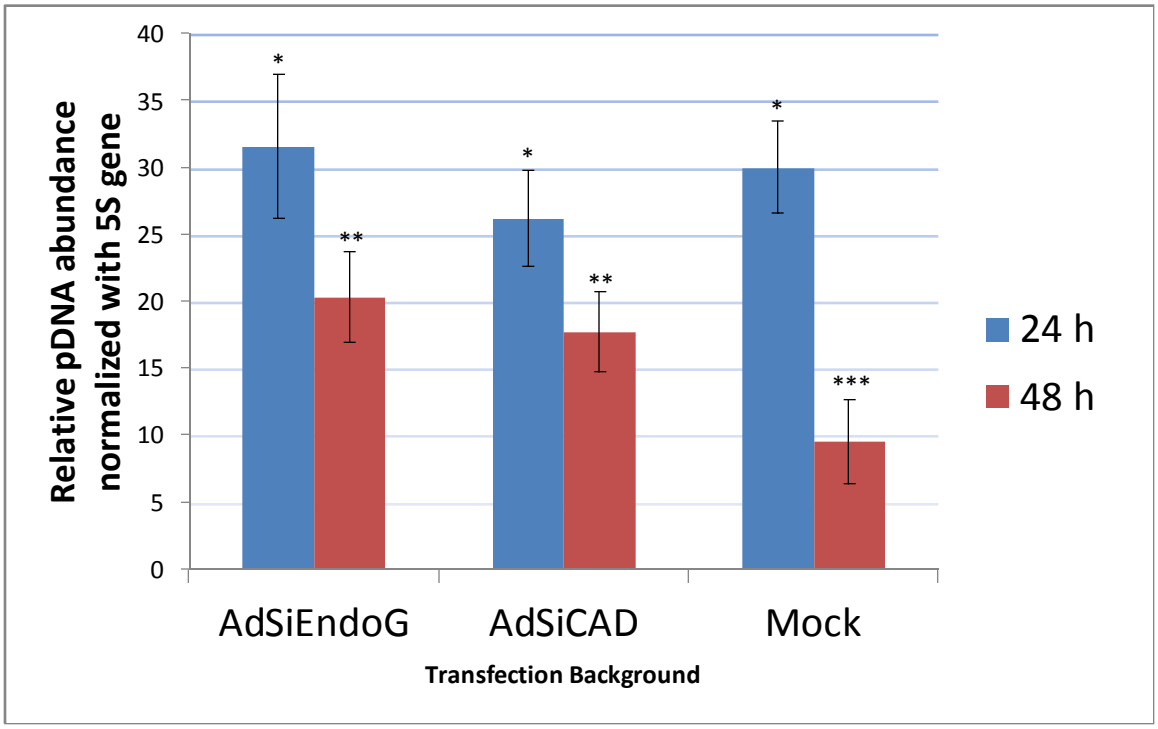

Figure 3.2: Effect of EndoG targeting on pDNA uptake in HeLa cells. Relative levels of pDNA in HeLa cells infected with AdsiEndoG, AdsiCAD, or mock PBS++ solution (N=3). Confluent cells cultured in 24-well plates were infected at MOI of 10 p.f.u/cell and 48 hours later transfected with 0.1 µg of pDNA. Twenty-four and 48 hours after transfection, DNA was isolated and amplified using primers specific for pDNA and the 5S gene. The pDNA levels were inferred based on ΔCt using the equation 2^(Ct, 5S – Ct, pDNA). At 24 hours there are no statistically significant differences between the means of all three conditions (one way ANOVA, p value 0.341973). At 48 hours, after transfection, the relative plasmid abundances in cells infected with AdsiEndoG and AdsiCAD are significantly higher than in mock-infected cells (Student's *t* test, 2 tailed, p value <0.05), but there is no significant differences between cells infected with AdsiEndoG and AdsiCAD (p value >0.05).

To interrogate whether differential DNA degradation was the reason for the observed differences in pDNA levels between infection conditions at 48 hours post-transfection, pDNA levels were examined on a "per well" basis rather than normalized with cellular

DNA (Fig. 3.3). The pDNA uptake was not different when comparing between conditions at 24 and 48 hours post-transfection, however when comparing between the two time points, the only statistically significant decrease in pDNA abundance was observed for the mock infected control. This was not a consequence of EndoG silencing, because AdsiEndoG-infected cells did not show differences in pDNA uptake when compared to AdsiCAD-infected cells (Fig. 3.3).

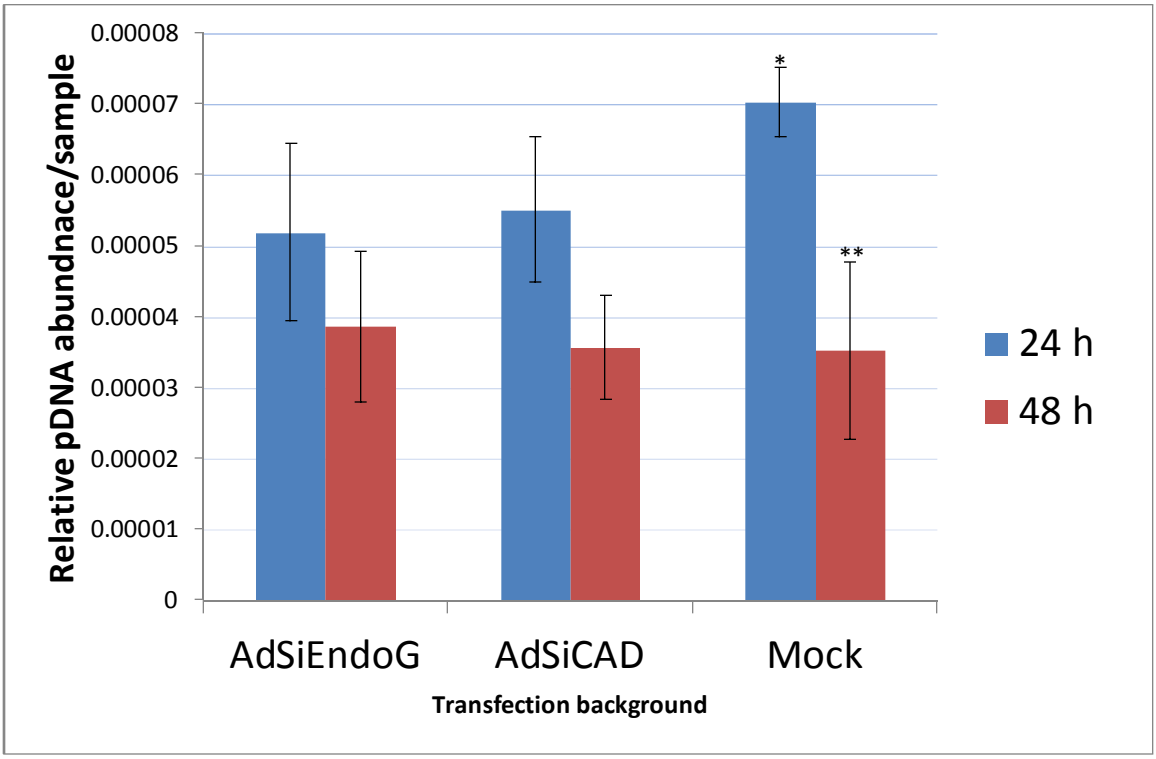

Figure 3.3: Effect of EndoG targeting on pDNA uptake in HeLa cells per well of transfected cells. Relative levels of pDNA in HeLa per well of cells infected with AdsiEndoG, AdsiCAD, or mock PBS++ solution (N=3). Confluent cells cultured in 24-well plates were infected at MOI of 10 p.f.u./cell and 48 hours later transfected with 0.1 µg of pDNA. Twenty-four and 48 hours after transfection, DNA was isolated and amplified using primers specific for pDNA. The pDNA levels were inferred based on average Ct using the equation 2^-Ct. No differences between all conditions in plasmid abundance per well were observed when compared at 24 and 48 hours post transfection (one way ANOVA, p value > 0.05). However, the difference in pDNA abundance per well between 24 and 48 hours was statistically different for the mock infected condition (Student's *t* test, 2 tailed, p value <0.05).

Although targeting EndoG failed to improve pDNA uptake in HeLa cells, the data left open the possibility that Ad5 ΔE1 infection in general may have a slight positive effect. To test for this, the experiment was repeated and included an additional condition where a control Ad5 ΔE1 (AdGFP), which does not target any endogenous mRNA, was used to infect HeLa cells at MOI 10 p.f.u./cell. Plasmid DNA uptake was measured at 48 hours post-transfection in an analogous manner to the above described method. However, there were no statistically significant differences in pDNA uptake between any of the conditions tested and Ad5 ΔE1 infection failed to improve pDNA uptake (Fig. 3.4).

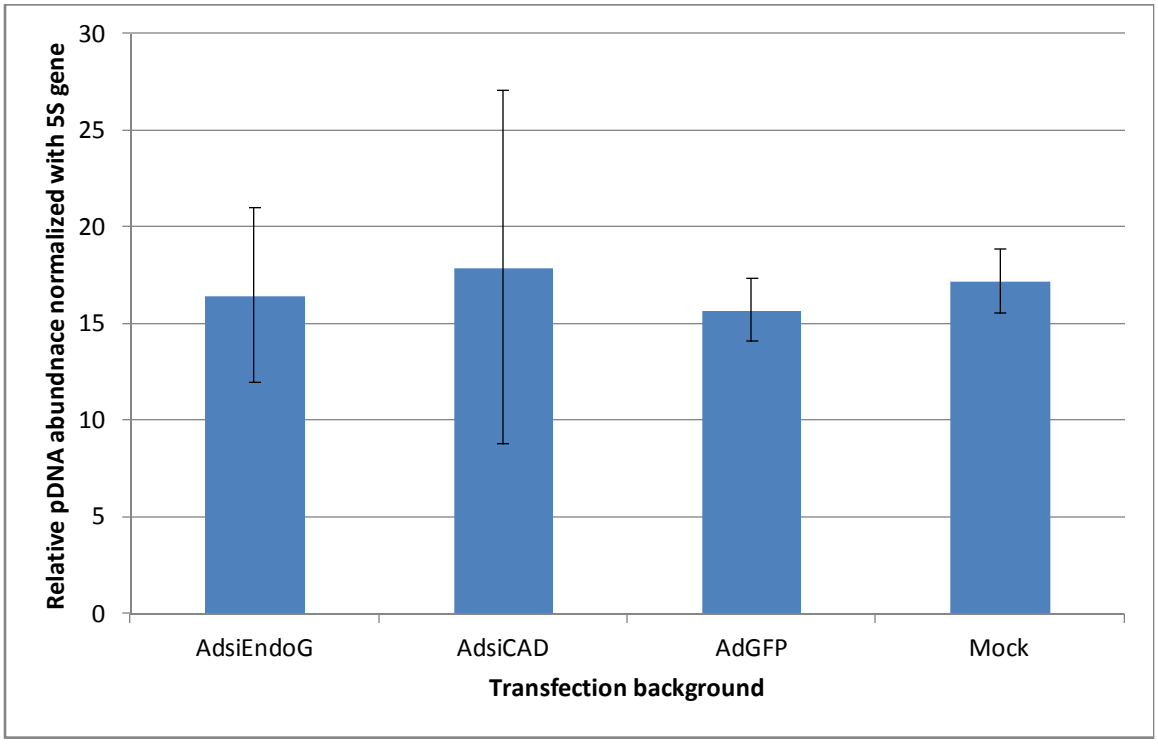

Figure 3.4: Effect of adenovirus infection on pDNA uptake in HeLa cells. Relative levels of pDNA in HeLa cells infected with AdsiEndoG, AdsiCAD, AdGFP or mock PBS++ solution (N=3). Confluent cells cultured in 24-well plates were infected at MOI of 10 p.f.u/cell and 48 hours later transfected with 1 µg of pDNA. Forty-eight hours after transfection, DNA was isolated and amplified using primers specific for pDNA and the 5S gene. The pDNA levels were inferred based on ΔCt using the equation 2^(Ct, 5S – Ct, pDNA. At 48 hours there are no statistically significant differences between the means of all four conditions (one way ANOVA, p value >0.05).

3.3.2 – Effects of EndoG silencing on levels of homologous recomination between plasmids in HeLa cells

EndoG has previously been implicated as a nuclease that facilitates recombination, a role first demonstrated for the HSV I genome. Since double stranded breaks in DNA increase recombination rates, the purpose of this study was to investigate whether silencing the nuclease EndoG would produce a measurable decrease in this process. In order to facilitate this experimental design, two plasmids with opposite deletions in the lacZ gene were co-transfected into HeLa cells with wild type or reduced EndoG levels (Fig. 3.5). Use of deletion plasmids has been widespread in recombination efficiency analysis, but mostly by interrogating expression of a gene reconstituted by homologous recombination. This study relied on quantification of recombination products by qPCR with primers designed specifically to detect the reconstituted LacZ gene.

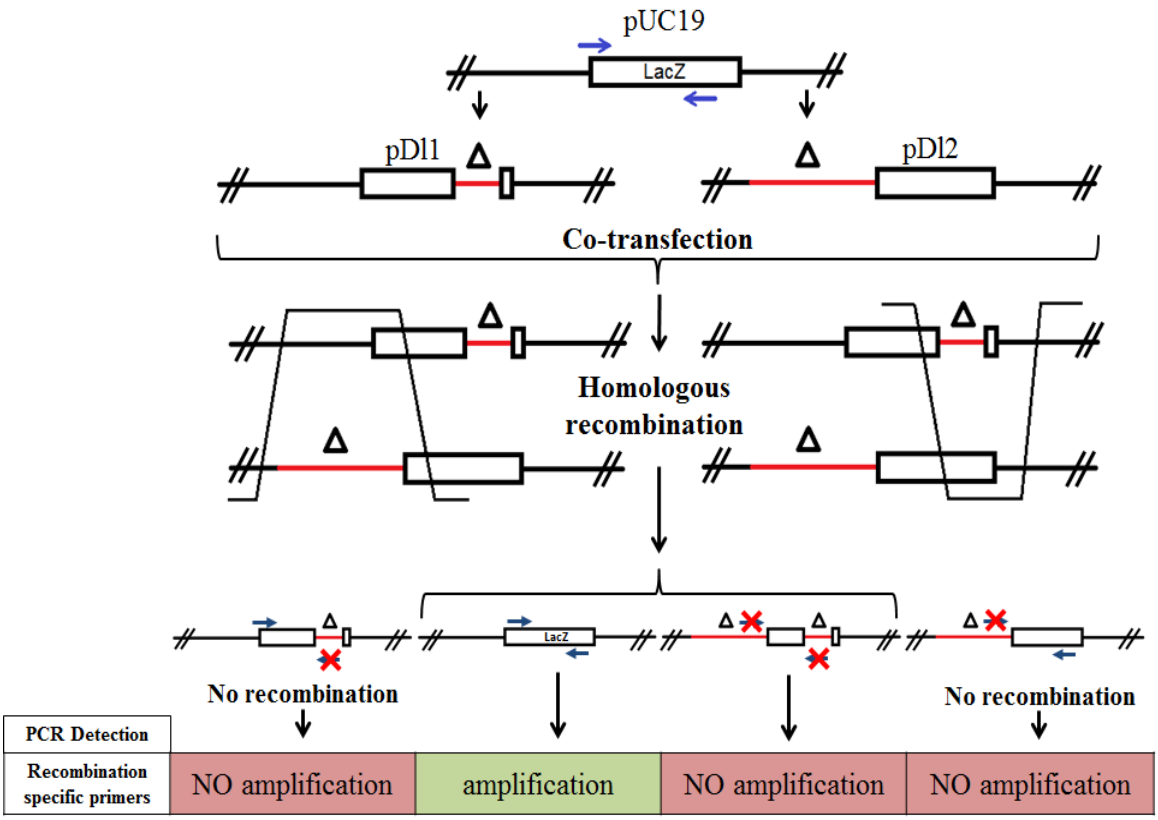

Figure 3.5: Schematic representation of the homologous recombination assay. Plasmid vector pUC19 was modified by enzymatic digestion to produce two plasmids with partial deletions in the lacZ gene (pDl1 and pDl2) that can recombine to reproduce pUC19 and a plasmid missing two portions of the lacZ gene. Recombination events were detected by qPCR using recombination specific primers (depicted in blue and placed corresponding to their approximate binding sites) and levels of homologous recombination were determined by the comparative threshold method using universal primers that were specific for the pUC19 backbone for normalization.

EndoG levels were decreased in HeLa by infection with AdsiEndoG, which targeted EndoG mRNA by an encoded shRNA. Control Ad5 ΔE1 vectors used were AdsiCAD and AdGFP. Cells were also mock infected. At 48 hours post-infection, HeLa cells were transfected with 0.5 µg of each deletion plasmid, since this was the time point where EndoG levels decreased in AdsiEndoG infected-cells (Fig. 3.1). Previous experiments by other groups (Wong and Capecchi, 1986; Brouillette and Chartrand, 1987) demonstrated

recombination between plasmids could be detected at 48 hours after co-transfection, so this time point was chosen for integration by qPCR (Fig. 3.5 for PCR detection method).

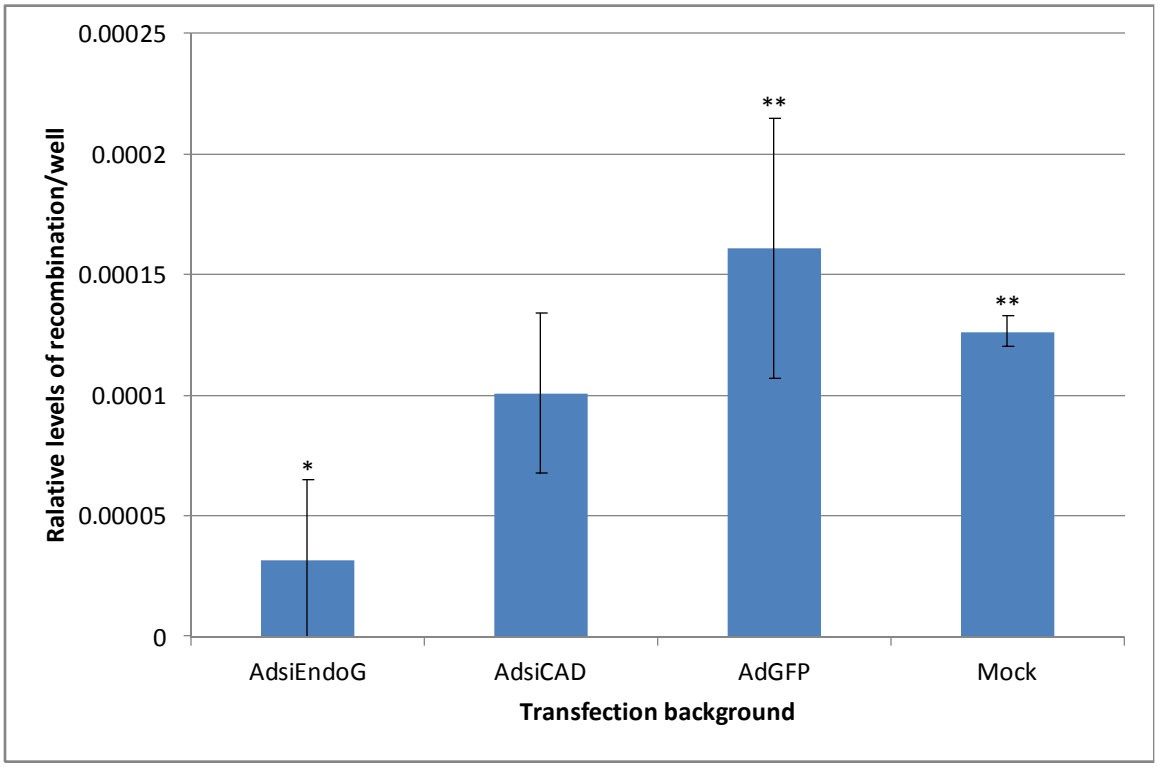

Figure 3.6: Effect of EndoG targeting on levels of homologous recombination between pDNA substrates in HeLa cells. Relative levels of recombination between two LacZ partial-deletion plasmids in wells of HeLa cells infected at MOI 10 p.f.u. with AdsiEndoG, AdsiCAD, and AdGFP or mock-infected (N=3). Recombination was assayed by qPCR 48 hours post co-transfection using primers specific for a fully reconstituted LacZ gene and normalized with total plasmid abundance inferred by universal primers specific for all plasmid variants using the equation 2^(Ct, universal – Ct, recombination). Recombination levels were significantly lower in AdsiEndoG infected HeLa cells compared with AdGFP infected or mock infected cells (Student's *t* test, p values <0.05).

Recombination rates for all conditions are summarized in Figure 3.6. Recombination levels were lowest in wells where HeLa cells were infected with AdsiEndoG, and this was statistically significant relative to wells of cells infected with AdGFP or mock-

infected. Recombination rates were also normalized with cellular DNA, by interrogating the 5S cellular gene, to determine relative per cell recombination (Fig. 3.7). Although recombination levels were still significantly lower in AdsiEndoG infected cells compared to AdGFP infected cells (p value <0.05), the difference relative to mock infected cells, just failed to reach statistical significance (p value 0.07).

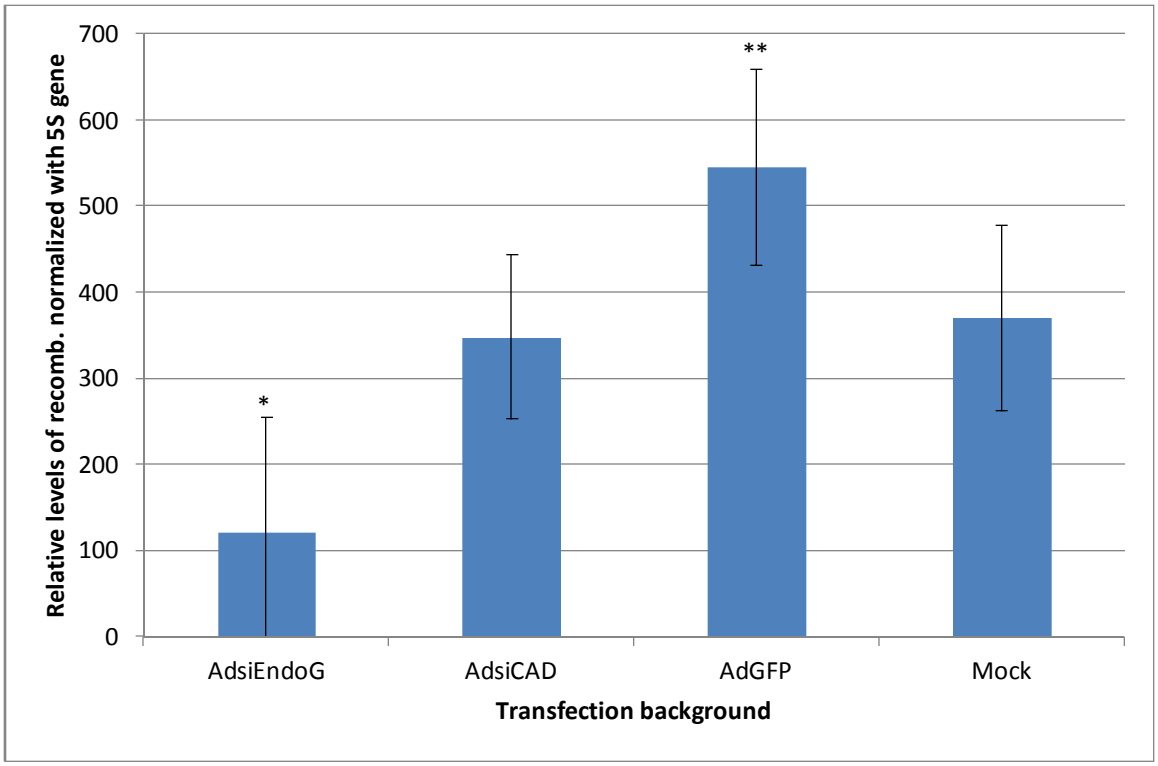

Figure 3.7: Effect of EndoG targeting on levels of homologous recombination between pDNA substrates in HeLa cells normalized against cellular DNA. Relative levels of recombination between two LacZ partial-deletion plasmids normalized with the cellular 5S rRNA gene (N=3). All cells were infected at MOI 10 p.f.u. with AdsiEndoG, AdsiCAD, and AdGFP or mock-infected. Recombination was assayed by qPCR 48 hours post co-transfection using primers specific for a fully reconstituted LacZ gene and normalized with total plasmid abundance inferred by primers specific for all plasmid variants (Fig. 5). Further normalization with the cellular 5S gene was performed to determine relative levels of recombination per cell using the equation 2^[Ct, 5S – (Ct, universal – Ct, recombination)]. Recombination levels were significantly lower in AdsiEndoG infected HeLa cells compared to AdGFP infected cells (Student's *t* test, p values <0.05).

The PCR products of the amplification generated by recombination assay primers were also examined by gel electrophoresis. This was done to determine if the generated plasmids reconstituted the LacZ gene by homologous recombination, in which case the expected amplicon size was 420bp. Amplicons that were not of this size could potentially be generated by non-homologous recombination, such as non-homologous end-joining following double stranded breaks in the two LacZ deletion plasmids or due to non-specificity.

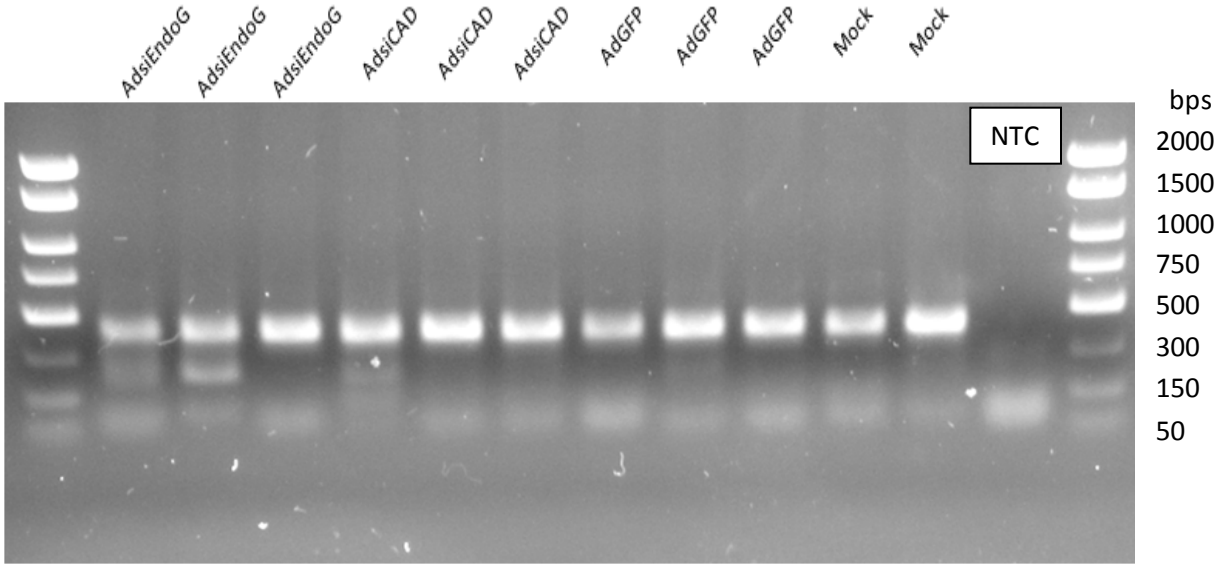

Figure 3.8: Detection of recombination specific PCR products. Gel electrophoresis (1% agarose gel) of PCR products facilitated by amplification of isolated DNA samples using assay primers specific for recombination between two LacZ deletion plasmids. Expected amplicon size was 420 bps for homologous recombination products. DNA was isolated from HeLa cells infected with AdsiEndoG, AdsiCAD, AdGFP or mock infected (MOI 10 p.f.u./cell) and co-transfected with two deletion plasmids (0.5 µg each). Two of the samples infected with AdsiEndoG showed non-specific amplification (~200 bps). This was also observed for one sample from AdsiCAD and Ad GFP infected cells. NTC denotes no template control.

From Figure 3.8, it was apparent that PCR interrogation of some samples produced amplicons that were not of the expected size (420 bps) for homologous recombination-generated templates. Specifically, two samples from AdsiEndoG infected cells and one from each other AdsiCAD and AdGFP infected cells. These could be products generated from templates that recombined in a non-homologous fashion, or non-specific amplification. Interestingly, the two samples with the highest amount of the non-specific product from cells that were infected with the AdsiEndoG, correspond directly to the two samples which showed the least amount of homologous recombination interrogated by quantitative PCR.

Since mock infected cells did not show this non-specific product, we analyzed whether Ad5 ΔE1 infection alone or in combination with transfection with either of the deletion plasmids (but not together) would result in non-specific amplification. However, none of the samples were amplified as none of the qPCRs reached threshold (data not shown) when recombination specific primers were used. However, all of the samples were amplified when universal primers were used, confirming that pDNA was isolated.

To summarize, targeting of EndoG by shRNA expressing Ad5 ΔE1, AdsiEndoG, reduced levels of detectable homologous recombination in HeLa cells between two deletion plasmids compared to a control Ad5 ΔE1 vector, Ad GFP.

3.4 Discussion

3.4.1 EndoG is not a cellular defence enzyme against pDNA uptake in HeLa cells

Successful uptake of exogenous DNA, such as pDNA, by mammalian cells is restricted by a number of cellular enzymes in order to prevent associated deleterious effects (Buzder et al., 2009). These include transformation or cell death by triggering apoptosis (Torchilin, 2006; Li et al., 1999; Nur et al., 2003). The greatest barrier for exogenous gene expression is the degradation of vectors by yet unidentified cellular nucleases (Chu et al., 2006). A recent report by Buzder *et al.* (2009) identified the level of nuclease activity of EndoG, a mitochondrial apoptosis regulator, as a determining factor in the efficiency of pDNA uptake of TKPTS and mouse PTE cells. Specifically, uptake of pDNA was enhanced by EndoG knockdown as measured by the level of expression of fluorescent reporter gene encoded on the vector. The observed effect was greater when measured at 48 hours post transfection, relative to 24 hours post-transfection.

In order to determine whether EndoG performs a similar function in human tumour cells, due to potential therapeutic implications, we tested the effect of EndoG knockdown on pDNA uptake in the cervical carcinoma cell line HeLa. To facilitate EndoG knockdown in HeLa, we made use of the previously constructed AdsiEndoG (Chapter II), a first generation adenovirus vector (Ad5 ΔE1) that encoded a cassette for the expression of shRNA directed against EndoG mRNA. Subsequently, HeLa cells were transfected with a test plasmid (pUC19) and the efficiency of the uptake was measured by quantitative PCR (qPCR).

EndoG knockdown in HeLa did not improve uptake of pDNA, assayed at 24 and 48 hours post-transfection, suggesting that EndoG is not a limiting factor for successful uptake of exogenous DNA. This result was not surprising considering the cellular localization of EndoG and its proposed roles in the cell.

Once pDNA transverses the cellular membrane and is released from endosomes, the bulk of vector degradation occurs in the cytoplasm, during intracellular trafficking to the nucleus (Chu et al., 2006). Therefore, cytoplasmic nucleases are the major effectors of pDNA degradation. Considering that the main cellular localization of EndoG is in the mitochondrial intermembrane space along with smaller concentrations in the nucleus, it is unlikely that EndoG is a mediator of cytoplasmic pDNA degradation (McDermott et al., 2011). However, upregulation of EndoG expression, due to extrinsic stimuli, may increase cytoplasmic EndoG levels (Varecha et al., 2007), which could in theory reduce pDNA uptake by the non-specific nuclease action of EndoG on vector substrates. In addition, apoptotic stimuli may induce both the upregulation and the translocation of high quantities of EndoG to the nucleus, where its nuclease action would non-specifically cleave chromatin and exogenous DNA substrates (Li et al., 2004; Zhao et al., 2009; Zhang et al., 2009; Lee et al., 2008; Mercer et al., 2010; Papa and Germain, 2011; Apostolov et al., 2011; Wu et al., 2010; Mitra et al., 2012; Ho et al., 2009; Yeh et al., 2011).

Another factor that could explain the contradictory results of this study in relation to those of Buzder et al. (2009) is the difference in cellular backgrounds used to evaluate EndoG activity on pDNA uptake. Although EndoG is ubiquitously expressed in mammalian cells, the levels of expression between tissues and cell lines can vary

considerably, which could determine the roles EndoG performs in the cell (Prats et al., 1997). This effect has been observed in relation to apoptosis phenotypes with other nucleases, such as the caspase activated DNase (CAD) and DNase γ in neuronal apoptosis, where differentiation-influenced expression levels of each nuclease determine which of the two enzymes catalyzes low molecular weight DNA degradation in response to apoptotic stimuli (Shiokawa and Tanuma, 2004).

Furthermore, experimental conditions also may have contributed to the discrepancy between the results. In this study, near-confluent HeLa cells were transfected using a cationic liposome transfection reagent (Lipofectamine2000, Invitrogen), which is inherently cytotoxic and induces apoptosis *via* the mitochondrial pathway due to an increase of intracellular reactive oxygen species (ROS) (Kongkaneramit et al., 2008; Takano et al., 2003; Aramaki et al., 2000; Aramaki et al., 1999; Iwaoka et al., 2006; Takano et al., 2001). In Chapter I of this study we have shown that Lipofectamine2000-mediated transfection of cells seeded at low initial density induced EndoG expression and may have contributed to increased pDNA vector degradation, which was absent in cells that were seeded at near-confluence at time of transfection. Degradation of pDNA most likely occurred due to induction of apoptosis which resulted in non-specific degradation of all intranuclear DNA, regardless of origin. Importantly, results from Chapter I showed that EndoG knockdown had a perceived positive effect on plasmid stability in sub-confluent HeLa cells, possibly by attenuating apoptosis in transfected cells. This is supported by other studies that demonstrated the protective effect of EndoG silencing upon treatment of cells with various apoptotic inducers (Li et al., 2004; Wang et al., 2008; Basnakian et al., 2006).

In the study performed by Buzder et al. (2009) Lipofectamine2000 was also used to transfect pDNA into TKPTS and mouse PTE cells. Although this cannot be stated with certainty, it is possible that part of the observed positive effect on pDNA uptake in EndoG deficient cells could have occurred due to an abrogated response to increased intracellular ROS. In their experimental design, Buzder et al. (2009) used the percentage of cells expressing the CFP fluorescent marker, which is encoded by the test pDNA vector, as measure of transfection efficiency. This could have contributed to the observed effect of EndoG knockdown on pDNA uptake, as cells that expressed wild type levels of EndoG could have underwent ROS induced apoptosis, thereby reducing the number of CFP expressing cells. In contrast, higher survival rates of EndoG depleted cells upon transfection could have produced a perceived positive effect on transfection efficiency. However, we are cautious in making this conclusion as the previously stated factors may be responsible for the discrepancy between our results and they may not be related to apoptosis or the cytotoxicity of the cationic liposome transfection reagent.

3.4.2 Knockdown of EndoG decreases homologous recombination between plasmids in HeLa cells

EndoG is primarily localized in the mitochondrial intermembrane space (IMS), however it is also found in the nucleus, albeit at much lower levels (Côté and Ruiz-Carrillo, 1993; Ikeda et al., 1997; Huang et al., 2002). To initiate high-scale chromatin degradation associated with apoptosis, EndoG requires a concentrated translocation from the mitochondrial IMS to the nucleus, in addition to H2B phosphorylation and possibly the

co-operation of other nucleases, such as DNase I, topoisomerase II and apoptosis inducing factor (AIF) (Zhang et al., 2007; Widlak et al. 2001, Buttner et al., 2007b; Varecha et al., 2012). Importantly, the nuclear concentration of EndoG in physiological circumstances may be important for DNA repair and recombination (Huang et al., 2006; Buttner et al., 2007a).

The first evidence for the role of EndoG in DNA recombination came from studies on herpes simplex type I (HSV I) replication (Huang et al., 2002). The characteristic inversion of the viral genome is dependent on alpha (α) sequence-mediated recombination, which is initiated by double stranded breaks in GC rich tracts within the sequence. The only enzyme isolated from HeLa cell nuclei capable of initiating HSV I recombination is EndoG, and furthermore, knockdown of EndoG in Vero cells resulted in decreased α sequence-mediated recombination (Huang et al., 2002; Huang et al., 2006). In addition, EndoG knockout mice exhibit reduced B cell immunoglobulin class switch DNA recombination, suggesting that EndoG is required for the generation of double stranded breaks in switch regions (Zan et al., 2011).

To investigate a potential role for EndoG in homologous recombination between exogenous DNA substrates, we co-transfected two pUC19-derived plasmids with non-overalpping deletions in the LacZ gene into HeLa cells with normal or reduced EndoG levels. Reconstitution of the LacZ gene, as measured by a very sensitive PCR-based approach, was used as a marker for successful homologous recombination.

Levels of homologous recombination between the two deletion plasmids were low (~0.01%) in HeLa cells, regardless of EndoG status. This was expected based on other

studies which reported low efficiencies of recombination between non-linearized extrachromosomal DNA substrates in mammalian cells (Wong and Capecchi, 1986; Brouillette and Chartrand, 1987). Furthermore, non-homologous recombination, exemplified by non-homologous end-joining, is a competing mechanism of DNA recombination and may reduce homologous recombination (Anderson and Eliason, 1986; Brouillette and Chartrand, 1987; Seidman, 1987; Zaunbrecher et al., 2008; reviewed in Hastings et al., 2009). Nonetheless, we were able to detect specific homologous recombination products in transfected cells, and our results showed that EndoG knockdown reduced levels of HR between two pDNA substrates in HeLa cells.

In Chapter I of this study, we confirmed previously reported activity of EndoG on a pDNA substrate in a standard EndoG activity assay using HeLa cell extracts. Although EndoG is an enzyme which preferentially introduces single stranded nicks in dsDNA, it is quite capable of degrading pDNA fully when those nicks accumulate on opposite strands of the DNA duplex and result in a double stranded break (Widlak et al., 2001). This is important in the context of its ability to initiate DNA recombination events, as double stranded break repair is a major driving force for homologous recombination (Dellaire et al., 2002; reviewed in Hastings et al., 2009).

Generation of double stranded breaks in cellular DNA occurs as a result of extrinsic stress, endonuclease activity or during normal cellular processes, such as DNA replication (reviewed in Hastings et al., 2009). Repair of double stranded breaks is facilitated in a large part by homologous recombination to ensure sequence fidelity and prevent deleterious chromosomal rearrangements. Although pDNA is extrachromosmal, it is nonetheless a suitable substrate for cellular DNA repair proteins (Dellaire et al.,

2002). Considering a common DNA repair model, once double stranded breaks are detected, cellular exonucleases mediate 5` end resection to generate long stretches of single stranded DNA with free 3` OH groups (reviewed in Hastings et al., 2009). The cellular DNA repair protein Rad51 guides single strand invasion into a homologous region of another DNA molecule. Extensive homology is required between recombination partners, which was facilitated by the design of the deletion plasmids used in our study (Ayares et al., 1986). Following the extension of the 3` OH of the invading strand and second end incorporation, crossing over can occur depending on how the double Holiday structure is resolved (reviewed in Hastings et al., 2009), resulting in the reconstitution of the LacZ gene. Therefore, it is likely that the negative effects of EndoG knockdown with respect to HR are a result of decreased nuclease activity available to generate double stranded breaks in homologous recombination substrates.

The results of this chapter are indirectly supported by those from Chapter II of this study, which demonstrated a cell proliferation defect in HeLa cells following EndoG knockdown. Other studies have also reported that depletion of EndoG leads to an accumulation of mammalian and yeast cells in the G2/M transition of the cell cycle, which is usually associated with an increase in unresolved DNA damage (Huang et al, 2006; Buttner et al., 2007a,b; Bunz et al., 1998). Since homologous recombination is a DNA damage repair pathway it is conceivable that absence of EndoG leads to a defect in this process. Furthermore, maintenance of polyploidy requires efficient homologous recombination, presumably to deal with the increased burden of DNA damage associated with a larger genome, and it may be telling that EndoG knockdown almost completely

eradicates this phenotype from mammalian and yeast cells growing in culture (Diener et al., 2010; Buttner et al., 2007a).

3.5 Conclusion:

In summary, the data presented in this chapter show that EndoG knockdown did not improve pDNA uptake in HeLa cells, making it an unlikely target for enhanced delivery/expression of therapeutic genes into tumour cells. However, the data show a small but statistically significant reduction in homologous recombination between exogenous DNA in HeLa cells following EndoG knockdown, implying a role for EndoG in this process.

Overall Conclusions of the Study

Using the gene knockdown approach, we studied the role of EndoG in the cervical cancer cell line HeLa, with a particular focus on its interaction with exogenous DNA due to potential considerations for gene therapy efforts. The results generated by this study demonstrated that EndoG knockdown in HeLa cells does not improve fDNA uptake, but may positively affect its short-term stability and encoded transgene expression in certain non-physiological circumstances that induce additional EndoG expression. These observations make it unlikely that EndoG has a universal defence role against the uptake and maintenance of fDNA. However, future experiments should be performed in other tumour and non-tumour cell lines before EndoG can be definitively dismissed as a defence DNase and a target for successful gene therapy. EndoG knockdown did induce a measurable HeLa cell proliferation defect, which supports previous claims that EndoG exerts control over the cell cycle. This effect coincided with enhanced DNA replication and encoded transgene expression of a first generation adenovirus vector in HeLa cells, most likely as a result of a prolongation of a favourable cellular environment for viral DNA replication. This finding may have potential implications for the use of first generation adenovirus vectors for viral oncolytic therapy, as EndoG targeting markedly improved their cytotoxicity when they were applied at higher concentrations. Utility of EndoG knockdown for adenovirus vector-mediated therapy of human malignancies should be further tested in other tumour cells to determine if the beneficial effects observed in HeLa cells are universal. Finally, knockdown of EndoG reduced homologous recombination between plasmid DNA substrates in HeLa cells. This finding demonstrated that the previously reported role of EndoG in homologous recombination of cellular DNA

also extends to exogenous DNA substrates. In conclusion, the results of this study are significant and relevant for the fields of gene therapy and virus oncolytic research. Continued work on the interaction of EndoG and adenovirus vectors, in particular, should be undertaken considering the promising initial results reported here, which may be of use for treatment of human carcinomas.

References:

Anderson RA, Eliason SL. (1986) Recombination of homologous DNA fragments transfected into mammalian cells occurs predominantly by terminal pairing. Mol Cell Biol. 6: 3246-52.

Apostolov EO et al. (2011) Endonuclease G mediates endothelial cell death induced by carbamylated LDL. Am J Physiol Heart Circ Physiol. 300: H1997-H2004.

Aramaki Y, Takano S, Arima H, Tsuchiya S. (2000) Induction of apoptosis in WEHI 231 cells by cationic liposomes. Pharm Res. 17: 515-20.

Aramaki Y, Takano S, Tsuchiya S. (1999) Induction of apoptosis in macrophages by cationic liposomes. FEBS Lett. 460: 472-6.

Arnoult D, Gaume B, Karbowski M, Sharpe JC, Cecconi F, Youle RJ. (2003) Mitochondrial release of AIF and EndoG requires caspase activation downstream of Bax/Bak-mediated permeabilization. EMBO J. 22: 4385-99.

Ayares D, Chekuri L, Song KY, Kucherlapati R. (1986) Sequence homology requirements for intermolecular recombination in mammalian cells. Proc Natl Acad Sci U S A. 83: 5199-203.

Bahi N, Zhang J, Llovera M, Ballester M, Comella JX, Sachis D. (2006) Switch from Caspase-dependent to Caspase-independent Death during Heart Development. J Biol Chem. 281: 22943-52.

Baker KP, Baron WF, Henzel WJ, Spencer SA. (1998) Molecular cloning and characterization of human and murine DNase II. Gene. 215: 281-9.

Baranovskii AG, Buneva VN, Nevinsky GA. (2004) Human deoxyribonucleases. Biochemistry (Mosc). 69: 587-601.

Baron WF, Pan CQ, Spencer SA, Ryan AM, Lazarus RA, Baker KP. (1998) Cloning and characterization of an actin-resistant DNase I-like endonuclease secreted by macrophages. Gene. 215: 291-301.

Basnakian AG, Apostolov EO, Yin X, Abiri SO, Stewart AG, Singh AB, Shah, SV (2006) Endonuclease G promotes cell death of non-invasive human breast cancer cells: Exp Cell Res. 312: 4139-49.

Benihoud K, Yeh P, Perricaudet M. (1999) Adenovirus vectors for gene delivery. Curr Opin Biotechnol. 10: 440-7.

Bernt KM, Steinwaerder DS, Ni S, Li ZY, Roffler SR, Lieber A. (2002) Enzyme-activated Prodrug Therapy Enhances Tumor-specific Replication of Adenovirus Vectors. Cancer Res. 62: 6089-98.

Berraondo P, González-Aseguinolaza G, Trocóniz IF. (2009) Semi-mechanistic pharmacodynamic modelling of gene expression and silencing processes. Eur J Pharm Sci. 37: 418-26.

Bos JL, Polder LJ, Bernards R, Schrier PI, van den Elsen PJ, van der Eb AJ, van Ormondt H. (1981) The 2.2 kb E1b mRNA of human Ad12 and Ad5 codes for two tumor antigens starting at different AUG triplets. Cell. 27: 121-31.

Bourbeau D, Lau CJ, Jaime J, Koty Z, Zehntner SP, Lavoie G, Mes-Masson AM, Nalbantoglu J, Massie B. (2007) Improvement of antitumor activity by gene amplification with a replicating but nondisseminating adenovirus. Cancer Res. 67: 3387-95.

Brand K, Klocke R, Possling A, Paul D, Strauss M. (1999) Induction of apoptosis and G2/M arrest by infection with replication-deficient adenovirus at high multiplicity of infection. Gene Ther. 6: 1054-63.

Bridge E, Ketner G. (1990) Interaction of adenoviral E4 and E1b products in late gene expression. Virology. 174: 345-53.

Brouillette S, Chartrand P. (1987) Intermolecular recombination assay for mammalian cells that produces recombinants carrying both homologous and nonhomologous junctions. Mol Cell Biol. 6: 2248-55.

Bunz F, Dutriaux A, Lengauer C, Waldman T, Zhou S, Brown JP, Sedivy JM, Kinzler KW, Vogelstein B. (1998) Requirement for p53 and p21 to sustain G2 arrest after DNA damage. Science. 282:1497-501.

Buttner S et al. (2007a) Depletion of Endonuclease G Selectively Kills Polyploid Cells. Cell Cycle. 6: 1072-6.

Buttner S et al. (2007b) Endonuclease G regulates budding yeast life and death. Mol. Cell. 25: 233–46.

Buzder T, Yin X, Wang X, Banfalvi G, Basnakian AG. (2009) Uptake of foreign nucleic acids in kidney tubular epithelial cells deficient in pro-apoptotic endonucleases. DNA Cell Biol. 28: 1-8.

Chu C, Zhang Y, Boado RJ, Pardridge WM. (2006) Decline in exogenous gene expression in primate brain following intravenous administration is due to plasmid degradation. Pharm Res. 23: 1586-90.

Côté J, Ruiz-Carrillo A. (1993) Primers for mitochondrial DNA replication generated by endonuclease G. Science. 261: 765-9.

David KK, Sasaki M, Yu S-W, Dawson TM, Dawson VL. (2006) EndoG is dispensable in embryogenesis and apoptosis. Cell Death Differ. 13: 1147-55.

Debbas M, White E. (1993) Wild-type p53 mediates apoptosis by E1A, which is inhibited by E1B. Genes Dev. 7: 546-54.

Dellaire G, Yan J, Little KC, Drouin R, Chartrand P. (2002) Evidence that extrachromosomal double-strand break repair can be coupled to the repair of chromosomal double-strand breaks in mammalian cells. Chromosoma. 111: 304-12.

Diener T, Neuhaus M, Koziel R, Micutkova L, Jansen-Durr P. (2010) Role of endonuclease G in senescenece-associated cell death of human endothelial cells. Exp Gerontol. 45: 638-44.

Dyson N. (1998) The regulation of E2F by pRB-family proteins. Genes Dev. 12: 2245-62.

Enari M, Sakahira H, Yokoyama H, Okawa K, Iwamatsu A, Nagata S. (1998) A caspase-activated DNase that degrades DNA during apoptosis, and its inhibitor ICAD. Nature. 391: 43-50.

Esche H, Mathews MB, Lewis JB. (1980) Proteins and messenger RNAs of the transforming region of wild-type and mutant adenoviruses. J Mol Biol. 142: 399-417.

Evans CJ, Aguilera RJ. (2003) DNase II: genes, enzymes and function. Gene. 322: 1-15.

Galluzzi L, Kepp O, Trojel-Hansen C, Kroemer G. (2012) Non-apoptotic functions of apoptosis-regulatory proteins. EMBO Rep. 13: 322-30.

Gavrilov K, Saltzman WM. (2012). Therapeutic siRNA: principles, challenges, and strategies. Yale J Biol Med. 85:187-200.

Gerschenson M, Houmiel KL, Low RL. (1995) Endonuclease G from mammalian nuclei is identical to the major endonuclease of mitochondria. Nucleic Acids Res. 23: 88-97.

Ghosh S, Duigou GJ. (2005) Decreased replication ability of E1-deleted adenoviruses correlates with increased brain tumor malignancy. Cancer Res. 65: 8936-43.

Glover DJ, Leyton DL, Moseley GW, Jans DA. (2010) The efficiency of nuclear plasmid DNA delivery is a critical determinant of transgene expression at the single cell level. J Gene Med. 12: 77-85.

Goldsmith KT, Dion LD, Curiel DT, Garver RI Jr. (1998) Trans E1 component requirements for maximal replication of E1-defective recombinant adenovirus. Virology. 248: 406-19.

Graham FL, Smiley J, Russell WC, Nairn R. (1977) Characteristics of a human cell line transformed by DNA from human adenovirus type 5. J Gen Virol. 36: 59-74.

Guo Z et al. (2008) Comprehensive Mapping of the C-terminus of Flap Endonuclease-1 Reveals Distinct Interaction Sites for Five Proteins That Represent Different DNA Replication and Repair Pathways. J. Mol. Biol. 377: 679-90.

Guse K, Hemminki A. (2009) Cancer gene therapy with oncolytic adenoviruses. J BUON. 14 Suppl 1:S7-15.

Han J, Sabbatini P, Perez D, Rao L, Modha D, White E. (1996) The E1B 19K protein blocks apoptosis by interacting with and inhibiting the p53-inducible and death-promoting Bax protein. Genes Dev. 10: 461-77.

Hastings PJ, Lupski JR, Rosenberg SM, Ira G. (2009) Mechanisms of change in gene copy number. Nat Rev Genet. 10: 551-64

Heacock CS, Eidsvoog KE, Bamburg JR. (1984) The influence of contact-inhibited growth and of agents which alter cell morphology on the levels of G- and F-actin in cultured cells. Exp Cell Res. 153: 402-12.

Higgins GC, Beart PM, Nagley P. (2009) Oxidative stress triggers neuronal caspase-independent death: endonuclease G involvement in programmed cell death-type III. Cell Mol Life Sci. 66: 2773-87.

Higgins GC, Devenish RJ, Beart PM, Nagley P. (2012) Transitory phases of autophagic death and programmed necrosis during superoxide-induced neuronal cell death. Free Radic Biol Med. 53: 1960-7.

Ho Y et al. (2009) Berberine Induced Apoptosis *via* Promoting the Expression of Caspase-8, -9 and -3, Apoptosis-inducing Factor and Endonuclease G in SCC-4 Human Tongue Squamous Carcinoma Cancer Cells. Anticancer Res. 29: 4063-70.

Holm PS et al. (2004) Multidrug-resistant cancer cells facilitate E1-independent adenoviral replication: impact for cancer gene therapy. Cancer Res. 64: 322-8.

Hong K, Sherley J, Lauffenburger DA. (2001) Methylation of episomal plasmids as a barrier to transient gene expression via a synthetic delivery vector. Biomol Eng. 18: 185-92.

Huang KJ, Ku CC, Lehman IR. (2006) Endonuclease G: A role for the enzyme in recombination and cellular proliferation. PNAS. 103: 8995-9000.

Huang KJ, Zemelman B, Lehman IR. (2002) Endonuclease G, a candidate human enzyme for the initiation of genomic inversion in herpes simplex type 1 virus. J Biol Chem. 277: 21071-9.

Ikeda S, Ozaki K. (1997) Action of mitochondrial endonuclease G on DNA damaged by L-ascorbic acid, peplomycin, and cis-diamminedichloroplatinum(II). Biochem Biophys Res Commun. 235: 291-4.

Ikeda S, Hasegawa H, Kaminaka S. (1997) A 55-kDa endonuclease of mammalian mitochondria: comparison of its subcellular localization and endonucleolytic properties with those of endonuclease G. Acta Med Okayama. 51: 55-62.

Imperiale MJ, Kao HT, Feldman LT, Nevins JR, Strickland S. (1984) Common control of the heat shock gene and early adenovirus genes: evidence for a cellular E1A-like activity. Mol Cell Biol. 4: 867-74.

Irvine RA et al. (2005) Generation and characterization of endonuclease G null mice. Mol Cell Biol. 25: 294-302.

Iwaoka S, Nakamura T, Takano S, Tsuchiya S, Aramaki Y. (2006) Cationic liposomes induce apoptosis through p38 MAP kinase-caspase-8-Bid pathway in macrophage-like RAW264.7 cells. J Leukoc Biol. 79: 184-91.

Jones N, Shenk T. (1979) Isolation of adenovirus type 5 host range deletion mutants defective for transformation of rat embryo cells. Cell. 17: 683-9.

Kalinowska M, Garncarz W, Pietrowska M, Garrard WT, Widlak P. (2005) Regulation of the human apoptotic DNase/RNase endonuclease G: involvement of Hsp70 and ATP. Apoptosis. 10: 821-30.

Kieper J et al. (2010) Production and characterization of recombinant protein preparations of Endonuclease G-homologs from yeast, C. elegans and humans. Protein Expr Purif. 73: 99-106.

Kim JS et al. (2008) Reactive oxygen species-dependent EndoG release mediates cisplatin-induced caspase-independent apoptosis in human head and neck squamous carcinoma cells. Int J Cancer. 122: 672-80.

Kobiyama et al. (2010) Extrachromosomal Histone H2B mediates Innate Antiviral immune Responses Induced by intracellular Double-Stranded DNA. J Virol. 84: 822-32

Kongkaneramit L, Sarisuta N, Azad N, Lu Y, Iyer AK, Wang L, Rojanasakul Y. (2008) Dependence of reactive oxygen species and FLICE inhibitory protein on lipofectamine-induced apoptosis in human lung epithelial cells. J Pharmacol Exp Ther. 325: 969-77.

Korn C, Scholz SR, Gimadutdinow O, Lurz R, Pingoud A, Meiss G. (2005) Interaction of DNA fragmentation factor (DFF) with DNA reveals an unprecedented mechanism for nuclease inhibition and suggests that DFF can be activated in a DNA-bound state. J Biol Chem. 280: 6005-15.

Krieser RJ, MacLea KS, Longnecker DS, Fields JL, Fiering S, Eastman A. (2002) Deoxyribonuclease IIalpha is required during the phagocytic phase of apoptosis and its loss causes perinatal lethality. Cell Death Differ. 9: 956-62.

La Thangue NB, Rigby PW. (1987) An adenovirus E1A-like transcription factor is regulated during the differentiation of murine embryonal carcinoma stem cells. Cell. 49: 507-13.

Lee S et al. (2008) Gene induction by glycyrol to apoptosis through endonuclease G in tumor cells and prediction of oncogene function by microarray analysis. Anti-Cancer Drugs. 19: 503-15.

Leppard KN, Shenk T. (1989) The adenovirus E1B 55 kd protein influences mRNA transport via an intranuclear effect on RNA metabolism. EMBO J. 8: 2329-36.

Li LH, Sen A, Murphy SP, Jahreis GP, Fuji H, Hui SW. (1999) Apoptosis induced by DNA uptake limits transfection efficiency. Exp Cell Res. 253: 541–50.

Li LY, Luo X, Wang X. (2001) Endonuclease G is an apoptotic DNase when released from mitochondria. Nature. 412: 95–99.

Li S, Bhatt R, Megyesi J, Gokden N, Shah SV, Portilla D (2004) PPAR-a ligand ameliorates acute renal failure by reducing cisplatin-induced increased expression of renal endonuclease G. Am J Physiol Renal Physiol 287:F990-F998.

Lieber A, He CY, Kirillova I, Kay MA. (1996) Recombinant adenoviruses with large deletions generated by Cre-mediated excision exhibit different biological properties compared with first-generation vectors in vitro and in vivo. J Virol. 70: 8944-60.

Martinez Valle F, Balada E, Ordi-Ros J, Vilardell-Tarres M. (2008) DNase 1 and systemic lupus erythematosus. Autoimmun Rev. 7: 359-63.

Marzetti E, Wohlgemuth SE, Lees HA, Chung HY, Giovannini S, Leeuwenburgh C. (2008) Age-related activation of mitochondrial caspase-independent apoptotic signaling in rat gastrocnemius muscle. Mech Ageing Dev. 129: 542-9.

McDermott-Roe C et al. (2011) Endonuclease G is a novel determinant of cardiac hypertrophy and mitochondrial function. Nature. 478: 114-8

McIlroy D et al. (2000) An auxiliary mode of apoptotic DNA fragmentation provided by phagocytes. Genes Dev. 14: 549-58.

Meck RA, Carsten AL, Kelsch JJ. (1976) Growth of HeLa cells in diffusion chamber cultures in vivo. Cancer Res. 36:2317-20.

Mercer KE et al. (2010) Expression of sulfotransferase isoform 1A1 (SULT1A1) in breast cancer cells significantly increases 4-hydroxytamoxifen-induced apoptosis. Int J Mol Epidemiol Genet 1: 92-103.

Middleton T, Sugden B. (1994) Retention of plasmid DNA in mammalian cells is enhanced by binding of the Epstein-Barr virus replication protein EBNA1. J Virol. 68:4067-71.

Mitra S et al. (2012) Copper-induced immunotoxicity involves cell cycle arrest and cell death in the spleen and thymus. Toxicology. 293: 78– 88.

Miyashita T, Reed JC. (1995) Tumor suppressor p53 is a direct transcriptional activator of the human bax gene. Cell. 80: 293-9.

Montell C, Fisher EF, Caruthers MH, Berk AJ. (1984) Control of adenovirus E1B mRNA synthesis by a shift in the activities of RNA splice sites. Mol Cell Biol. 4: 966-72.

Nadano D, Yasuda T, Kishi K. (1993) Measurement of deoxyribonuclease I activity in human tissues and body fluids by a single radial enzyme-diffusion method. Clin Chem. 39: 448-52.

Nakagami Y, Ito M, Hara T, Inoue T, Matsubara S. (2003) Nuclear translocation of DNase II and acid phosphatase during radiation-induced apoptosis in HL60 cells. Acta Oncol. 42: 227-36.

Nelson JE, Kay MA. (1997) Persistence of recombinant adenovirus in vivo is not dependent on vector DNA replication. J Virol. 71: 8902-7.

Ng P, Cummings DT, Evelegh CM, Graham FL. (2000) The yeast recombinase FLP functions effectively in human cells for construction of adenovirus vectors. BioTechniques 29: 524-8.

Nur EKA, Li TK, Zhang A, Qi H, Hars ES, Liu LF. (2003) Single-stranded DNA induces ataxia telangiectasia mutant (ATM)=p53-dependent DNA damage and apoptotic signals. J. Biol. Chem. 278: 12475–81.

Ochiai H, Harashima H, Kamiya H. (2006a) Intranuclear disposition of exogenous DNA in vivo: silencing, methylation and fragmentation. FEBS Lett. 580: 918-22.

Ochiai H, Harashima H, Kamiya H. (2006b) Silencing of exogenous DNA in cultured cells. Biol Pharm Bull. 29: 1294-6.

Ohsato T et al. (2002) Mammalian mitochondrial endonuclease G: digestion of R-loops and localization in intermembrane space. Eur. J. Biochem. 269: 5765-70.

Papa L, Germain D. (2011) Estrogen receptor mediates a distinct mitochondrial unfolded protein response. J Cell Sci. 124: 1396-402.

Parrish J, Li L, Klotz K, Ledwich D, Wang X, Xue D. (2001) Mitochondrial endonuclease G is important for apoptosis in C. elegans. Nature. 412: 90–4.

Phelps WC, Yee CL, Münger K, Howley PM. (1988) The human papillomavirus type 16 E7 gene encodes transactivation and transformation functions similar to those of adenovirus E1A. Cell. 53: 539-47.

Pilder S, Logan J, Shenk T. (1984) Deletion of the gene encoding the adenovirus 5 early region 1b 21,000-molecular-weight polypeptide leads to degradation of viral and host cell DNA. J Virol. 52: 664-71.

Prats E, Noël M, Létourneau J, Tiranti V, Vaqué J, Debón R, Zeviani M, Cornudella L, Ruiz-Carrillo A. (1997) Characterization and expression of the mouse endonuclease G gene. DNA Cell Biol. 16: 1111-22.

Rao L, Debbas M, Sabbatini P, Hockenbery D, Korsmeyer S, White E. (1992) The adenovirus E1A proteins induce apoptosis, which is inhibited by the E1B 19-kDa and Bcl-2 proteins. Proc Natl Acad Sci U S A. 89: 7742-6.

Rein DT, Breidenbach M, Curiel DT. (2006) Current developments in adenovirus-based cancer gene therapy. Future Oncol. 2: 137-43.

Roth J, König C, Wienzek S, Weigel S, Ristea S, Dobbelstein M. (1998) Inactivation of p53 but not p73 by adenovirus type 5 E1B 55-kilodalton and E4 34-kilodalton oncoproteins. J Virol. 72: 8510-6.

Sabbatini P, Han J, Chiou SK, Nicholson DW, White E. (1997) Interleukin 1 beta converting enzyme-like proteases are essential for p53-mediated transcriptionally dependent apoptosis. Cell Growth Differ. 8: 643-53.

Samejima K, Earnshaw WC. (1998) ICAD/DFF regulator of apoptotic nuclease is nuclear. Exp Cell Res. 243: 453-9.

Samejima K, Earnshaw WC. (2005) Trashing the genome: the role of nucleases during apoptosis. Nat Rev Mol Cell Biol. 6: 677-88.

Sarnow P, Ho YS, Williams J, Levine AJ. (1982) Adenovirus E1b-58kd tumor antigen and SV40 large tumor antigen are physically associated with the same 54 kd cellular protein in transformed cells. Cell. 28: 387-94.

Schafer P et al. (2004) Structural and functional characterization of mitochondrial EndoG, a sugar non-specific nuclease which plays an important role during apoptosis. J Mol Biol. 338: 217–28.

Seidman MM. (1987) Intermolecular homologous recombination between transfected sequences in mammalian cells is primarily nonconservative. Mol Cell Biol. 7: 3561-5.

Shenk, T. (1996). Adenoviridea. In Fields' Virology, B.N. Fields, D.M. Knipe, and P.M. Howley, eds. (Lippincott-Raven, Philadelphia) pp. 2111–48.

Shiokawa D, Kobayashi T, Tanuma S. (2002) Involvement of DNase gamma in apoptosis associated with myogenic differentiation of C2C12 cells. J Biol Chem. 277: 31031-7.

Shiokawa D, Tanuma S. (2001) Characterization of Human DNase I Family Endonucleases and Activation of DNase γ during Apoptosis. Biochemistry. 40: 143-52.

Shiokawa D, Tanuma S. (2004) Differential DNases are selectively used in neuronal apoptosis depending on the differentiation state. Cell Death Differ. 11: 1112-20.

Spergel JM, Chen-Kiang S. (1991) Interleukin 6 enhances a cellular activity that functionally substitutes for E1A protein in transactivation. Proc Natl Acad Sci U S A. 88: 6472-6.

Steinwaerder DS, Carlson CA, Lieber A. (2000) DNA replication of first-generation adenovirus vectors in tumor cells. Hum Gene Ther. 11: 1933-48.

Steinwaerder DS, Carlson CA, Lieber A. (2001) Human papilloma virus E6 and E7 proteins support DNA replication of adenoviruses deleted for the E1A and E1B genes. Mol Ther. 4: 211-6.

Strauss G et al. (2008) 4-hydroperoxy-cyclophosphamide mediates caspase independent T-cell apoptosis involving oxidative stress-induced nuclear relocation of mitochondrial apoptogenic factors AIF and EndoG. Cell Death Differ. 15: 332-43.

Takahashi Y, Nishikawa M, Takiguchi N, Suehara T, Takakura Y. (2011) Saturation of transgene protein synthesis from mRNA in cells producing a large number of transgene mRNA. Biotechnol Bioeng. 2011 Apr 21. doi: 10.1002/bit.23179. [Epub ahead of print]

Takano S, Aramaki Y, Tsuchiya S. (2001) Lipoxygenase may be involved in cationic liposome-induced macrophage apoptosis. Biochem Biophys Res Commun. 288: 116-20.

Takano S, Aramaki Y, Tsuchiya S. (2003) Physicochemical properties of liposomes affecting apoptosis induced by cationic liposomes in macrophages. Pharm Res. 20: 962-8.

Torchilin VP. (2006) Recent approaches to intracellular delivery of drugs and DNA and organelle targeting. Annu Rev Biomed. Eng. 8: 343–75.

Varecha M, Amrichová J, Zimmermann M, Ulman V, Lukásová E, Kozubek M. (2007) Bioinformatic and image analyses of the cellular localization of the apoptotic proteins endonuclease G, AIF, and AMID during apoptosis in human cells. Apoptosis. 12: 1155-71.

Varecha M, Potěšilová M, Matula P, Kozubek M. (2012) Endonuclease G interacts with histone H2B and DNA topoisomerase II alpha during apoptosis. Mol Cell Biochem. 363: 301-7.

Vousden KH. (1995) Regulation of the cell cycle by viral oncoproteins. Semin Cancer Biol. 6: 109-16.

Wang X, Tryndyak V, Apostolov EO, Yin X, Shah S.V, Pogribny IP, Basnakian, AG. (2008) Sensitivity of human prostate cancer cells to chemotherapeutic drugs depends on EndoG expression regulated by promoter methylation: Cancer Lett. 270: 132-43.

Wersto RP, Rosenthal ER, Seth PK, Eissa NT, Donahue RE. (1998) Recombinant, replication-defective adenovirus gene transfer vectors induce cell cycle dysregulation and inappropriate expression of cyclin proteins. J Virol. 72: 9491-502.

White E, Grodzicker T, Stillman BW. (1984) Mutations in the gene encoding the adenovirus early region 1B 19,000-molecular-weight tumor antigen cause the degradation of chromosomal DNA. J Virol. 52: 410-9.

Widlak P, Lanuszewska J, Cary RB, Garrard WT. (2003) Subunit structures and stoichiometries of human DNA fragmentation factor proteins before and after induction of apoptosis. J Biol Chem. 278: 26915-22.

Widlak P, Li LY, Wang X, Garrard WT. (2001) Action of Recombinant Human Apoptotic Endonuclease G on Naked DNA and Chromatin Substrates. J Biol Chem. 276: 4804-9.

Winnard PT Jr, Botlagunta M, Kluth JB, Mukadam S, Krishnamachary B, Vesuna F, Raman V. (2008) Hypoxia-induced human endonuclease G expression suppresses tumor growth in a xenograft model. Cancer Gene Ther. 15: 645-54.

Wong EA, Capecchi MR. (1986) Analysis of homologous recombination in cultured mammalian cells in transient expression and stable transformation assays. Somat Cell Mol Genet. 12: 63-72.

Woo EJ, Kim YG, Kim MS, Han WD, Shin S, Robinson H, Park SY, Oh BH. (2004) Structural mechanism for inactivation and activation of CAD/DFF40 in the apoptotic pathway. Mol Cell. 14: 531-9.

Wu S et al. (2010) Curcumin Induces Apoptosis in Human Non-small Cell Lung Cancer NCI-H460 Cells through ER Stress and Caspase Cascade- and Mitochondria-dependent Pathways. Anticancer Res. 30: 2125-34.

Xiong Y, Hannon GJ, Zhang H, Casso D, Kobayashi R, Beach D. (1993) p21 is a universal inhibitor of cyclin kinases. Nature. 366: 701-4.

Yamada Y, Kamiya H, Harashima H. (2005) Kinetic analysis of protein production after DNA transfection. Int J Pharm. 299: 34-40.

Yao XL, Nakagawa S, Gao JQ. (2011) Current targeting strategies for adenovirus vectors in cancer gene therapy. Curr Cancer Drug Targets. 11: 810-25.

Yeh RD et al. (2011) Gallic acid induces G_0/G_1 phase arrest and apoptosis in human leukemia HL-60 cells through inhibiting cyclin D and E, and activating mitochondria-dependent pathway. Anticancer Res. 31: 2821-32.

Zacal NJ, Francis MA, Rainbow AJ. (2005) Enhanced expression from the human cytomegalovirus immediate-early promoter in a non-replicating adenovirus encoded reporter gene following cellular exposure to chemical DNA damaging agents. Biochem Biophys Res Commun. 332: 441-9.

Zan H et al. (2011) Endonuclease G plays a role in immunoglobulin class switch DNA recombination by introducing double-strand breaks in switch regions. Mol Immunol. 48: 610-22.

Zaunbrecher GM, Dunne PW, Mir B, Breen M, Piedrahita JA. (2008) Enhancement of extra chromosomal recombination in somatic cells by affecting the ratio of homologous recombination (HR) to non-homologous end joining (NHEJ). Anim Biotechnol. 19: 6-21.

Zhang S et al. (2009) Hypoxia influences linearly patterned programmed cell necrosis and tumor blood supply patterns formation in melanoma. Lab Invest. 89: 575–86.

Zhang Z, Yang X, Zhang S, Ma X, Kong J. (2007) BNIP3 Upregulation and EndoG Translocation in Delayed Neuronal Death in Stroke and in Hypoxia. Stroke. 38: 1606-13.

Zhao ST et al. (2009) Mitochondrial BNIP3 upregulation precedes endonuclease G translocation in hippocampal neuronal death following oxygen-glucose deprivation. BMC Neurosci. 10: 113-22.